Dissertation Thesis

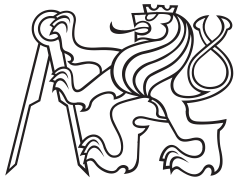

Czech Technical University in Prague

F3

Faculty of Electrical Engineering
Department of Control Engineering

Demand Side Management System for Optimizing Operation of Power Grids with Renewable Energy Sources

Ondřej Malík

Supervisor: Ing. Petr Havel, Ph. D.
PhD Programme: Electrical Engineering and Information Technology
Branch of study: Control Engineering and Robotics
August 2016

Acknowledgements

First and foremost I would like to thank Petr Havel for his relentless guidance, reviews and comments not only on this thesis but on all the work that I had done within the course of the whole PhD study and before.

I would also like to thank Petr Horáček, who, being an original supervisor of this thesis, helped to define the goals it should achieve and he also helped to organize meetings with the parties that could be interested in the results of the presented work.

My thanks also go to my colleagues at the Czech Technical University, especially to the closest co-workers Ondřej Novák, Michal Dvořák and Jan Zábojník. Some of them were directly involved in the SIRES project and therefore helped me with various aspects of the work presented in this thesis, others helped me by giving useful consultations and comments even though the focus of their work was not related to the work presented here.

Last, but not the least, I would like to thank my family and friends. They all contributed to creating such an environment that motivated me during the course of all my studies.

This work was supported by the Technology Agency of the Czech Republic under the project number TA01020865 and by the Ministry of Education of the Czech Republic under the project number 1M0567.

Declaration

This doctoral thesis is submitted in partial fulfillment of the requirements for the degree of doctor (Ph. D.). The work submitted in this dissertation is the result of my own investigation, except where otherwise stated. I declare that I worked out this thesis independently and I quoted all used sources of information in accord with Methodical instructions about ethical principles for writing academic thesis. Moreover, I declare that it has not already been accepted for any degree and is also not being concurrently submitted for any other degree.

Prague, August 2016

Ondřej Malík

Abstract

Integration of renewable energy sources is one of the most challenging issues that is being dealt with in the today's electricity networks. In order to facilitate such integration, new technologies and adequate control systems and algorithms need to be developed and put into practice.

In this thesis, a three-level demand side management system based on direct load control of electric water heaters is proposed. The system utilizes load shifting capabilities of electric water heaters in households in order to optimize operation of power system at different voltage levels, particularly focusing on networks with high penetration of renewable energy sources.

The first control level of the proposed concept operates at low-voltage level of the power system. Its objective is to control the power balance of the low-voltage area by shifting the load of electric water heaters to the time periods with high renewable energy sources production. This should ensure reduction of adverse effects of renewable energy sources on power quality in the low-voltage networks since it reduces line loading and reverse power flows, which in turn reduces voltage fluctuations observed in the network.

The second control level operates at medium-voltage level of the power system while pursuing the same objective as the first control level. The objective is achieved by coordinating operation of multiple systems at the low-voltage level which allows to improve control performance by accessing additional demand-side potential in low-voltage networks with low renewable energy sources penetration and also allows to incorporate medium-voltage network transmission constraints into the control process.

Finally, the third control level aggregates demand-side management potential from multiple medium-voltage networks in order to provide ancillary service to the transmission system operator which is then used for load-frequency control in real-time. When the transmission system operator decides to activate the provided ancillary service, the two lower control levels ensure distribution of the request among the electric water heaters in the aggregation so that the regulation energy is delivered as required. Despite that in this case mitigation of issues associated with renewable energy sources is not a direct objective of the system, the two lower levels of the control system ensure that when delivery of regulation energy is requested by the transmission system operator, the distribution of the request to activate electric water heaters is performed in a way that minimizes negative impacts on power quality.

The optimal dispatch of electric water heaters with regard to the given

objective at each control level is computed utilizing a two-stage optimization. The first phase solves a linear or quadratic programming problem and finds optimal operation of electric water heaters on longer time horizon. The second stage is based on mixed-integer linear programming and it corrects the dispatch in real-time based on instantaneous measurements and corrected predictions. In case of autonomous operation of the first control level, both stages are performed at the low-voltage level, while in case when the second control level is present, the first phase is performed on the medium-voltage level and the second phase at the low-voltage level. If the third control level is present, the principle of operation of the system at the two lower levels remains the same, only the objective changes from matching load and generation to following regulation energy delivery requests of the transmission system operator.

The simulation results indicate that the first two control levels of the proposed concept are capable of significantly reducing energy imports and exports of their network and also reducing voltage fluctuations observed in the network. The results also show that the third control level of the proposed concept is able to ensure reliable delivery of regulation energy to the transmission system operator without reducing power quality in the networks providing the demand side management potential compared to the current state.

Keywords: demand-side management, optimization, direct load control, hierarchical control system, power quality, renewable energy sources, ancillary services

Supervisor:
Ing. Petr Havel, Ph. D.

Abstrakt

Integrace obnovitelných zdrojů energie do elektrických sítí je jedním z nejaktuálnějších témat, která jsou v současnosti v oblasti energetiky řešena. Aby byla tato integrace umožněna, je třeba vyvinout a uvést do praxe takové technologie a řídicí systémy, které omezí negativní dopady obnovitelných zdrojů energie na elektrické sítě.

V této práci je navržen tříúrovňový řídicí systém založený na ovládání elektrických bojlerů v domácnostech. Tento systém využívá schopnosti elektrických bojlerů uložit energii a přesunout jejich odběr elektřiny tak, aby bylo dosaženo zlepšení provozních parametrů elektrických sítí na různých napěťových úrovních, přičemž se zaměřuje zejména na sítě s vysokým zastoupením obnovitelných zdrojů energie.

První úroveň řídicího systému je navržena pro sítě nízkého napětí. Cílem řízení je přesunout odběr elektrických bojlerů do doby vysoké výroby obnovitelných zdrojů v oblasti. Tento přesun zajistí zlepšení kvality dodávky energie v dané síti, protože snižuje zatížení vedení, omezuje zpětné toky energie do vyšších napěťových úrovní a tím zároveň snižuje výkyvy napětí v řízené síti.

Druhá úroveň řídicího systému se snaží dosáhnout stejného cíle v sítích vysokého napětí. Tohoto cíle je dosaženo koordinováním provozu řídicích systémů instalovaných v sítích nízkého napětí, které jsou napájeny ze sítě vysokého napětí, ve které je instalována uvedená druhá úroveň řídicího systému. Oproti samostatnému provozu řídicích systémů v sítích nízkého napětí umožňuje nadřazená úroveň systému využít potenciál elektrických bojlerů i v sítích nízkého napětí s nízkým zastoupením obnovitelných zdrojů energie a zároveň umožňuje řídit provoz těchto systémů s ohledem na kapacitu linek sítě vysokého napětí.

Třetí úroveň řídicího systému umožňuje sloučit potenciál řízení odběru elektrických bojlerů v několika sítích vysokého napětí tak, aby bylo možno tento potenciál poskytnout provozovateli přenosové soustavy jako podpůrnou službu, kterou pak může použít k řízení výkonové bilance soustavy. Ve chvíli, kdy provozovatel přenosové soustavy aktivuje tuto podpůrnou službu, řídicí systémy na úrovních vysokého a nízkého napětí zajistí, že tento požadavek je rozdělen mezi ovládané elektrické bojlery tak, aby požadovaná regulační energie byla provozovateli přenosové soustavy dodána. Přestože v tomto případě není primárním účelem systému omezit negativní dopady obnovitelných zdrojů energie v síti, dodávka regulační energie je řídicími systémy na úrovních vysokého a nízkého napětí realizována tak, aby byly dopady na kvalitu dodávky energie co nejvíce minimalizovány.

Optimální provoz elektrických bojlerů vzhledem k cíli dané úrovně řídicího systému je hledán ve dvou fázích. První fáze řeší problém lineárního nebo kvadratického programování a optimalizuje provoz elektrických bojlerů na delším časovém horizontu. Druhá fáze řeší problém smíšeného celočíselného lineárního programování a jejím úkolem je korigovat provoz elektrických bojlerů v reálném čase na základě okamžitých měření a aktualizovaných predikcí. V případě, že je použita pouze první úroveň řídicího systému, obě fáze optimalizace jsou prováděny řídicím systémem na úrovni nízkého napětí. Pokud je použita i druhá úroveň řídicího systému, první fáze optimalizace je prováděna řídicím systémem na úrovni vysokého napětí, druhá fáze optimalizace pak jednotlivými řídicími systémy na úrovni nízkého napětí. Pokud je použita i třetí úroveň řídicího systému, princip funkce systému na dvou nižších úrovních zůstává stejný, pouze se změní cíl řízení z přesunu odběru bojlerů do doby výroby obnovitelných zdrojů energie na splnění požadavků provozovatele přenosové soustavy na dodávku regulační energie.

Výsledky simulací naznačují, že první dvě úrovně řídicího systému jsou schopny výrazně snížit import a export energie oblastí, které řídí a zároveň jsou schopny snížit výkyvy napětí v daných oblastech. Simulace provozu třetí úrovně řídicího systému ukazují, že systém je schopen zajistit spolehlivou dodávku regulační energie provozovateli přenosové soustavy a zároveň dodat regulační energii tak, aby nebyla zhoršena kvalita dodávky energie v distribučních sítích ve srovnání se současným stavem.

Klíčová slova: řízení odběru, optimalizace, hierarchický řídicí systém, kvalita dodávky energie, obnovitelné zdroje energie, podpůrné služby

Contents

Figures

Tables

Acronyms

DSM demand side management. 3–8, 17–21, 23, 24, 26, 31–34, 36–48, 51, 59, 62–64, 66, 68–72, 75, 80, 82, 83, 87, 88, 90, 92, 93, 96–98, 100, 101, 103, 105, 106, 109–112, 114, 115, 129–136, 138, 140, 141

DSO distribution system operator. 9–11, 13, 40, 44, 73–75, 141

EWH electric water heater. 4–7, 45, 46, 48–69, 71, 72, 74–76, 79–83, 85, 87, 88, 90, 92–98, 100, 101, 103, 104, 106, 111, 112, 114, 130–135, 138, 140, 141

HV high-voltage. 5, 7, 62, 93, 94, 100, 101, 103, 106

LV low-voltage. 4–8, 10, 12, 17, 43, 47–54, 59–63, 67–72, 75, 77, 79, 80, 82, 87–90, 92–98, 110–112, 114, 129–135

MV medium-voltage. 5–8, 10, 46, 48, 60–62, 87–90, 92–94, 96–98, 100, 101, 103–106, 110–112, 114, 129–135, 138, 141

PV photovoltaic. 3–6, 11, 13–15, 48, 53, 67–69, 72, 74, 75, 77, 80–85, 92, 93, 95–97, 100, 101, 103, 106, 135

RES renewable energy sources. 3–11, 13, 17, 34, 43, 44, 67, 69–71, 73, 75, 87–89, 96, 98, 100, 101, 106, 141

TSO transmission system operator. 5–8, 10, 34–36, 40, 44, 109–112, 114, 115, 119, 120, 129–131, 134–136, 140, 147

Chapter 1

Introduction

With increasing penetration of renewable energy sources (RES) in power systems, new challenges for the operation of power systems arise. In low or moderate penetrations, the RES may help to supply some of the local load, resulting in reduced energy imports from higher levels of distribution or transmission networks. However, as soon as the penetration increases to the point at which the energy production exceeds load and the distribution network starts to export power, the RES may introduce problems, since the distribution systems were not traditionally designed to deal with energy production. Moreover, the phenomena associated with high RES penetration, such as voltage rise or increased power losses, are intensified by the intermittent production of RES, which further decreases power quality and puts additional strain on distribution system equipment.

One of the key problems associated with RES is that the time period in which RES produce energy often does not coincide with the period when the energy is demanded. This is particularly true for rural areas with photovoltaic (PV) sources. Such a discrepancy may be corrected by utilizing energy storage or by shifting energy consumption.

The concept presented in this thesis follows the second approach. It proposes a three-level control system depicted in Fig. 1.1, each level of which utilizes demand side management (DSM) potential of household appliances in order to pursue objective specific to the given level of the power system while capitalizing on capabilities of lower levels of the control system. These control levels are designed to be independent in a way that the lower level of the control system does not require the superior control level to be present, however, having the superior control level allows the system as a whole to pursue additional objectives based on information that is not available at the lower levels of the system.

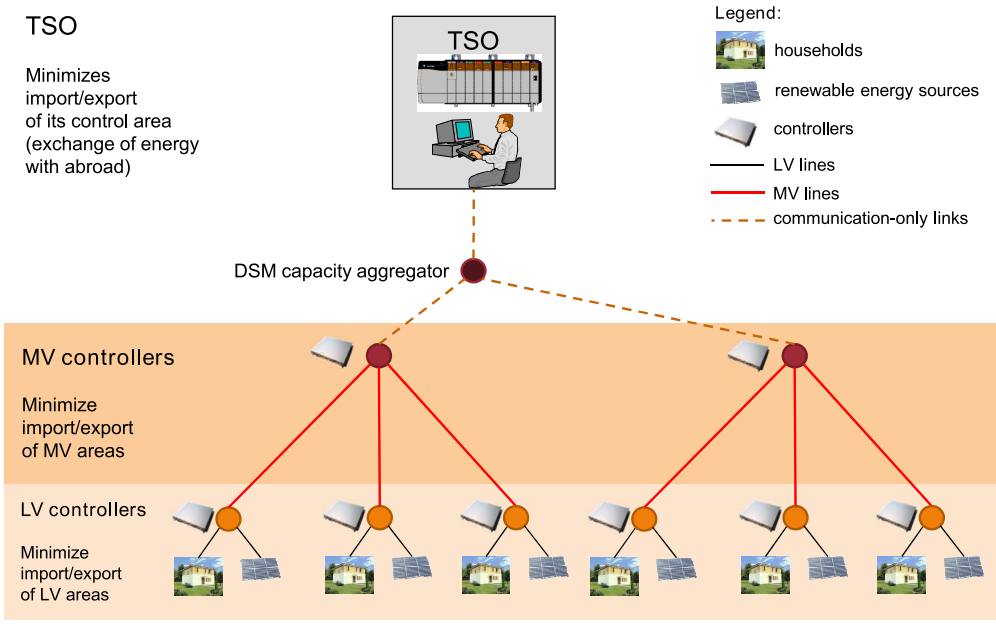

Figure 1.1: Control levels of the proposed DSM concept.

1.1 Control levels of the system

The lowest control level and the core part of the concept is a DSM system based on centralised direct control of electric water heaters in low-voltage (LV) parts of distribution networks with high RES penetration (particularly PV sources). The basic objective of the system is to shift the electric water heater (EWH) load to the time periods with high RES energy production capitalizing on energy storage capabilities of EWHs. In an interconnected power system, this objective may be equivalently expressed as minimizing energy exchange (energy import and export) with a higher level of a power system as illustrated in Fig. 1.1. The EWH dispatch is computed utilizing two stage linear and mixed-integer linear programming based optimization, where the first stage computes the overall EWH load distribution on longer time horizon while the second stage corrects the dispatch in real-time based on instantaneous power balance of the area (i. e. the difference between energy production and load in the area resulting in power flow into or from the area through the feeding transformer). Such a system should reduce the aforementioned adverse effects of RES and facilitate

safe operation of distribution network with existing equipment at higher voltage levels.

In order to expand the potential benefits of the LV DSM system, a second control level formed by a medium-voltage (MV) extension of the DSM system is also presented. The additional control layer coordinates operation of multiple LV DSM systems in order to:

- provide possibilities to exploit DSM capabilities of LV areas with small or no penetration of RES,
- introduce capability to control the load with respect to MV network transmission constraints.

The coordination of the LV DSM systems is performed by computing a dispatch reference (i. e. the target power balance) for each LV DSM system in the controlled MV distribution network which replaces the reference that was computed by the LV DSM system itself in case of autonomous operation of the LV DSM system. The dispatch references for the LV DSM systems are again computed with an objective to maximize local consumption of the energy produced by RES and levelling the transmission profile at the interconnection of the MV network and the high-voltage (HV) network. With the additional control level in the MV network, it is possible to exploit the DSM capabilities even of the LV areas with low or no penetration of PV sources, since the EWHs in such LV areas may be utilized to store energy of neighbouring LV areas that have excess of PV sources production that they cannot accommodate on their own. Moreover, when computing the optimal dispatch references for the individual LV areas, the controller at the MV level takes into account transmission constraints of the MV network. Similarly to the LV DSM system, the EWH dispatch is computed in two stages with different update intervals. The first stage is performed at the MV level and computes the dispatch references for each LV DSM system on at least 24 hour horizon by solving quadratic-programming (QP) problem. The second phase is performed by the LV DSM systems in each LV area in the same way as if the LV DSM systems operate autonomously.

Finally, the highest level of the control system aggregates the DSM potential of multiple DSM systems at MV level in order to provide the DSM potential to the transmission system operator (TSO) in a form of ancillary service so that it can be used for load-frequency control of the TSO's control area. Real-time utilization of the DSM-based ancillary service by the TSO dispatchers is facilitated by using modification of decision support tool proposed in an earlier work of the author. The two lower control levels of the DSM system then ensure

that when the TSO requests to activate such an ancillary service, the regulation energy is delivered as required. Although when the DSM potential is used to provide ancillary services for the TSO, it cannot directly focus on mitigating issues associated with RES at lower levels of the power system, the MV and LV control levels ensure that when delivery of regulation energy is requested by the TSO, the request is distributed among the EWHs in the aggregation in a way that minimizes negative impacts on power quality in the MV and LV networks.

1.2 Connection with the SIRES project

Most of the research towards the aforementioned concept was undertaken within a Technology Agency of the Czech Republic project number TA01020865 co-denamed BIOZE, which is a Czech acronym for *Safe Integration of Renewable Energy Sources* hence an according English acronym SIRES will be used to reference the project in the text of this thesis. The SIRES project targeted issues with integration of RES into distribution and transmission network systems, with emphasis put on (but not limited to) current issues associated with RES in the Czech Republic. The baseline situation at the project start was determined by two major factors:

- steep increase of small and medium-scale RES (particularly PV sources) in the LV and MV distribution systems, which brought about various problems, mostly connected with power quality,
- intended roll-outs of smart-metering pilot projects.

As SIRES is an application-oriented project, it influenced the fundamental design principles of the presented DSM system with the key requirements being:

- focus on controlling load already existing in the households,
- design the system so that it can be rolled-out with minimal investment costs aside from the smart-meter installation,
- design the system so that it requires minimal possible end-user interaction.

Adhering to the above requirements should have enabled the system to be rapidly put into practice had the initial research shown that the system brings appreciable benefits over the current way how the household load is controlled.

As a part of the SIRES project, a small-scale pilot implementation of the LV DSM system was set up in a part of the LV distribution network in the Czech Republic. While the scale of the pilot project was insufficient to show the actual potential of the DSM system in terms of influence on improving the power quality in the network, it allowed to collect important data and prepare and test key parts of the concept such as algorithms for estimating of hot water consumption of the households with controlled EWHs.

1.3 Goal of the thesis

To summarize, the goal set out for this thesis is to propose a demand side management system that should attempt to deal with one of the key problems associated with RES which is that the time period in which RES produce energy often does not coincide with the period when the energy is demanded. In an interconnected power system, this objective may be equivalently expressed as minimizing energy exchange (energy import and export) with a higher level of a power system as illustrated in Fig. 1.1. As a result, the goal of this thesis breaks into three subtasks, each dealing with one of the control levels described in Section 1.1:

- **Low-voltage (LV) DSM system** objective of which is to control the load such that the energy exchange of the controlled LV area with MV network is minimized. As a part of the design of the LV DSM system, the fundamental aspects of the proposed DSM system such as hardware configuration, communication between individual components of the system and implementation of functions necessary for the operation of the system (predictions, EWH state estimation, etc.) should be discussed. These aspects should be designed in line with requirements given in the SIRES project that were described in Section 1.2.

- **Medium-voltage (MV) DSM system** which aims to minimize energy exchange of the controlled MV network with the HV network by coordinating operation of the LV DSM systems connected within the MV network.

- **Provision of the DSM capabilities to the transmission system operator (TSO)** so that it can be used for load-frequency control of the TSO's control area. The objective of the load-frequency control is mainly to minimize the unscheduled energy exchange of the control area (typically transmission system of one country) with neighbouring control areas.

1.4 Structure of the thesis

The rest of this thesis is organised as follows: Chapter 2 summarizes what effects the RES have on power quality and also presents several traditional voltage control methods and how effective they are in networks with high RES penetration. Chapter 3 presents what potential several studies see in various DSM capacity holders and DSM programmes. Then, the proposed three-level control concept is presented: First, the important aspects influencing all the control layers such as what type of load to control or selection of load control principle are discussed based on relevant literature survey in Chapter 4. Then the LV DSM system is presented in Chapter 5. As the design of the LV DSM system was closely related to the pilot installation realized within the SIRES project, the chapter also gives insights into possible hardware configuration and implementation of the DSM system functions. The MV DSM system is detailed in Chapter 6 and how the DSM capabilities may be provided to and efficiently utilized by the TSO is shown in Chapter 7. Finally, the main findings and results are summarized in Chapter 8.

Chapter 2

Impacts of renewable energy sources on power quality in distribution grids

High penetration of RES in the distribution grids impacts the quality of power delivered to the end-consumers mainly for two reasons: first, the distribution grids equipment was not designed to deal with generation and second, the RES generation is intermittent, i. e. the amount of power delivered by RES may be subject to fast fluctuations as a result of changes in weather, temperature etc. This section will summarize the voltage quality requirements, the issues that may arise with increased RES penetration in the distribution grids, traditional methods of voltage control in distribution grids and what effects were observed and what measures were proposed in several studies to deal with issues introduced by RES integration.

2.1 Power quality standards and influence of renewable energy sources on power quality in distribution grids

One of the primary concerns of the distribution system operator (DSO) is to keep the voltage quality at the customers' feed-in points within specified limits. In the Czech Republic, these limits are specified mainly by the CSN 50160 norm, which is an implementation of the European Union EN 50160 norm. The main requirements are as follows:

- The nominal frequency is 50 Hz and the mean frequency shall remain within ±1% of the nominal frequency (i. e. 49.5Hz - 50.5Hz) during 99.5% of the

year and shall never deviate more than -6% and +4% (i. e. 47Hz - 52Hz) from the nominal frequency.

- The nominal voltage in LV networks is 230V phase to neutral and 400V phase to phase. In MV networks, the nominal phase to phase voltages are 3, 6, 10, 22 and 35 kV. The norm defines, that 95% of 10-minute RMS voltage averages over a week time shall remain within ±10% of the nominal voltage (i. e. 207V - 253V phase to ground in LV networks).

- The flicker (fast voltage fluctuations) shall not exceed 5% of the nominal voltage in LV networks and 4% of the nominal voltage in MV networks.

- Further specifications in the Czech norms define for example duration of short-term voltage drops resulting from appliances switching, duration of short and long-term voltage outages, requirements on voltage symmetry etc.

Since the network frequency is common for the whole transmission and distribution system and is primarily maintained by a TSO, the main concerns of the DSOs are the impacts of RES on voltage quality and other factors influencing the distribution system reliability and economics. These impacts were summarized in article [1]. The article divides the impacts into two categories: steady-state impacts, i. e. the impacts that may be quantified using a steady-state load flow analysis, and dynamic impacts, that need to be assessed using dynamic model of the studied network. The following steady state impacts were mentioned in [1]:

- *Reverse power flow* - As soon as the production exceeds consumption, the area will export power, which can influence overcurrent protection or voltage regulators in the distribution system, which were not traditionally designed for power exports.

- *Voltage rise and fluctuations* - Since the generation of RES is dependent on ambient conditions, the power output varies with changes in weather. The power output directly influences voltage levels at the RES connection points and the effects are especially pronounced if the RES are installed at the end of long lines with low loading.

- *Interaction with distribution system voltage control equipment* - The aforementioned voltage fluctuations may induce frequent switching of voltage control equipment, such as capacitor banks, voltage regulators or on-load tap changing transformers, which can lead to shortening of their life cycle.

- *Reactive power fluctuations* - The frequent switching of voltage control equipment influences the amount of reactive power that is produced in the distribution system. The missing reactive power then has to be supplied from the transmission system which increases losses and transmission lines loading.
- *Modification of feeder section loading* - Depending on penetration, the RES may positively or adversely influence the loading of the feeders where the RES are connected. With low penetration, the RES may help to locally supply part of the feeder load, however, with high penetration, the exported power may cause the feeder overloading.
- *Increase in power losses* - Here, the situation is similar to changes in feeder loading - with high RES penetration, the feeder power flows are increased compared to normal situation due to the exported power. Moreover, if the capacitor banks are switched off because of voltage rise, the feeder has to also supply the missing reactive power which further increases the feeder losses.

Among the dynamic effects that need to be studied in context of RES integration, the article [1] lists the following:

- quick and large fluctuations of RES power output,
- sudden connection and disconnection of RES,
- accidental islanding,
- impacts on power quality - voltage sags, flicker, etc.,
- RES behaviour during faults,
- interaction with voltage control devices.

Although the article [1] addresses these issues in connection with PV generation, similar effects are associated with other types of RES as well, albeit with different magnitudes.

2.2 Traditional voltage control methods

According to [2], most DSOs control the voltage at the customers' feed-in points by adjusting the voltage on the distribution feeder. The impedance of feeder

conductors, LV transformer and load causes a voltage drop on the feeder and subsequently also at the customers' feed-in points which increases with distance from the distribution transformer.

Since the voltage drop depends on the current flowing through the feeder which in turn depends on the active and reactive power drawn by the load, the distribution transformer has to adapt its secondary voltage according to load variations. This is usually achieved by using on-load tap-changing (OLTC) distribution transformer which allows to control primary to secondary voltage ratio by switching the transformer taps. The OLTC measures the voltage and current and estimates the voltage at the customers' feed-in points. If this voltage is found to be out of the specified limits, the OLTC adjusts the tap positions in order to increase or lower the secondary voltage and bring the voltage at the customers' feed-in points back to the required bounds. As specified in [2], the OLTC is typically capable of adjusting the voltage within $\pm 10\%$ of the nominal voltage in 32 steps.

If the voltage drop along the feeder causes voltage limits violation at customers' feed-in points a capacitor bank may be used to locally compensate (supply) some of the reactive power required by the load. This causes reduction in reactive power flow from the distribution network and as a result the voltage drop along the feeder is also reduced. According to [2] due to frequent changes in reactive power requirements of the network load and the fact, that the capacitor banks may only be switched in several discrete increments, the reactive power delivered by the capacitor banks cannot perfectly match the reactive power required by the load. Two more issues of capacitor banks were mentioned in [2] - first, the amount of reactive power delivered by the capacitor banks decreases with voltage squared, hence as the voltage drops, the capacitor banks deliver less reactive power instead of more and therefore their contribution to voltage control is limited. Moreover, if the feeder becomes overcompensated the capacitor banks may cause substantial voltage rise which would require corrective action from the distribution transformer.

The article [3] mentions a static VAR compensator (SVC) as another means to control voltage on the feeder. The SVC, similarly to the capacitor banks, compensates the impedance of the feeder to match the reactive power required by the load. The SVC consists of a capacitor bank for coarse impedance control accompanied by thyristor-controlled inductor, which is used to fine-tune the impedance. Main advantage of the SVC over the capacitor banks is that it is able to perform continuous and smooth control of the line impedance, hence it is able to track fast changes in impedance of the load.

Finally, the article [3] suggests, that a step voltage regulator (SVR) may be used to control the voltage along the feeder. The SVR principle is equivalent to that of the OLTC - it is a transformer with variable primary to secondary voltage ratio, however, the tap change is not directly initiated by changes of power drawn by the load, but rather by an external signal (e. g. by the DSO control system).

2.3 Performance of traditional voltage control in networks with high RES penetration

As already mentioned, the high penetration of RES in the distribution networks introduces unexpected situations and control issues in the specific area. While on one hand, the local generation may help to reduce power in-feed from the distribution substation resulting in reduction of power losses on the transmission lines, on the other hand, without proper voltage control, phenomena like overvoltage or power flow reversals might occur.

A study [4] investigated the impacts of high PV penetration in a residential area. Rooftop PV installations with 1-2 kW rating per house were considered. A part of Leicester, UK distribution network supplying more than 1200 customers was selected for simulations. The study stresses out the importance of precise load modelling based on 1-minute load data in order to capture fast load fluctuations resulting in short-term voltage extremes and power reversals. The generation of the PV arrays was modelled based on irradiance data from nearby meteorological station. The study compared the probability of occurrence of voltage in specific range and reduction in power losses for several levels of PV penetration (0%, 30% and 50%).

The simulation results have shown, that the probability of higher voltage at the customers' feed-in points increases with increased PV penetration most notably on summer days when the PV generation is high. For the 50% penetration level, the study reported probability of exceeding the voltage limits and suggested that for safe operation, the PV penetration should not exceed 30%. The study has also shown that for the 50% PV penetration, some of the transmission lines experienced reversed power flow during the whole selected summer day.

The power losses were reduced by approx. 10% in winter and 15% in summer for the 30% PV penetration case and by 13% in winter and 20% in summer for 50% PV penetration case. The reduction in power losses for 50% PV penetration case over the 30% case is comparatively low, which is caused by increased reversed

power flows in the 50% case. The study also notes, that high penetration of PV may cause issues with OLTCs and automatic voltage control relays as a result of frequent changes in power factor due to the variable PV generation.

The paper [5] presented a study of impacts of PV penetration in Anatolia III Residential Community, Rancho Cordova, California, USA. It is expected that after full rollout 600 out of 795 houses will be SolarSmart, i. e. the houses will be equipped with 2 kW rooftop PV system each, resulting in total potential capacity of 1.2 MW. The area is supplied by substation equipped with 20 MVA OLTC transformer capable of controlling voltage in range ±1.5 V around 123 V with time delay for tap adjustment 60 seconds. A capacitor bank is also installed in the substation.

The study presented measurements from a cold summer sunny day, i. e. a day, when the PV arrays should generate maximum energy. At the time, only 115 out of expected houses 600 were SolarSmart. During the night, the voltage at homes was lower than that of the substation, which is typical for passive distribution networks (without generation). During the day, however, the voltage rose to maximum of 0.7 V above the substation voltage, resulting in energy export from the area after the morning load peak has ended. However, the voltage remained within limits. The measurements were used to develop model of the distribution network, which will be used to estimate acceptable PV penetration levels.

2.4 Control strategies to improve voltage control in networks with high RES penetration

The article [2] investigated the impacts of high PV penetration on the distribution network and potential of PV arrays inverters for improving voltage control. The selected system consisted of 7 aggregated loads with the total load of 11 MVA. The system was fed from substation with 20 MVA OLTC transformer. A SVR and switched capacitor bank were also installed on the feeder. The photovoltaics were modelled as constant negative load with size proportional to the PV penetration level. The PV arrays were considered to be equipped with inverters with 10% greater kVA rating than their rated active power to allow for reactive power generation/voltage control even when generating the maximal active power.

The simulations were performed for 5, 10, 30 and 50% PV penetration levels with PV inverters configured to pursuit different control targets (to supply reactive power only, to control voltage, to control power flow etc.). The presented results

compared voltage profiles for the case of peak PV production and low load using different control strategies and PV penetration levels. A case with no PV production with PV inverters supplying only reactive control was also shown.

In the case of low load, high PV generation, 50% PV penetration and PV inverters controlling the voltage the study has shown, that although the PV inverters managed to produce almost flat voltage profile, this control strategy caused increase in reactive power transmissions since the inverters reduced the voltage by absorbing the reactive power, which resulted in increased transmission losses.

The second presented strategy for this case was as follows: the PV inverter control was combined with feeder voltage control to allow exporting of reactive power. For this case, both voltage controllers reduced the voltage to minimum levels, facilitating the export of active power as well as reactive power. It should be noted that apart from allowing the energy export, this strategy had an adverse effect in increasing the feeder transmission losses.

The third strategy was to control the feeder power factor using the PV inverters. This strategy allows the export the active power with reduced reactive power transmissions resulting in reduction of transmission losses.

The paper [6] suggested that a droop control based coordinated active power curtailment of grid-connected PV inverters may be an effective method to deal with overvoltage caused by PV generation in areas with high PV penetration. An advantage of this control method is that all the connected inverters act in coordinated way without need for communication infrastructure, because the control action is proportional to the voltage deviation from the nominal voltage, which can be measured locally. The paper suggests, that the controller should not take any action until the voltage crosses a specified threshold (a limit for "normal operating state" in this case). The droop coefficient is then set to such a value, so that the PV inverter supplies no active power when the voltage reaches "extreme operation limit". A deficiency of this approach is that the houses located further from the distribution substation are more susceptible to voltage variations hence in case of overvoltage, they are the first to be curtailed. Since the curtailment of active power delivery is associated with reduction of revenues of the PV installation owners, such a situation should be avoided in order to assure fair opportunities for all PV owners. To compensate this deficiency, the paper proposes to modify the droop coefficient based on voltage sensitivity at the point of each PV installation. Such a modification levels the amount of active power delivered by each PV installation, however, it also reduces the net active power exported from the area.

Chapter 3

Demand side management potential analyses

As already mentioned, one of the main problems with RES integration lies in the fact that they are being installed into LV parts of distribution networks which are not equipped with adequate equipment to deal with associated issues. One way to deal with this inadequacy is to install additional voltage control equipment and use traditional methods for voltage control as described above even in LV networks. An alternative approach might be to control the load of consumers connected in the network, so that the load locally compensates the fluctuating RES generation. Such an active management of consumers' load is a part of the smart grids concept as a DSM.

However, traditionally the DSM is perceived as a way to deal with problems on a transmission system level, such as high peak demand. The traditional DSM programmes attempt to modify the consumption patterns so that the consumption is lowered in peak hours and if possible shifted to periods with generally lower energy demand. With proper market design, technology and incentives, this type of DSM could play a significant role by providing similar opportunities to increase the efficiency of the power system as the dedicated energy storage facilities, i. e. to allow for better utilization of generation capacities by levelling the load curve, and therefore avoiding construction of peaking power plants or to defer construction of new transmission lines by accumulating energy in off-peak hours and serving it locally during the peak demand.

This section attempts to demonstrate the DSM potential on both - the transmission and the distribution system levels - by presenting a survey of analyses

of DSM potential in the world and also own estimates of the DSM potential in the Czech Republic.

3.1 Potential providers of the demand side management services

According to [7], two prospective groups of consumers have the potential to provide the DSM services. The first group is formed by the large industrial consumers with the possibility to lower their energy demand for limited time period. The lowering of the energy demand is usually associated with substantially limiting or completely stopping the underlying industrial process leading to reduction of profit. If the process does not need to be stopped completely, for example if a storage of some intermediate product is available or if the lost production may be recovered later, then the price, at which the industry would be willing to halt its production, might be competitive with conventional generation. In other cases, however, the opportunity costs may be so high that using the DSM capabilities of the particular industry would be prohibitively expensive.

Apart from high opportunity costs, the other factors influencing the decision of the industrial consumers whether to provide the DSM services or not are more favourable. The DSM potential may range up to several MW per industrial consumer and the investment costs per MW of DSM service are usually negligible. Moreover, large industrial consumers are expected to act in a rational way, i. e., it is reasonable to expect that they will provide the DSM services in case they find it cost-effective.

The second group of the prospective DSM services providers are small energy consumers such as households or commercial buildings. The most energy demanding household appliances, e. g. electric water heaters, refrigerators, freezers or air-conditioners have relatively high load shifting potential. If properly controlled, these appliances allow to accumulate thermal energy in off-peak periods and lower their energy demand in peak hours. While the DSM potential of individual households might be small, the aggregated potential of all small consumers is substantial. As a result, the level of penetration of DSM enabling technologies (e. g. smart meters with load control capabilities) is critical for exploiting the DSM potential in households.

One of the most important tasks associated with the DSM of small energy consumers is to provide proper incentives to the consumers so that they invest

in the DSM enabling technologies. The households do not only care about what economic benefits would such a technology provide, but other factors such as comfort reduction or ease of use of the new technologies are equally important. Due to the aforementioned factors and other technical, economical and legislative barriers, the penetration of the DSM enabling technologies is increasing at slow pace.

3.2 Demand side potential studies

Several studies dealt with assessment of the DSM potential and its value as an alternative to conventional measures for compensating the peak electricity demand and transmission lines overloading as well as a means to improve the power system efficiency.

3.2.1 Studies in the USA

A number of studies assessed the DSM potential in the USA. These studies usually consider two types of DSM potential - energy efficiency (i. e. replacement of current appliances and technologies by more energy efficient ones) and demand response (i. e. active control of electricity consumption). This analysis is only interested in demand response programmes, hence the energy efficiency programmes will not be dealt with as long as they do not influence the estimates of demand response potential in a particular study. The contribution of commercial, industrial and residential consumers to the peak demand reduction by 2020 as estimated in selected studies is presented in figure 3.1. Since each study dealt with different area/state of the USA, only peak demand reductions relative to the 2020 peak demand estimate presented in each study are shown in figure 3.1. Note, that each of the studies might have used slightly different methods to produce the peak demand estimate, so care should be taken when comparing the peak demand reduction estimates. The key assumptions used when producing the estimates of the demand response potential to reduce peak electricity demand along with known differences between the peak demand estimates in individual studies will be further presented.

In 2009, the Federal Energy Regulatory Commission (FERC) published "a first nationwide study of demand response potential using a state-by-state approach" [8]. The DSM potential is analysed mainly in context of consistently growing peak power consumption in the USA, associated with for example

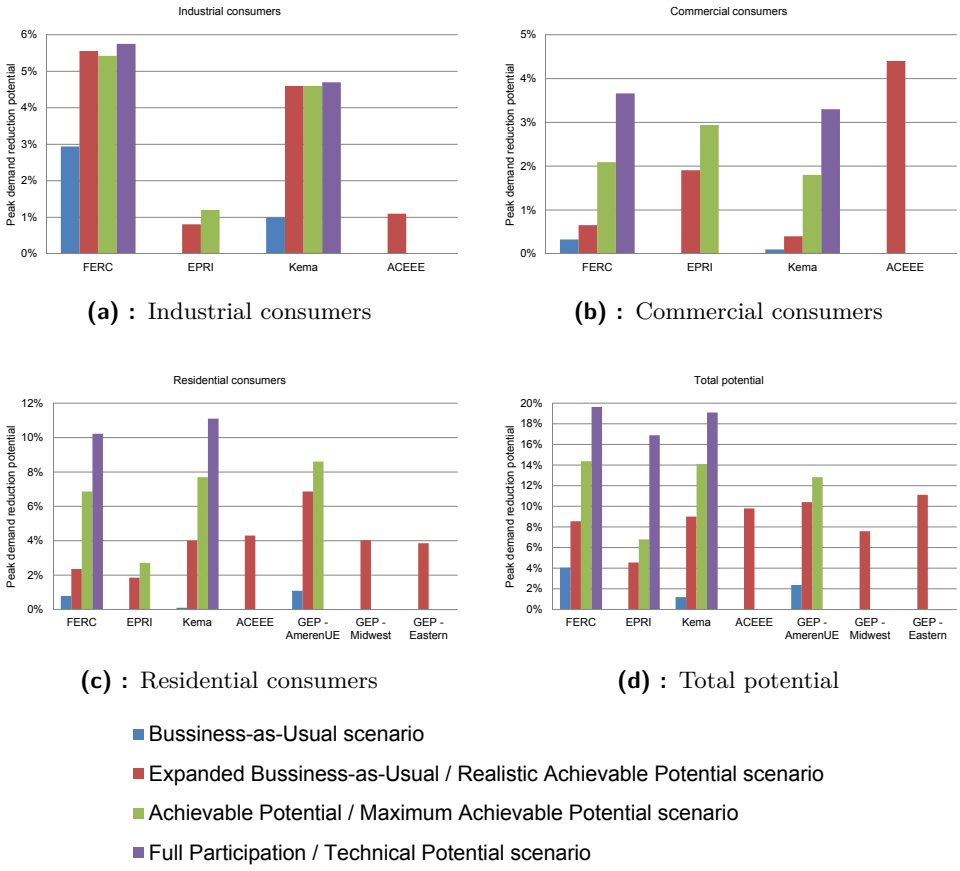

(a) : Industrial consumers

(b) : Commercial consumers

(c) : Residential consumers

(d) : Total potential

Figure 3.1: Demand response potential by 2020 as estimated in US analyses.

with increase in air conditioning penetration. Without any demand response programmes (even without those that were in place by 2009), FERC expects that the peak demand will increase at rate 1.7% per year, growing from 810GW to 950GW over a 10-year horizon.

The study investigated the effects of several types of DSM programmes:

- *Dynamic pricing* (DP, with or without enabling technology) is a type of DSM programme in which the electricity prices are dynamically variated (either day-ahead or in real-time) in order to respond to various situations in the power system, primarily to power system load with high prices during peak demand and low prices in off-peak hours, but also to unexpected

situations such as generation outages etc. The enabling technology allows for an automatic response of consumers to price signals instead of having to respond manually, leading to increased effect of price variations on consumers' electricity demand.

- *Direct load control* (DLC) is similar to dynamic pricing with enabling technology, however, the control of consumers' appliances is not necessarily connected with energy prices, but reacts on current needs of the transmission or distribution system operator.
- *Interruptible tariffs* (IT) are targeted at large energy consumers. For a specified payment, the consumers agree to reduce their energy consumption on demand of the transmission or distribution system operator.
- *Other programmes* encompass other possibilities how the medium and large energy consumers may sell their DSM potential, such as bidding into capacity markets.

The overall impact of all demand response programmes was computed based on three key inputs: the average load of a given group of consumers in peak demand periods, the average peak demand reduction of a particular demand response programme and finally by number of consumers participating in each programme. The average load profiles for several consumer classes (categorized based on peak demand) were estimated from hourly load data from utilities in 21 states using statistical analysis.

The estimates of per consumer peak demand reduction in dynamic pricing tariffs were produced based on various pilot projects. The study points out that the price responsiveness (i. e. the power demand change as a reaction to a price change) differs state to state, which may be attributed to climate differences, differences in central air conditioning penetration and availability of enabling technologies. The price responsiveness is also varies with type of consumers (residential, commercial or industrial). Finally, the price responsiveness is influenced by peak to non-peak price ratio. The examples of peak reductions with 4 to 1 and 8 to 1 price ratio as estimated in the study [8] are presented in table 3.1. The 8 to 1 price ratio was used in the study for estimating the demand response potential of dynamic pricing programmes.

For other demand response programmes, which are already commonly used in practice, information from current programmes was used to estimate peak demand reductions and participation rates. For the direct load control programmes, only direct control of central air conditioning was modelled; other

State	Central air conditioning penetration	Peak demand reduction (4 to 1 price ratio)	Peak demand reduction (8 to 1 price ratio)
Massachusetts	12.70%	6.20%	9.83%
Maryland	78.00%	12.56%	19.66%
Arizona	86.80%	14.28%	22.33%

Table 3.1: FERC study: Examples of peak demand reduction as a function of price ratio and central air conditioning penetration.

Consumer class	Dynamic pricing without technology	Dynamic pricing with technology	Direct load control	Interruptible tariffs	Other DR
Residential	7% to 18%	21% to 34%	19% to 52%	N/A	N/A
Small C&I	1%	15%	7% to 17%	N/A	N/A
Medium C&I	9%	14%	2% to 5%	27% to 100%	39% to 100%
Large C&I	7%	14%	N/A	13% to 100%	10% to 100%

Table 3.2: FERC study: Per consumer peak demand reductions by demand response programme.

devices such as water heating were not included because of small impacts compared to central air conditioning and lack of state-level saturation data. All assumed per consumer peak demand reductions in various programmes are summarized in table 3.2.

The numbers of consumers participating in demand response programmes were estimated from the total number of consumers of given class eligible for a particular demand response programme (i. e. those who own a particular technology/appliance and enabling technology) and assumed programme participation rate. For dynamic pricing programmes, the participation rates were based on number of consumers with enabling technology and dynamic pricing tariff as defined below for each scenario. For other demand response programmes, the participation rates were based on experience from the current programmes and are summarized in table 3.3.

	Residential	Small C&I	Medium C&I	Large C&I
Direct Load Control	25%	1%	7%	N/A
Interruptible Tariffs	N/A	N/A	2%	17%
Other DR	N/A	N/A	0%	19%

Table 3.3: FERC study: Non-Pricing demand response programmes participation rates estimates.

The study analysed the DSM potential over the 10-year horizon in various DSM participation scenarios:

- *Business-as-Usual* (BAU) scenario assumes that current and planned DSM programmes remain unchanged, i. e. the participation rates will increase at current rates.
- *Expanded Business-as-Usual* (EBAU) scenario expands DSM programmes to all states and achieve a "best practices" participation levels.
- *Achievable Participation* (AP) assumes universal deployment of smart meters with dynamic pricing as a default tariff. The consumers are allowed to opt-out (choose another tariff). It is assumed that no more than 25-40% of consumers will opt out of the dynamic pricing tariff.
- *Full Participation* (FP) is identical to the Achievable Participation scenario, but consumers are not allowed to opt-out. Such a scenario served as a benchmark of what potential the DSM actually hold if there were no barriers in enabling technology penetration growth.

The potential peak demand reductions by 2019 for each scenario are presented in figure 3.1. For example, the 20% peak reduction achieved in the FP scenario translates into 184 GW. This is roughly equivalent to expected peak demand increase over the 10 year horizon, hence under the FP scenario, the demand response could help keeping the peak demand unchanged. Note, that in order to allow for comparison of the results with other studies, the Small C&I and Medium C&I were included in commercial consumers class and Large C&I in industrial consumers class in figure 3.1.

Among the DSM programmes, the dynamic pricing with enabling technology was found to hold the largest peak demand reduction potential. However, due to the dependence on smart meters penetration and number of consumers with dynamic pricing tariff, in other participation scenarios, the contribution of

this DSM programme to the reduction of peak demand decreases considerably. Moreover, the study assumes that with global smart meter rollout in AP and FP scenarios, the consumers with direct load control programmes will switch to dynamic pricing, with the direct load control only remaining available for the consumers who choose to opt-out of the dynamic pricing. In this aspect, the author agrees with [9], where this fact was discussed and concluded, that such a situation is unlikely, since direct load control programmes potentially provide more benefits to the utility because direct load control yields more predictable effects than price variations.

Another statewide energy efficiency and demand response potential study was conducted by Electric Power Research Institute (EPRI) [10] in 2009. The EPRI study states, that average peak demand increase in the USA was around 2.3% per year until 2008, but expects it to decrease to around 1.5% as a result of air conditioning saturation. EPRI expects the peak demand to increase from 826 GW in 2010 to 964 GW in 2020, which is quite consistent with FERC estimates.

Since the EPRI study considers energy efficiency programmes and demand response at the same time, the adoption of energy efficiency measures naturally influences the demand response potential as well. The energy efficiency programmes reduce the peak demand by replacing the technologies, which are active in peak demand periods, by more efficient ones. This reduces the demand response programmes potential as the more efficient technologies have lower power input and as a result less load may be controlled by demand response programmes. This effect is illustrated in table 3.4 which compares the technical potential to reduce the peak demand of the energy efficiency programmes and demand response programmes in years 2010, 2020 and 2030. Initially, demand response programmes have higher potential as the replacement of appliances or technologies in the energy efficiency programmes is assumed at the end of their life, however, the demand response programmes may (technically) be deployed faster. As more technologies are replaced by more energy efficient ones, the energy efficiency programmes potential increase while the demand response programmes potential remains the same or even decrease. Since while evaluating the demand response programmes potential, the EPRI considers the energy efficiency programmes first, and evaluates the demand response potential afterwards, the demand response programmes potential estimates turn out lower than for example in the FERC study.

	2010	2020	2030
Energy Efficiency	67	222	304
Demand Response	170	163	175

Table 3.4: EPRI study: Illustration of energy efficiency and demand response programmes interactions: technical potential of both programmes in peak demand reduction [GW].

The EPRI study considered three types of demand response programmes for three consumer classes and three scenarios:

- Demand response programmes available to the consumer classes
  - *Residential consumers*: Direct load control (air conditioning, water heating), Dynamic pricing (time-of-use, critical-peak, real-time).
  - *Commercial consumers*: Direct load control (cooling, lighting), Interruptible tariffs (interruptible demand, demand bidding, emergency programmes, ancillary services), Dynamic pricing (same as for residential consumers).
  - *Industrial consumers*: Direct load control of industrial processes, Interruptible tariffs and Dynamic pricing (both same as for commercial consumers).
- Scenarios
  - *Technical potential* (TP): All eligible consumers participate in the according demand response programme (if they are eligible for more programmes, they participate in the programme according to the following priorities: 1. Direct load control, 2. Dynamic pricing, 3. Interruptible tariffs).
  - *Maximum achievable potential* (MAP): Technical potential reduced by the potential not accessible due to the market barriers.
  - *Realistic achievable potential* (RAP): Maximum achievable potential reduced by the potential not accessible due to the regulatory or administrative barriers.

The table 3.5 gives the estimates of maximum achievable and realistic achievable peak demand reduction potentials of each consumer class/demand response programme combination by 2020. Unfortunately, the EPRI study does not

	Residential		Commercial		Industrial		Total	
	RAP	**MAP**	**RAP**	**MAP**	**RAP**	**MAP**	**RAP**	**MAP**
DLC - cooling	0.85%	0.99%	0.4%	0.45%	N/A	N/A		
DLC - water heating	0.3%	0.36%	N/A	N/A	N/A	N/A	1.86%	2.26%
DLC - lighting	N/A	N/A	0.11%	0.14%	N/A	N/A		
DLC - other	N/A	N/A	0.09%	0.14%	0.12%	0.19%		
Interruptible tariffs	N/A	N/A	0.91%	1.42%	0.41%	0.47%	1.33%	1.89%
Dynamic pricing	0.72%	1.36%	0.42%	0.79%	0.29%	0.53%	1.42%	2.69%
Total	1.87%	2.71%	1.92%	2.94%	0.82%	1.20%	4.61%	6.84%

Table 3.5: EPRI study: Peak demand reduction potentials of according to consumer class and demand response programme by 2020 [% of projected 2020 peak demand].

publish details on how these estimates were obtained (e. g. the per consumer and programme peak demand reductions as presented in the FERC study) other than that the Global Energy Partners' (GEP) LoadMAP tool was used for the analysis.

When comparing the peak demand reduction potential of consumer classes, the EPRI study predicts approximately the same potential for residential consumers and considerably lower potential for the industrial sector. Among the demand response programmes, the DLC has the highest potential in the RAP scenario, while in the MAP scenario, DP takes the lead as a result of removing the barriers for the enabling technologies penetration. Comparison with the FERC study shows, that distribution of the demand response potential among programmes strongly depends on which programme is prioritized (DP in FERC study, DLC in EPRI study). This provides the utility a possibility to choose which demand response programme to support according to its own criteria, such as how difficult it is to deploy and manage each of the programmes.

In figure 3.1, the EPRI RAP scenario is presented alongside the FERC EBAU scenario, EPRI MAP alongside the FERC AP scenario and EPRI TP alongside the FERC FP scenario. While the EPRI's and FERC's scenario definitions differ, these pairs are believed to be the closest matches. Moreover, since the EPRI study does not present technical potentials of individual consumer classes, they could not be included in figure 3.1.

Two studies, a multi-volume study published by GEP [11, 12, 13, 14] and study published by KEMA [15], dealt with DSM potential in state Missouri, USA. The KEMA study [15] presents own methodology for assessing potential of energy efficiency programmes, however, when evaluating the impact of demand response programmes on peak demand reduction, the KEMA study utilizes the FERC

model [8] with updated Missouri data. Therefore the potential peak demand reductions presented in figure 3.1 are very close to the FERC study results, with the differences resulting only from regional specifics and different initial state of demand response programmes.

When assessing the impact of demand response programmes on peak demand reduction, programmes participation rates etc., the GEP's AmerenUE study [11, 12, 13, 14] uses the LoadMAP model, similarly to the EPRI study. The potential of the following demand response programmes is investigated for each consumer class:

- *Residential consumers*: Direct load control (air conditioning, water heating), Dynamic pricing (time-of-use, critical-peak, real-time).
- *Commercial consumers*: Direct load control (air conditioning), Dynamic pricing (same as for residential consumers), Demand bidding, Demand response aggregator contracts.
- *Industrial consumers*: Interruptible tariffs, Dynamic pricing, Demand bidding, Demand response aggregator contracts.

The demand response aggregator contracts programme is similar to demand bidding, but instead of consumers directly bidding their demand reduction potential, an additional entity aggregates the bids from individual consumers and is then able to bid a larger capacity into the market. The study assumes that each consumer may only participate in one of the available programmes, and that each of the programmes reaches full participation rates in four years (2009-2013). Furthermore, the study expects, that smart meter penetration will be 15% in 2015 and will gradually increase, reaching full penetration in 2019. The study uses the same demand response programmes participation scenarios as the EPRI study and adds a Business-as-Usual scenario, which represents the state of the demand response programme in 2008.

The table 3.6 presents the peak demand reduction potentials of demand response programmes by 2020 in each scenario. Unfortunately, the results for programmes type aimed at C&I sector are presented in aggregated form, which prevents from determining the potentials of commercial and industrial consumers. As a result, only residential consumers' potential and total potential are shown in figure 3.1. Otherwise, the estimated potentials are quite close to the FERC estimates: for example, under the MAP scenario, which is closest to the FERC AP scenario, the demand response potential is estimated as 12.83% of peak demand in 2020, compared to the FERC's 14.1%. The results also confirm the largest potential of

	BAU	RAP	MAP
Residential DLC	0.85%	1.00%	0.76%
Residential DP	0.24%	5.86%	7.85%
C&I DLC	0.00%	0.26%	0.37%
C&I DP	0.27%	1.80%	2.40%
Demand bidding	0.45%	0.69%	0.65%
Interruptible tariffs	0.57%	0.43%	0.45%
DR aggregator contracts	0.00%	0.36%	0.36%
Total	2.38%	10.41%	12.83%

Table 3.6: GEP AmerenUE study: Peak demand reduction potentials of according to demand response programme by 2020 [% of projected 2020 peak demand].

DP programmes in RAP and MAP scenarios, however, this is again associated with the DP being the default tariff for smart meter equipped consumers.

The Global Energy Partners also elaborated two studies for the Midwest ISO - one concerning the Midwest ISO region [16] and one the whole Eastern interconnection [17] (excluding the Midwest ISO). An important difference from the studies presented so far is that the Midwest ISO studies only present potential achievable under current conditions (comparable for example to FERC's BAU or EBAU scenarios), i. e. it does not assume substantial increase in programmes funding, changes in legislation or smart meter roll-out.

The study for the Midwest ISO region built upon data provided by the utilities in the Midwest ISO area, such as load and peak demand historical data and 20-year forecasts, smart meter roll out schedule and data on current demand response and energy efficiency programmes (participation rates, energy and peak demand savings etc.). The peak demand forecast for the Midwest ISO region was created by aggregating forecasts from individual utilities and estimating the missing data. Without demand response and energy efficiency programmes, the study expects the peak demand to increase at a rate 0.8% per year between years 2009 and 2020.

The Eastern interconnection study utilized external data to obtain estimates of participation rates, peak demand reductions or peak demand forecasts, with the EBAU scenario of the FERC study being the primary information source. As a result, the expected peak demand increase rate is 1.7% per year, identical to the FERC study estimate.

The studies modelled three types of demand response programmes: direct load control and dynamic pricing for both, residential and C&I consumers

	Participation rate	Per consumer impact [kW]
DLC - residential	15%	1
DP - residential	20%	2
DLC - C&I	2.5%	3.2
DP - C&I	10%	30
Interruptible tariffs	0.13%	1056

Table 3.7: GEP Midwest ISO study: Participation rates and per consumer demand reductions [kW] of demand response programmes.

and Interruptible tariffs for C&I consumers. The Eastern interconnection study additionally modelled "Other demand response programmes" class, which includes, similarly to the FERC study, programmes available to medium and large consumers, such as demand bidding, aggregator contracts etc. Only consumers with central air conditioning or hot water heating were considered eligible for direct load control or dynamic pricing programmes; if the consumer already participates in the direct load control programme, such a consumer is not eligible for dynamic pricing programme. The table 3.7 shows the participation rates and per consumers peak demand reductions as estimated in the Midwest ISO region study. The Eastern interconnection study does not provide such information, however, the study states that FERC estimates were used, therefore the participation rates and peak demand impacts should be similar to those presented for the FERC study.

The table 3.8 shows the peak demand reduction estimates determined in both studies. Similarly to the AmerenUE study, the C&I programmes results are presented in aggregated form, hence only residential consumers' potential and total potential are shown in figure 3.1. The Midwest ISO region and Eastern interconnection results are comparable, the slightly higher residential potentials in the Midwest ISO region may be attributed to high central air conditioning penetration (around 65%). Since both studies used participation rates equivalent to the EBAU scenario, the C&I sector has higher potential, mainly formed by interruptible tariffs. The residential sector potential is lower than in the other studies due to low penetration of enabling technologies.

The last study presented in the figure 3.1 is the American Council For an Energy-Efficient Economy (ACEEE) study that dealt with energy efficiency, demand response and on-site renewable energy sources in Texas. The potential of these measures was evaluated as a reaction to increasing peak demand, associated for

	Midwest ISO	Eastern interconnection
DLC - residential	2.32%	2.08%
DP - residential	1.72%	1.46%
DLC - C&I	0.16%	0.10%
DP - C&I	0.39%	0.34%
Interruptible tariffs	2.99%	3.00%
Other DR	N/A	3.24%
Total	7.58%	10.22%

Table 3.8: GEP Midwest ISO and Eastern interconnection studies: Peak demand reduction potentials of according to demand response programme by 2020 [% of projected 2020 peak demand].

example with population increase. The study states, that the peak demand in Texas was growing at a rate 2.5% per year from 1990 to 2006 and that Electric Reliability Council of Texas (ERCOT) expected 2.3% per year increase in years 2007-2012. Own estimates presented in the study predict, that this rate will remain almost unchanged until 2023 with the peak demand increase proceeding at rate of 2.26% per year.

The study assessed peak demand reduction potential of rather limited selection of demand response programmes:

- direct load control of air conditioning for residential consumers,
- energy management systems capable of reducing 5% of peak demand in 2008 and 20% of peak demand in 2023 for commercial and small industrial consumers,
- demand reduction bids into Responsive Reserve market.

It was assumed, that beginning from 2008, all new houses equipped with air conditioning will be required to install smart thermostat facilitating the DLC programme participation. Moreover, it was expected, that at the end of the service life of air conditioning in existing households, the replacement air conditioning system will be equipped with the smart thermostat as well. Each DLC controlled air conditioner was expected to provide 1 kW of peak demand reduction potential.

A requirement for installation of energy management systems into each new non-residential facility was also anticipated to be put into practice as of 2008.

The average peak demand reduction per commercial building was expected to rise from 5 kW in 2008 to 12 kW in 2020.

In the industrial sector the study assumed removing of all barriers that would prevent industrial consumers participation in Responsive Reserve market.

According to the study, these three measures could allow for reducing the peak demand by 9.8% in 2020, with 4.3% contribution of the residential sector, 4.4% contribution of the commercial sector and small industries and 1.1% contribution of the large industries.

3.2.2 European studies

The study [18] gives a basic outlook into the future of DSM in Europe. According to the study, the EU energy consumption increased at rate 1.5% per year in years 2001-2006 and the peak demand at rate 2% per year in the same period. Until 2020, the energy consumption increase is expected to continue at 1.5% rate and the peak demand at 1.8% rate.

Based on experience from DSM research projects, the study concludes, that the automated DSM systems are capable of shaving up to 50% of peak household demand and 10-15% of energy consumption. Moreover, it has been reported, that customer satisfaction with DSM projects has been high, with 85-99% of customers being positive towards them.

The DSM potential was estimated for two scenarios: in a *moderate* scenario, it is expected, that the DSM programmes implementation will continue at the current rate, reaching only partial penetration of smart meters in 2020 as well as partial adoption of energy conservation policies and use of energy efficient equipment. Under this scenario, the model assumes 100% smart meter penetration in several EU-15 countries by 2020 (France, Ireland, Italy, Netherlands, Sweden) and 30-90% penetration in other countries. In *dynamic* scenario, optimal DSM programmes implementation is assumed with smart meter penetration reaching 100%, relevant energy policies being put into practice and equipment being replaced by energy efficient counterparts. Under the Moderate scenario, the study expects that DSM will help reducing the annual energy consumption in the EU-15 by 59 TWh and the peak demand by 28 GW. In the Dynamic scenario, the energy savings reach 202 TWh and peak demand savings reach 72 GW. The study also states that significant investments into new generation facilities and associated network infrastructure could be avoided by implementing DSM programmes.

	Daily consumption [GWh]	Percentage of the daily consumption of Germany	Aggregated power input [MW]	Achievable contemporal activation time estimate [h]	Load shifting capacity (aggregated) [MWh]
Chloralkali electrolysis	40	2.64	660	2	1 320
Aluminium electrolysis	26	1.75	277	N/A	N/A
Cement mills	6	0.40	314	9.6	3 014
Wood pulp production	6	0.40	312	1.5	468
Electric arc furnaces	20	1.30	1 097	N/A	N/A

(a) : Industrial processes

	Daily consumption [GWh]	Percentage of the daily consumption of Germany	Power input per unit [kW]	Aggregated power input [MW]	Achievable contemporal activation time estimate [h]	Load shifting capacity (aggregated) [MWh]
Electric water heaters	19	1.25	1.4	5 700	7.8	44 400
Electrical heating	102	6.73	14	34 900	5.3	185 000
Fridges, freezers	52	3.43	0.3	10 600	2.7	29 000
Washing machines	41	2.71	0.73	20 800	2	41 600
Heat pumps	67	4.41	0.03	2 200	N/A	N/A

(b) : Household appliances

Table 3.9: DSM potential in Germany.

The paper [7] analysed the DSM potential in Germany. The study examined long term economic benefits of the DSM using the Dispatch and Investment Model For Electricity Markets in Europe (DIME). In particular, the DSM was assessed as a prospective measure to deal with increased demand for regulating power resulting from planned extension of wind power plants in Germany. Several industrial processes with aggregate yearly consumption of 33.7 TWh and household appliances with 79 TWh per year were identified as suitable for DSM and modelled in DIME. These processes and appliances are listed in table 3.9.

The achievable contemporal activation time estimate and shifting capacity express the following: If all the appliances/processes of the specified type are blocked for sufficiently long time period, and then all are activated at the same time, the contemporal activation time estimate is a time for how long the appliances/processes will (contemporally) draw the maximal power input until they reach their full capacity (e. g. the water in electric water heaters is heated up to the maximum temperature). The load shifting capacity is then the energy

consumption that was avoided while the appliances/processes were blocked or the energy that was consumed during their activation. Note that the paper [7] does not give the achievable contemporal activation time estimates but in order to facilitate the comparison with estimates of the potential in the Czech Republic (see Section 3.3.2.1), they were computed by dividing the shifting capacity by the power input. As a result the contemporal activation time estimates are not available for processes without storage capacity. The amount of time by which the consumption of the appliances or processes may be shifted depends on the appliance type and other conditions - for example, the activation of washing machines may be shifted by a long time period, whereas activation of fridges and freezers may be withheld for only as long, as the temperature does not exceed a point, when a fast degradation of stored food would occur.

Also, to allow for easier comparison with the potential estimates for the Czech Republic, the yearly consumptions of the processes and appliances were converted to daily consumptions with an assumption, that the daily consumption is equal over the whole year. Such an assumption is reasonable for industrial processes as well as for electric water heaters, fridges, freezers and washing machines, consumption of which is not highly dependent on season. When converting the consumption of heating appliances (electrical heating, heat pumps) it was assumed that such appliances are used on average 225 days a year among which the consumption is equally distributed. The consumption data presented in the study [7] represent the real consumption in Germany in 2005. The total consumption in Germany in 2005 amounted in 554 TWh, i. .e. 1.52 TWh per day on average, which was the base for computation of the daily consumption contribution of the selected industrial processes and household appliances.

The table 3.9 shows that the aggregated consumption, power input and shifting capacity of household appliances exceeds that of industrial processes. However, only limited amount of the DSM potential in household appliances was actually proposed to be utilized by the DIME until 2020 due to high investment costs and other technical barriers. On the other hand, the optimization results indicated that due to the low investment costs, the whole DSM potential of energy intensive industries could be quickly exploited. The simulation results indicated prospective savings reaching €481 million in years 2007-2020, which were mostly achieved by reduction in investment costs into peaking gas turbines.

In [19] the author points out that due to the dimensioning of the UK electricity system for supplying the peak load, most of the time the power system operates inefficiently with generation capacity on average utilised below 55% and transmission capacity below 50%. The article suggests that the DSM could be used

to help dealing with large but infrequent generation shortages for which it is inefficient to permanently keep reserves at conventional generators. Moreover, the DSM is also envisaged as a measure to shave the peak load and transmissions and thus preventing investments into the network infrastructure. Finally, similarly to [7], the DSM is seen as an alternative source of power reserves that will be increasingly required to compensate the increasing penetration of RES, particularly wind power. However, the presented study reveals, that the DSM might be economically competitive with traditional power reserves providers only in case of significant amounts of intermittent energy sources and inflexible conventional generation at the same time.

The article [20] estimates the DSM potential in Russia in connection with peak demand and energy consumption growth, which is expected in the next decade. Same as in [7], the DSM is considered a complement, not an alternative to increase of conventional generation. The study identified controllable loads such as electric vehicles, resistance heating plants or household, industrial and agricultural consumers with aggregate power input more than 100 GW, however the article does not present the load shifting capacities. Optimization software was used to determine the optimal investments in power generation, storage, DSM and other power system components in order to deal with increasing consumption. The optimization software however proposed to utilize only 11 GW of the total DSM capacity, majority of which was formed by industrial consumers accompanied by electric vehicles and resistance heating plants. None of the potential of household consumers was proposed to be exploited by 2030 similarly to [7] due to the high investment and operating costs.

3.3 The demand side management in the Czech Republic

The DSM state and potential in the Czech Republic will be analysed separately for the two groups of the potential DSM services providers described in Section 3.1 - the industrial and the household and commercial consumers.

3.3.1 Industrial consumers

Currently, the main possibility for the industrial consumers to sell their DSM potential is to provide the Load Change ancillary service to the Czech TSO

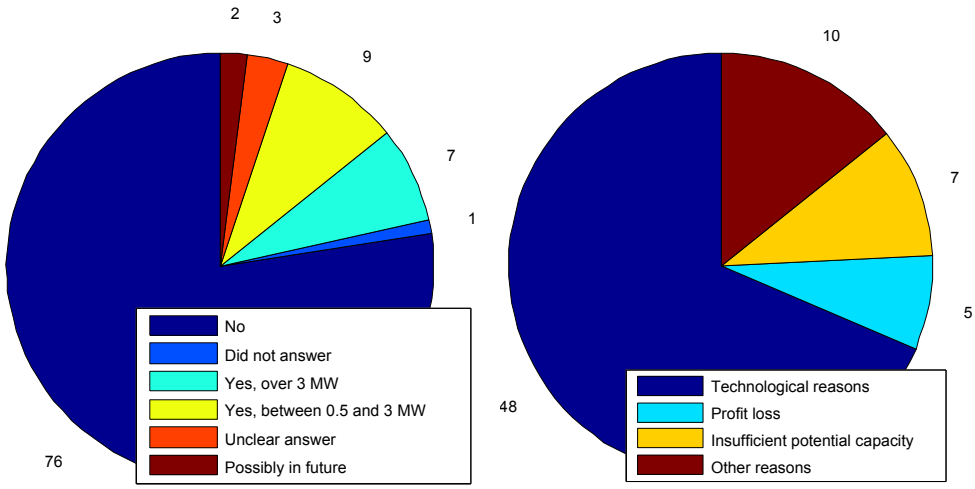

(a) : Responses to question: Are you capable of providing the Load Change ancillary service?

(b) : Responses to question: What is the reason of declination to provide the Load Change ancillary service?

Figure 3.2: Results of survey [23] carried out by ORGREZ, a. s.

ČEPS, a. s. The grid code [21] specifies the following requirements for providers of the Load Change ancillary service:

- the service must be activated within 30 minutes from the activation request,
- the provider must be capable of delivering the service for at least 120 minutes,
- the minimum capacity per one provider is 10 MW.

According to [22], in 2008 the Load Change ancillary service was provided by three industrial consumers operating in paper, mining and cement industry. The ancillary services provided by these consumers formed 1.36% of the total ancillary services available to the Czech TSO in 2008.

In 2005 the company ORGREZ, a. s., analysed whether there is an additional potential to provide the Load Change ancillary service among the large industrial consumers in the Czech Republic. The survey [23] attempted to identify the technological possibilities to provide Load Change ancillary service and to find an optimal minimum capacity per one provider. The survey addressed 96 industries with annual consumption greater than 40 GWh and with potential capacity at least 3 MW.

The figure 3.2 summarizes the responses of the surveyed industries. The figure 3.2a presents responses to question "Are you capable of providing the Load Change ancillary service?" and the figure 3.2b responses to question "What is the reason of declination to provide the Load Change ancillary service?" Out of 96 respondents, only 16 claimed to be capable of providing the Load Change ancillary service, 9 of which indicated, that they would only be capable of providing a capacity of 0.5-3 MW. The technological structure of the underlying energy intensive industrial process was identified as main reason for inability to provide the Load Change ancillary service. Other frequently quoted reasons included insufficient potential capacity and excessive profit loss.

The largest load change capabilities were found in cement and mining industries. In total 7 industrial consumers claimed to be capable of providing more than 3 MW of their DSM potential out of which 3 were able to meet the current requirement of 10 MW minimal capacity. The total capacity of these 3 consumers was 32 MW while the remaining four were capable of providing 13 MW of the DSM services. If all of the capacity was contracted, the TSO could achieve demand reduction of 45 MW for 2 hours, i. e. could avoid consumption of 90 MWh of energy. However, the study concluded that due to the relatively small capacity addition of the smaller potential providers and increased complexity of controlling the Load Change ancillary service with more providers, the minimal capacity of 10 MW should remain unchanged.

3.3.2 Residential and commercial consumers

To date, the DSM potential of residential and commercial consumers in the Czech Republic is utilized to a very low degree. To give an insight into what DSM potential the residential and commercial consumers hold, the Section 3.3.2.1 presents estimates of the DSM potential of selected household appliances and commercial buildings technologies and the Section 3.3.2.2 gives an overview of prospective ways to access the potential.

3.3.2.1 Estimates of the residential and commercial consumers' demand side management potential

The study [7] stated that around 50% of household energy is consumed by only few types of household appliances - electric water heaters, electrical heating, fridges and freezers, washing machines (including dish washers and tumble dryers) and heat pumps. It may be expected that the household consumption

	Unit count [thousand units]	Daily consumption per unit [kWh]	Aggregated daily consumption [GWh]	Percentage of the daily consumption of the Czech Republic	Power input per unit [kW]	Aggregated power input [MW]	Achievable contemporal activation time estimate [h]	Load shifting capacity (per activation, aggregated) [MWh]
Electric water heaters	1 245	6.24	7.77	4.79	2	2 491	2	4 982
Electrical heating	166	74	12.3	7.58	10	1 657	2	3 315
Fridges, freezers	3 828	1	3.83	2.36	0.10	383	2	766
Air conditioning	77	8	0.61	0.38	1	76	0.33	24
Washing machines	3 675	0.55	2.01	1.24	2	4 027	0.33	1 329

Table 3.10: Estimated technical potential of selected household appliances in the Czech Republic

distribution in the Czech Republic is similar, hence the aforementioned appliances were selected for the DSM potential analysis with an exception of heat pumps which were excluded due to the low penetration in the Czech Republic, low power input and no load shifting capabilities. Air conditioners, although they are not nearly as widespread in the Czech Republic as was shown in the USA studies, were included in the list of appliances with DSM potential because of their convenient characteristics for DSM - comparatively high power input and load shifting potential. Also, the air conditioning oriented DSM programmes could benefit from experience gained in the USA upon their launch.

Table 3.10 presents estimates of DSM potential of the selected household appliances in the Czech Republic. The information on household appliances is based on data collected in census performed in 2001 by the Czech Statistical Office [24] and penetration of refrigeration and washing equipment was updated based on the REMODECE project report [25]. Since the Czech Statistical Office does not record the number of households equipped with air conditioners, the penetration level was estimated from the penetration in the European Union (EU) in 2005 [26], by assuming that the penetration in the Czech Republic is 50% of the EU average. The meaning of the table entries is the same as was described for the table 3.9 presented for study [7]. The base for computation of percentage of daily energy consumption of the Czech Republic was 162.34 GWh, which was computed from annual consumption of the Czech Republic in 2010, which reached 59.25 TWh as stated in [27].

For individual appliances, the following assumptions were used:

- electric water heaters - used in 33% of households (based on [24]), volume 120 litres, cold water temperature 15°C, hot water temperature 60°C, power input 2 kW, the whole capacity is consumed over the day, the achievable contemporal activation time estimate assumes that around 60% of the water boiler capacity needs to be recovered,
- electrical heating - used in 4.3% of households (based on [24]), annual heat energy consumption 60 GJ (16.7 MWh, average heat energy consumption according to [28]) per household, heating used 225 days in year, yearly consumption is assumed equally distributed over these 225 days, power input 10 kW,
- fridges and freezers - used in 100% of households (based on [24] and [25]), combined fridge and freezer (used in majority of households according to [25]), energy consumption 1 kWh/day (a slightly lower value than presented in [25], accounting for efficiency increase of new appliances), power input 100 W, cooling/idle cycle length 2 hours,
- air conditioning - used in 2% of households (explained above), in operation for 8 hours a day, power input 1 kW (a typical power input of one split air conditioning unit for room space up to 90 m^3), cooling/idle cycle length 20 minutes,
- washing machines - used in 96% of households (based on [24] and [25]), energy consumption 1 kWh per washing cycle, 200 washing cycles per year (i. e. around 55% of washing machines are available for control each day, hence the aggregated power input is lower than the product of number of appliances and per unit power input), power input during water heating 2 kW, heating for 20 minutes after the washing start.

It should be noted that the DSM potential of some appliances varies significantly throughout the day (i. e. air conditioning is seldom used during the night, the potential of electric water heaters depends on water consumption etc.) and also throughout the year (especially the potential of air conditioning and electrical heating). Based on the appliance, the presented load shifting potential may be either accessed several times a day (especially fridges and freezers or air conditioners), once a day (typical for washing machines) or may be distributed throughout the day as needed (mainly electric water heaters, which have high storage capacity).

	Unit count	Floor space per unit [m^2]	Aggregated daily consumption [GWh]	Percentage of the daily consumption of the Czech Republic	Power input per unit [kW]	Aggregated power input [MW]	Achievable contemporal activation time estimate [h]	Load shifting capacity (per activation, aggregated) [MWh]
Refrigeration (large stores)	250	4 600	0.88	0.54	276	69	2	138
Refrigeration (medium stores)	600	1 300	0.51	0.32	78	47	2	94
Air conditioning (business centres)	100	16 600	0.24	0.15	239	24	0.33	8

Table 3.11: Estimated technical potential of selected commercial buildings technologies in the Czech Republic.

The table 3.11 presents two commercial building technologies that are likely to have significant DSM potential - refrigeration in large and medium size warehouses and air conditioning systems in business centers. Both of these technologies form a significant portion of energy consumption of the respective commercial buildings (for example refrigeration in warehouses may present up to 50% of its energy consumption) and have load shifting capabilities.

The information presented in table 3.11 is based on environmental impact assessments (EIA) of several warehouses and commercial centres publicly available in the Czech EIA Information System [29]. In each case, at least 10 EIAs for the particular type of commercial building were examined and average floor size and overall power input and daily energy consumption were computed. Then, the daily consumption of the particular technology (refrigeration, air conditioning) was computed based on the typical distribution of energy consumption for this type of commercial building, which was presented in the AmerenUE study [11, 12, 13, 14]. Several EIAs also presented information about what portion of the power input forms the particular technology. Based on this information, an average power input of the particular technology per square meter was computed and used to produce estimates presented in table 3.11. The information on number of stores and business centres were based on [30, 31].

Although the aggregated consumption, power input and shifting capacity is lower than that of household appliances, the main advantage lies in a greater per unit potential and as a result lower investment costs, which should facilitate exploiting the commercial buildings DSM potential.

If all the potential of household and commercial consumers was made available to the TSO as an ancillary service, the estimated power of 8774 MW and energy of 10656 MWh would be available to control. Moreover, this potential could be deployed in a very short time, with the delays resulting only from time required to deliver the control signals to the consumers. That would allow to provide a comparable reaction time to the Quick-start reserve used by the Czech TSO, which according to the definition in [21] has to be deployed within 10 or 15 minutes. The article [32] states, that the Czech TSO typically has around 600 MW of the Quick-start reserve available, hence the estimated DSM potential of household and commercial consumers is more than 10 times higher. However, the DSM potential could not be offered as the Quick-start reserve mainly due to the requirement, that the provider of the Quick-start reserve has to ensure, that the reserve deployment is sustainable for at least 4 hours for the 10-minute Quick-start reserve and 24 hours for the 15-minute Quick-start reserve. Hence, either a new category for the DSM services would have to be created, or a sophisticated control of the DSM providers load would have to ensure gradual deployment of the DSM capacity, so that the 4-hour sustainability requirement of the Quick-start reserve could be met, albeit with lower offered MW capacity.

3.3.2.2 Technologies for accessing the residential and commercial consumers' demand side management potential

Except for programmes oriented strictly on changing the energy-related behaviour of the end consumers, the access to household DSM potential is always connected with enabling technology such as smart meters. In the Czech Republic several smart-grids or automatic metering demonstration projects have started. For instance, in the FUTUREMOTION project [33], led by the largest Czech electricity producer ČEZ, a. s., more than 30000 households were equipped with automatic meters. In global view, however, the penetration of smart meters in the Czech Republic is currently negligible. Another possibility to access the DSM potential in Czech households is using the Centralised Ripple Control (CRC) system. The article [34] dealt with topic of the CRC in the Czech Republic and barriers disallowing its use for effective DSM of households. The basic principle of CRC lies in broadcasting audio frequency signals, superimposed on base waveform with frequency around 200 Hz, from switching stations in distribution networks. The signals are received by receivers installed in households and used to control mainly heating appliances such as electric water heaters or electrical heating. The DSO may switch these appliances off for a specified amount of time in exchange for lower energy costs for the customers.

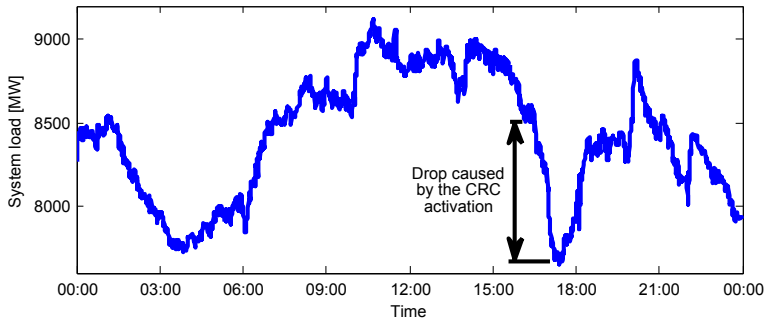

Figure 3.3: Illustration of CRC capabilities: load drop caused by the CRC activation.

The article [34] estimates the total CRC controlled load to 10-15% of the total load connected in the distribution system in the Czech Republic which translates into around 1350 MW of accessible load. This is illustrated in figure 3.3 which, according to study [35], shows a load drop in the Czech transmission system that occurred after a significant part of the CRC controlled load was instructed to disconnect.

One of the main problems that limits the applicability of CRC for the DSM that was mentioned in [34] is that after legal unbundling in 2005, the distribution companies may no longer operate the CRC in real-time. This situation is caused by the fact that in order for the energy dealers to have equal possibilities, the load curve, for which they buy electricity, should not be altered by a third party. If the load was changed using the CRC and as a consequence, the load would deviate from the expected load curve, such a deviation would incur penalties for the energy dealer for causing an energy disbalance. Some of the DSM capabilities may be recovered by optimising the load curve as proposed in [36] but in order to exploit the full DSM potential of CRC, a legislative change is needed.

Another problem lies in fact that, unlike when using the automatic meters for the DSM, the CRC system provides no direct feedback and its effects may only be observed by measuring load at various measuring points within the distribution system. Moreover, the load caused by the CRC controlled devices is not constant, but changes in time as individual thermal storage devices reach its full capacity and shut down irrespective of the CRC signal. This issue might be partially overcome by estimating the current load caused by groups of CRC controlled devices as described in [35] and [36].

As was mentioned earlier, the larger per unit DSM capacity of commercial buildings should allow for quick exploitation of their DSM potential, since

the investment costs are comparatively low. Moreover, the warehouses and commercial centres usually already have sophisticated control systems which - in case it is economically beneficial - could be updated to support the DSM functions without the need to install additional hardware.

Chapter 4

Literature survey

The Section 3 gave an overview of the DSM potential of different types of consumers and different DSM programmes. The presented studies, such as [8, 11, 12, 13, 14, 15, 10], concluded that out of industrial, commercial and residential consumers, it is the households that have the highest potential. However, traditionally only industrial or large commercial consumers were provided with possibilities to offer their load shifting or load shedding capabilities mostly in a form of interruptible tariffs or time-of-use tariffs. Since with the household-oriented DSM programmes the per consumer DSM potential is low, the low penetration of technologies allowing to control the load and their installation costs are the most important of the barriers identified in [19] which prevent fast implementation of these programmes.

Despite these barriers, the residential consumers were selected as a target users of the proposed system. The main reason is that in order to counteract problems associated with RES integration in distribution networks, it is important to introduce means to control the load at the place where the problems are originated. In order to minimize the investment costs and facilitate overcoming other barriers that may prevent the system from being put into practice, the following principles were followed while designing the LV DSM system:

- focus on controlling load already existing in the households,
- design the system so that it can be rolled-out with minimal investment costs aside from the smart-meter installation,
- design the system so that it requires minimal possible end-user interaction.

In order to adhere to the above principles, two important steps needed to be accomplished at the very beginning of the DSM system design: select an appropriate method of load control (real-time price (RTP) signals, direct load control (DLC), or another method) and select the household appliance or appliances to be controlled.

To accomplish the first step, a survey of existing household-oriented DSM concepts was carried out. A recent survey of DSM concepts was presented in [37]. Many of such concepts published to date [38, 39, 40] were based on RTP signals supplied by the utility (TSO, DSO or real-time energy markets). The consumers participating in RTP programmes adjust their consumption based on actual and predicted energy price either manually or with help of energy management systems (EMS). The possible issues include how to ensure effectiveness of manual control (i. e. how to motivate the consumers to perform manual load adjustments) or how to design an effective in-house EMS at minimum costs. Moreover, the users are required to actively interact with the system even when EMS is installed in order to set their appliances utilization preferences. These aspects were discussed in a pilot project carried out in Norway [39]. The paper [41] also indicated that without further coordination of participating consumers, the RTP systems may succeed in their primary goal (e. g. in shifting the load from typical peak to typical non-peak periods), however, due to the load synchronization by the price signals, aspects such as peak to average load ratio may remain unimproved.

Since the price signals usually reflect lack or surplus of energy in the transmission system, the RTP based systems cannot be used to compensate local problems caused by the RES production unless the RES are installed in households equipped with EMS which schedules the load considering the RES production [40].

The DSM systems may also be designed to react on information universally available in the grid, such as grid frequency [42, 43, 44] or voltage [45]. The key advantage of such approach is that the household installations may be completely autonomous, i. e. no communication with utility is required, yet they act in a synchronized manner. However, the lack of communication does not allow to coordinate the load dispatch of multiple households on a longer term horizon, since generally only instantaneous value of the controlled variable is available.

Finally, the DSM systems may be designed to participate in load-frequency or voltage control based on control signals obtained from TSO or DSO, i. e. to perform similar functions as ancillary services. Since provision of such services

is usually subject to strict regulations, the DSM system is required to have reliable and predictable response. As concluded in [46], such qualities may be achieved by using DLC based DSM systems which directly control specific group of appliances, usually employ detailed modelling of the controlled appliances and coordinate the load dispatch using a centralized controller. An interesting example of such system may be found in [47, 48, 49, 50]. First, a state model of thermostatically controlled appliances (TCA) was developed in [47, 48] in order to evaluate effects, such as load synchronization when controlling large number of TCAs. Second, DLC systems controlling thermostat settings of EWHs [49] and cycling of heating, ventilation and air conditioning (HVAC) systems [50] were developed in order to verify their possible application to perform load-frequency control based on area control error (ACE) signals and to participate in US load following service [51].

Based on the survey, the direct load control (DLC) was selected as a means to control the selected household appliances, since it ensures fast and predictable response to the control signals. With proper control signals, this should allow the system to be used for a broad range of purposes, even for demanding ones, such as provision of ancillary services.

The second step, i. e. the selection of an appliance to be controlled, was based on analysis which was presented in Section 3.3.2.1. The EWHs were selected as an initial appliance to be used in the proposed DSM system since they have several convenient characteristics:

- according to the table 3.10, the EWHs have the highest load shifting capacity and aggregate achievable power input,
- they are much more widespread than for example electrical heating, therefore controlling EWHs would allow the system to be used in wide range of localities,
- EWHs are usually connected directly to the main distribution board of the household, which allows to install the household part of the DSM system conveniently on the distribution board rack,
- the household part of the system may be formed by a majority of smart meters without any modifications, since the traditional EWHs may be controlled by a circuit breaker installed in the circuit on which the EWH is connected,

- in the Czech Republic, control of EWHs using a circuit breaker is actually already used in the CRC system (see Section 3.3.2.2), therefore the consumers are familiar with the concept. It should be therefore seamless to exchange the CRC control with the direct load control performed by the proposed DSM system.

Finally, the survey also attempted to find DSM concepts that use multiple control layers similarly to the concept proposed in this thesis with a particular focus on practical requirements of the given system with regards to instrumentation and communications infrastructure. The article [52] describes a two-phase hierarchical EWH dispatch algorithm which applies a multi-period AC-OPF to allow the load to participate in load-frequency and voltage control in a MV network. Effects of application of two-level DSM system controlling several household appliances on peak demand reductions and voltage quality at various voltage levels of the distribution system were studied in [53]. A hierarchical system aggregating controllable load into virtual power plants in order to enable them to participate in spinning reserve market is proposed in [54]. A common factor of the referenced concepts is that they either assume presence of advanced in house energy management system required to support the DSM system operation or assume presence of high-bandwidth communication links required to spread out control signals at various levels of the distribution networks.

Chapter 5

Low-voltage demand side management system

This chapter describes the proposed LV DSM system which is a key part of the three-level control system presented in Chapter 1 as it is the level at which the actual control of the controlled load is being performed. Main ideas of the LV DSM system concept were presented in the author's article [55] that was published in IEEE Transactions on Sustainable Energy. The chapter is organised as follows: the Section 5.1 outlines the basic principles of the LV DSM system functionality, Section 5.2 specifies the formulation of optimization problems solved as a part of the control process, Section 5.3 describes implementation of individual functions of the LV DSM system, Section 5.4 presents pilot installation realised within the SIRES project along with the network used for simulations in the case study, Section 5.5 describes the model of the LV pilot installation network that was used to perform simulations of the LV DSM system operation, Section 5.6 outlines the process of LV DSM system operation simulation and the Section 5.7 presents results of the case study which illustrates how the LV DSM system influences operation of the LV network under study.

5.1 Basic principles

The principles of the LV DSM system are illustrated in Fig. 5.1 and 5.2. The Fig. 5.1 isolates the LV level from the Fig. 1.1 to illustrate that without additional control levels, each of the LV DSM system operates autonomously with no communication with other LV DSM systems or any other subjects.

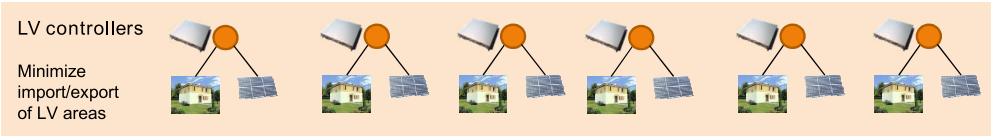

Figure 5.1: LV level of the proposed DSM concept.

The Fig. 5.2 then presents the LV DSM system operation in a more detailed way. It reveals that in order to accomplish the task of minimizing export and import of energy of the LV area (i. e. to minimize the energy exchange with the MV network that the LV area is connected to), the power balance of the LV area which is at any time instant defined as

$$\begin{aligned} \text{power balance} = \text{uncontrolled load} + \text{controlled load} \\ - \text{uncontrolled generation} \end{aligned} \tag{5.1}$$

must be kept close to zero as possible. This can be only achieved if the total load of the LV area, which consists of the controlled load (i. e. power input of the controlled EWHs) and uncontrolled load (i. e. power required by any other appliances in the households), matches the power generated by PV sources in the LV area in the best possible way. How the individual elements of equation 5.1 form the resulting power balance of the area and also how the control of EWHs may help to reach the given objective is also illustrated in Fig. 5.3. The sign convention used in figures throughout this thesis is that load always has a positive sign whereas generation has a negative sign. Positive power balance of the area therefore means that the area is importing energy and negative power balance signifies power export.

The possibility to control the power input of the EWHs is limited by

- **Aggregate power input of all controlled EwHs** which limits the maximal achievable controlled load at any instant,
- **Energy storage capacity of the EWHs** which follows from the fact that the EWHs may store only as much energy as the total energy that needs to be delivered by the heating element to heat the water in the EWH to the maximal temperature,
- **Consumption of hot water by the households** since if the water in the EWH is at the maximal temperature, the heating cannot be resumed or conversely, if the hot water is depleted, the heating must be started irrespective of the power balance of the area.

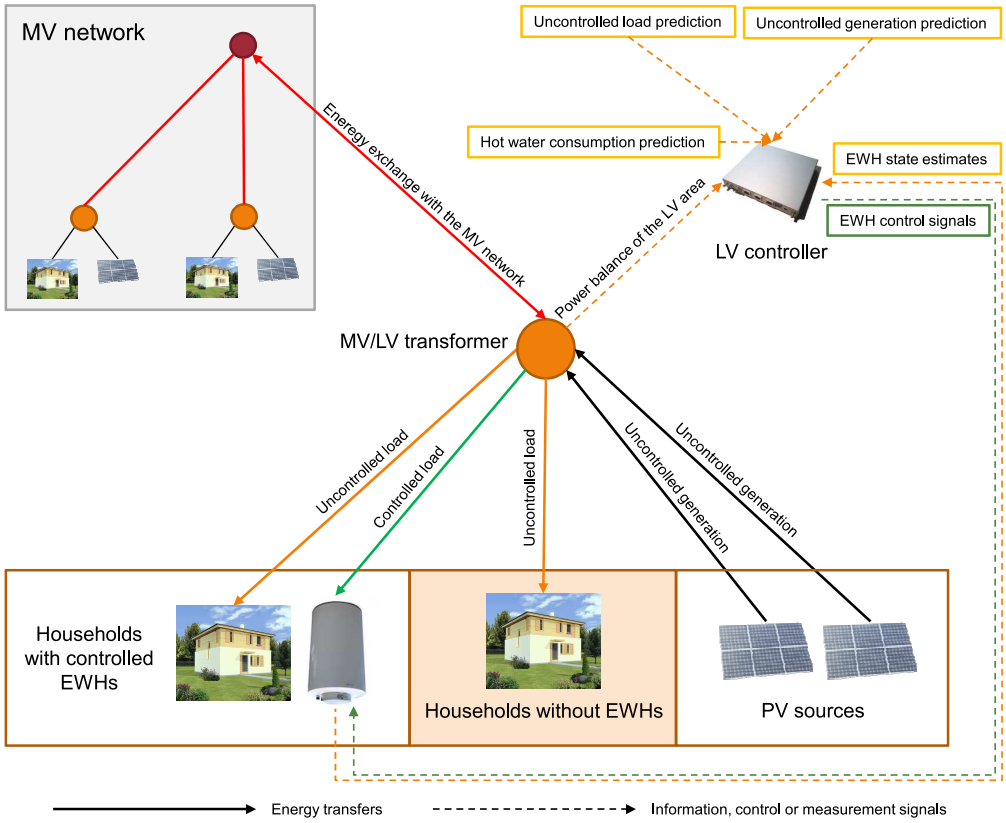

Figure 5.2: Details of the LV DSM system operation.

As a result, the control system must carefully plan how the EWH load should distributed in time in order to achieve the aforementioned objective. Such an optimization is done in two stages:

1. **Dispatch reference optimization**, which computes the best possible power balance of the LV area in each time instant (dispatch reference) in terms of the given control objective that is achievable on a longer time horizon (e. g. 48 hours) based on
   - uncontrolled load prediction,
   - uncontrolled generation prediction,
   - current energy stored in the EWHs,
   - expected hot water consumption of the households with controlled EWHs.

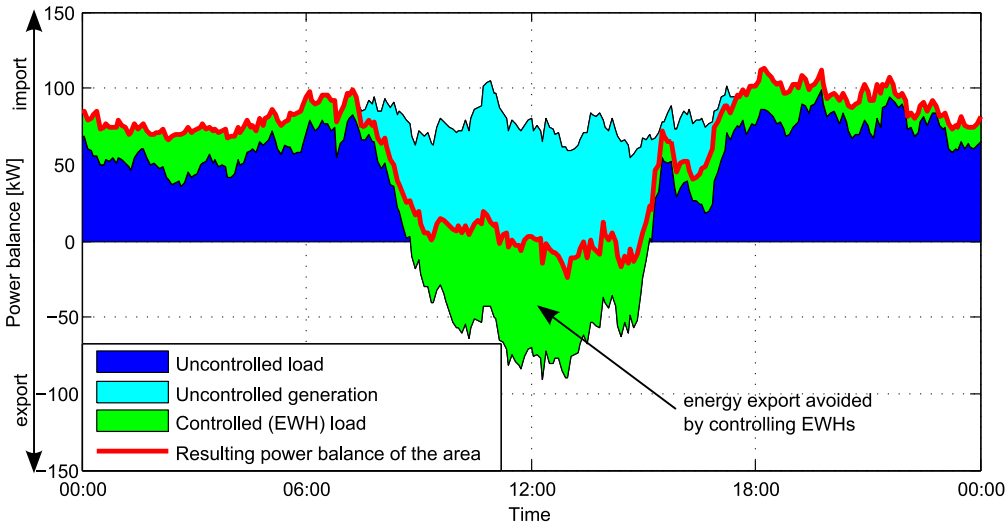

Figure 5.3: Illustration of how the individual elements form the resulting power balance of the LV area.

2. **Dispatch schedules optimization** which optimizes operation of each EWH (its dispatch schedule) on a shorter time horizon (e. g. 6 hours) with the objective that the resulting power balance of the area matches the dispatch reference computed in the first phase as closely as possible. The inputs of the dispatch schedule optimization are
   - short-term uncontrolled load prediction,
   - short-term uncontrolled generation prediction,
   - current energy stored in the EWHs,
   - expected hot water consumption of the households with controlled EWHs,
   - current measured or computed power balance of the area.

To better understand the reasons for dividing the optimization into the two stages, the sequence of the individual actions of the LV controller will be outlined. The process consists of the following steps, which are also graphically represented in Fig. 5.4:

1. *Generation of power balance prediction:* Prediction of the power balance of the controlled area (i. e. the difference between the predicted energy

production and the predicted load in the area) for a selected horizon (e. g. 48 hours) is computed.

2. *Dispatch reference optimization:* Based on the current EWHs state estimates and the aforementioned power balance prediction, the dispatch reference (i. e. the power balance with optimal distribution of EWHs load according to the selected criterion) is computed and passed on to the dispatch optimization module.

3. *Dispatch schedules optimization:* With a specified frequency (e. g. 5 minutes) the following steps are performed, similarly to the receding horizon optimization principle, until new relevant information for the power balance prediction are available:

   i) The power balance prediction is updated with measured or estimated instantaneous power balance.

   ii) The optimal dispatch schedules of each EWH (i. e. switching schedules of the controlled EWHs, such that the difference from the dispatch reference is minimized) for a shorter time interval (e. g. 6 hours) are computed and sent to the household units.

   iii) First action in the EWH dispatch schedules is executed in each household unit. The rest of the dispatch schedule is kept in a household unit and used only in case of the failure of communication with the LV controller.

4. *Power balance prediction update:* If new information used for the power balance prediction is available (e. g. a new weather forecast) the process is repeated from the step 1. Typically, this would happen several times a day.

The main reasons to perform the optimization in two stages are:

- **Computation complexity**. Due to the limited capacity of the EWHs to store energy, the DSM system needs to optimize the power balance on a sufficiently long horizon (at least 1 day) in order to be able to optimally distribute the EWH load. However, the optimization also needs to be performed with sufficiently short time-sampling of the optimization horizon in order to capture the short-term variations of generation, load and hot water consumption. Moreover, to correctly model the binary nature of the EWH operation (the EWH may only be on or off), MILP problem formulation is preferable. Should the whole optimization be performed in

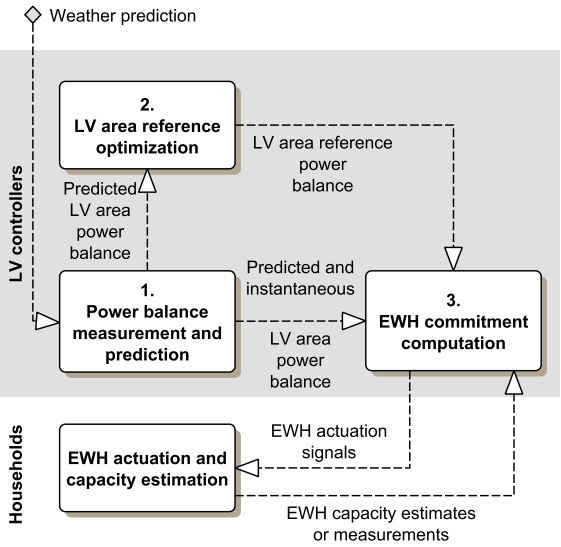

Figure 5.4: Detailed description of control process performed by the LV controller.

a single step, the resulting problem would be too complex to be solved in a sufficiently short time, especially if the computation capabilities of the LV controller are limited. Moreover, this complex optimization would have to be performed with the frequency with which the dispatch schedules optimization is performed (e. g. every 5 minutes). The two-phase approach allows to use a simplified LP formulation with longer time horizon for the dispatch reference optimization which provides the required outlook into the future, while the shorter time-horizon in the dispatch schedules optimization allows to use MILP formulation to reach the required precision.

- **Safeguard against power balance prediction and EWH state estimation errors**. As will be shown in the problems formulation, it is possible (and advisable) to only use a part of the capacity of EWHs for the control to prevent hot water depletion even in case EWH state estimation errors or to be able to keep the resulting power balance of the LV area close to the dispatch reference even in case of power balance prediction errors. This is achieved by using smaller part of the capacity in the first stage to obtain a more conservative dispatch reference which should be achievable to adhere to in the second stage even if larger than expected amount of

energy needs to be stored in EWHs (this would happen for example if the actual PV sources production is higher than was its prediction that was used for the dispatch reference computation).

- **Cooperation of control layers**. The two phase approach is used as a means to coordinate operation of the LV controller with the other control layers. In such a case, the dispatch reference is computed by the superior control layer while the dispatch schedules optimization remains unchanged. This allows to seamlessly switch to hierarchical operation with minimal modification of the LV controller operation.

5.2 Optimization problem formulations

The formulations of the problems for both optimization stages, i. e. the dispatch reference optimization and the dispatch schedule optimization as described in the previous section, are given here. The problems are defined as follows:

Dispatch reference optimization

minimize import and export of the LV area
subject to

- EWH power input constraints (continuous)
- EWH energy and hot water consumption constraints

Dispatch schedules optimization

minimize difference between resulting power balance of the LV area and the dispatch reference
subject to

- EWH power input constraints (discrete)
- EWH energy and hot water consumption constraints
- minimum on time constraints

The dispatch reference optimization is formulated as a LP problem and uses relaxed (continuous) EWH constraints whereas the dispatch schedules optimization is formulated as MILP problem and uses discrete version of EWH constraints that correctly reflect the binary nature of the EWHs operation. The MILP formulation also allows to incorporate minimum on time constraints in the model which are used to prevent excessive switching of the EWHs on and off.

5.2.1 Dispatch reference optimization problem formulation

The dispatch reference B_P is a sum of the predicted uncontrolled power balance $\hat{B}_P$ (i. e. the power balance that is a sum of uncontrolled load and uncontrolled generation) of the area and optimally distributed EWHs load such that the objective of minimizing of imports and exports of the LV area is achieved. Since from the distribution system perspective, the most important is to avoid the export and import peaks, as such peaks increase the line loading, requirements on power system dimensioning and also voltage fluctuations, minimizing of the daily peak exports $P_{max,E}$ and the daily peak imports $P_{max,I}$ of the LV area was selected as an objective function of the dispatch reference optimization. As will be shown in case study, such an objective also ensures reduction of energy transfers to/from the controlled area. The optimal dispatch reference is therefore found as a solution of the following optimization problem:

minimize

$$\sum_{d} \left[w_I(d) \cdot P_{max,E}(d) + w_E(d) \cdot P_{max,I}(d) \right] \tag{5.2}$$

subject to

(daily maximal import and export constraints)

$$\forall k \in D_d : P_{max,I}(d) \geq B_P(k), \tag{5.3}$$

$$P_{max,E}(d) \geq -B_P(k), \tag{5.4}$$

$$P_{max,I}(d) \geq 0, P_{max,E}(d) \geq 0, \tag{5.5}$$

(dispatch reference and EWH power input constraints)

$$B_P(k) = \hat{B}_P(k) + \sum_{i} P_i(k), \tag{5.6}$$

$$0 \leq P_i(k) \leq P_{nom,i}, \tag{5.7}$$

$$k = 1 \ldots N_S.$$

(EWH energy constraints)

$$\hat{E}_i(k+1) = \hat{E}_i(k) + P_i(k+1) \cdot T_S(k+1) - \hat{E}_{consumed,i}(k+1), \tag{5.8}$$

$$\hat{E}_{min,i} \leq \hat{E}_i(k) \leq \hat{E}_{max,i} \tag{5.9}$$

$$\hat{E}_{max,i} = V_i \cdot \rho_{water} \cdot c_{water} (t_{out,i} - t_{in,i}), \tag{5.10}$$

$$k = 0 \ldots N_S - 1,$$

(maximal average relative energy constraints)

$$\frac{1}{N_{EWH}} \sum_{i=1}^{N_{EWH}} \left[\hat{E}_{rel,i}\left(k\right)\right] \leq \hat{E}_{rel,max} \leq 1, \tag{5.11}$$

$$\hat{E}_{rel,i}\left(k\right) = \frac{\hat{E}_i\left(k\right)}{\hat{E}_{max,i}}, \tag{5.12}$$

$$k = 1 \ldots N_S,$$

where

$P_{max,E}, P_{max,I}, B_P, P_i, \hat{E}_i, \hat{E}_{rel,i}$ are continuous decision variable vectors,
$w_I, w_E, \hat{B}_P, T_S, \hat{E}_{consumed,i}$ are real number vectors,
$P_{nom,i}, \hat{E}_{min,i}, \hat{E}_{max,i}, \hat{E}_{rel,max}$ are real number scalars,
i is EWH index, $i = 1 \ldots N_{EWH}$,
k is time index (bounds given in each constraint set),
N_{EWH} is number of the controlled EWHs,
N_S is number of samples in the optimization horizon.

The daily maximal import and export constraints define how the daily peak imports $P_{max,I}\left(d\right)$ and peak exports $P_{max,E}\left(d\right)$ are computed. Since positive values of the dispatch reference B_P denote the energy import to the area, negative values of B_P denote the energy export and D_d is a set of time samples of the optimization horizon belonging to the day d, the daily peak imports $P_{max,I}$ and daily peak exports $P_{max,E}$ are defined by constraints (5.3) and (5.4) respectively. The constraints (5.5) ensure non-negativity of $P_{max,I}\left(d\right)$ and $P_{max,E}\left(d\right)$. The terms $w_I\left(d\right), w_E\left(d\right)$ are the objective weights of the maximal imports and exports in the day d. Since the prediction uncertainty typically increases on longer time horizons, the weights defined for each day provide the means to compensate the increasing uncertainty by setting the weights in a decreasing manner from the beginning of the optimization horizon towards its end. Such a setting helps to achieve optimal distribution of EWH load over the entire optimization horizon.

According to (5.6) the dispatch reference B_P is expressed as a sum of the predicted power balance (without the power drawn by the EWHs) $\hat{B}_P$ [W] and the aggregate power input of all controlled EWHs, i. e. the sum of $P_i\left(k\right)$ [W]. Although the EWH heating power cannot be continuously controlled in most cases (the EWH can only be switched on or off), for the purpose of the dispatch reference optimization, the EWH power input $P_i\left(k\right)$ is treated as a continuous variable. Such a simplification is used since in the dispatch reference

optimization, only the overall EWH load distribution is of interest, therefore the more precise modelling of the EWH power using binary variables (5.22) would not considerably improve the resulting dispatch reference, but would increase optimization times. The power input of each EWH $P_i\,(k)$ is bounded by the constraint (5.7) where $P_{nom,i}$ [W] is a nominal power input of EWH i.

The estimated amount of energy stored in the EWH $\hat{E}_i$ [Wh] in each time sample is given by the constraint (5.8) where $T_S\,(k)$ [h] is the length of the time sample k and the term $\hat{E}_{consumed,i}\,(k)$ [Wh] denotes the energy of water that is expected to be consumed in time k. The term $\hat{E}_i\,(0)$ is an estimate of the energy stored in the EWH at the beginning of the optimization horizon. The amount of energy that may be stored in the EWH is limited by the constraint (5.9). Since only additional energy supplied by the EWH heating element is of interest, $\hat{E}_i\,(k)$ is defined as zero if the temperature of the water in the EWH is equal to the temperature of feed-in water $t_{in,i}$ [°C]. Similarly, the $\hat{E}_i\,(k)$ is maximal if the temperature of the water in the EWH is equal to the desired hot water temperature $t_{out,i}$ [°C] as defined by the formula (5.10), where V_i [l] is the volume of the EWH, ρ_{water} is the water density ($1\ kg \cdot l^{-1}$) and c_{water} is the specific heat capacity of water ($4180\ J \cdot kg^{-1} \cdot K^{-1}$).

Note that the estimate of the energy stored in the EWH might be subject to a substantial cumulative error resulting mainly from an imprecise hot water consumption prediction. To limit the cumulative error, synchronization of the EWH energy estimate and the real state needs to be ensured with sufficient frequency as discussed in Section 5.3.2.1. Depending on the EWH energy estimation quality, it might be necessary to set $\hat{E}_{min,i}$ to a non-zero positive value in optimization as a safety margin to avoid hot water depletion.

Besides the safety margin for the water consumption prediction error, the two stage optimization approach makes it possible to reserve a part of the total capacity of controlled EWHs for power balance prediction errors. This is done by limiting the maximum average relative energy in EWHs according to the constraint (5.11) where $\hat{E}_{rel,i}$ [-] is the energy stored in a EWH relative to the maximal energy $\hat{E}_{max,i}$ defined by the constraint (5.12) and $\hat{E}_{rel,max}$ [-] is the desired maximum average relative energy. If $\hat{E}_{rel,max}$ is set lower than 1, then a part of the energy storage capacity of all controlled EWHs equivalent to $1-\hat{E}_{rel,max}$ may not be utilized in the dispatch reference optimization. Since the constraint (5.11) is not used in the second stage of the optimization, the EWHs will be capable of storing additional energy if the actual energy production in the area is higher than was predicted when computing the dispatch reference. As a result, in such case, the maximal power export scheduled by the dispatch

reference will not be exceeded, unless the amount of additionally produced energy is higher than $1 - \hat{E}_{rel,max}$ of the total energy storage capacity of the controlled EWHs.

5.2.2 Dispatch schedules optimization problem formulation

The dispatch schedules optimization module utilizes the dispatch reference B_P and attempts to find EWHs dispatch schedules so that the difference ΔB_P between the dispatch reference B_P and the final power balance $B_{P,final}$ is minimal. The ΔB_P is defined as:

$$\Delta B_P = B_{P,final} - B_P. \tag{5.13}$$

By decomposing the ΔB_P as $\Delta B_P = \Delta B_{P,I} + \Delta B_{P,E}$ where $\Delta B_{P,I}$ and $\Delta B_{P,E}$ are differences from the scheduled import and the scheduled export defined as

$$\Delta B_{P,I}(k) = \begin{cases} \Delta B_P(k) & \forall k : B_P(k) \geq 0, \\ 0 & \text{otherwise}, \end{cases} \tag{5.14}$$

$$\Delta B_{P,E}(k) = \begin{cases} -\Delta B_P(k) & \forall k : B_P(k) < 0, \\ 0 & \text{otherwise}. \end{cases} \tag{5.15}$$

the problem in the second phase may be formulated as:

minimize

$$\begin{aligned} & w_{\Delta I}^{over} \cdot \Delta B_{P,I}^{over} + w_{\Delta I}^{under} \cdot \Delta B_{P,I}^{under} \\ & + w_{\Delta E}^{over} \cdot \Delta B_{P,E}^{over} + w_{\Delta E}^{under} \cdot \Delta B_{P,E}^{under} \end{aligned} \tag{5.16}$$

subject to

(deviation from the dispatch reference constraints (5.13-5.15))
(over- and under-import and export constraints)

$$\Delta B_{P,I}^{over} \geq \Delta B_{P,I}(k), \Delta B_{P,I}^{under} \geq -\Delta B_{P,I}(k), \tag{5.17}$$

$$\Delta B_{P,E}^{over} \geq \Delta B_{P,E}(k), \Delta B_{P,E}^{under} \geq -\Delta B_{P,E}(k), \tag{5.18}$$

$$\Delta B_{P,I}^{over} \geq 0, \Delta B_{P,I}^{under} \geq 0, \tag{5.19}$$

$$\Delta B_{P,E}^{over} \geq 0, \Delta B_{P,E}^{under} \geq 0, \tag{5.20}$$

$$k = 1 \ldots N_S.$$

(final power balance and EWH power input constraints)

$$B_{P,final}(k) = \hat{B}_P(k) + \sum_i P_i(k), \tag{5.21}$$

$$P_i(k) = u_i(k) \cdot P_{nom,i}, \tag{5.22}$$
$$k = 1 \dots N_S,$$

(EWH energy constraints (5.8-5.10))
(minimum on time constraints)

$$\forall j, j \in \left\{k \dots k + N_i^{min,ON}(k)\right\} : u_i(j) \geq \Delta u_i(k), \tag{5.23}$$

$$\Delta u_i(k+1) \geq u_i(k+1) - u_i(k) \tag{5.24}$$

$$N_i^{min,ON}(k) = \left(\min l : \sum_{m=k}^{l} T_S(m) \leq T_i^{min,ON}\right) \tag{5.25}$$
$$k = 0 \dots N_S - 1.$$

(minimum on time at the start of the horizon constraints)

$$\forall j, j \in \left\{1 \dots N_i^{remain,ON}\right\} : u_i(j) = 1, \tag{5.26}$$

$$N_i^{remain,ON} = \left(\min l : \sum_{m=1}^{l} T_S(m) \leq T_i^{min,ON} - T_i^{ON}\right) \tag{5.27}$$

where

$u_i, \Delta u_i$ are binary decision variable vectors,
$\Delta B_P, \Delta B_{P,I}, \Delta B_{P,E}, B_{P,final}$ are continuous decision variable vectors,
$\Delta B_{P,I}^{over}, \Delta B_{P,I}^{under}, \Delta B_{P,E}^{over}, \Delta B_{P,E}^{under}$ are continuous decision variable scalars,
$N_i^{min,ON}$ is a real number vector,
$N_i^{remain,ON}, w_{\Delta I}^{over}, w_{\Delta I}^{under}, w_{\Delta E}^{over}, w_{\Delta E}^{under}, T_i^{min,ON}, T_i^{ON}$ are real number scalars,

The rest of the symbols have the same meaning and are of the same type as in the dispatch reference optimization.

Utilizing the objective (5.16) facilitates separately penalizing the maximal over- and under-import compared to the dispatch reference ($\Delta B_{P,I}^{over}, \Delta B_{P,I}^{under}$) as well as the maximal over- and under-export compared to the dispatch reference ($\Delta B_{P,E}^{over}, \Delta B_{P,E}^{under}$). Typically, the over-import and over-export weights $w_{\Delta I}^{over}, w_{\Delta E}^{over}$ would be set higher than the under-import and under-export weights

$w_{\Delta I}^{under}, w_{\Delta E}^{under}$ since exceeding the dispatch reference in both directions is undesirable. However, the under-import and under-export weights are also important to ensure that the resulting power balance is as close to the dispatch reference as possible. This is required since the dispatch reference optimization is performed on a longer optimization horizon than the dispatch schedules optimization, therefore the dispatch reference may take into account predictions beyond the horizon of the dispatch schedules optimization.

The final power balance $B_{P,final}$ is computed according to (5.21), i. e. similarly to the dispatch reference optimization with the only difference, that the first value of the predicted power balance $\hat{B}_P$ is replaced by the measured or estimated instantaneous power balance. Since in the dispatch schedules optimization, the dispatch schedules of individual EWHs are of interest, the power input of individual EWHs needs to correctly reflect its binary nature as defined by the constraint (5.22) where $u_i(k)$ indicates if the EWH i is switched on in time k.

Moreover, in order to prevent excessive switching of the EWH heating, the minimum on time $T_i^{min,ON}$ is ensured by constraint (5.23), where Δu_i is a startup indicator defined by the constraint (5.24) and the term $N_i^{min,ON}$ is a minimal number of samples for which the EWH heating has to remain in operation computed according to the formula (5.25).

If the EWH heating was on at the beginning of the optimization (i. e. $u_i(0) = 1$), the constraints (5.26-5.27) guarantee, that the EWH heating stays on for the remainder of minimal on time given the time T_i^{ON} for which the EWH heating was on prior to the beginning of the dispatch schedules optimization.

5.3 Hardware setup and implementation of demand side management system functions

The preceding sections described the basic principles of the LV DSM system operation and formulated optimization problems that are solved as a part of the process of controlling the power balance of the LV area. This section presents the necessary components that would allow to put the LV DSM system based on the aforementioned principles into practice, i. e. the hardware setup of the LV DSM system and implementation of individual functions of the system. Moreover, this section also gives some insights into required communication between the individual parts of the LV DSM system.

5.3.1 Hardware setup of the low-voltage DSM system

As shown in Fig. 5.2, physically, the control system consists of the following elements:

- **LV controller**, which generates the control signals for the EWHs in the LV area in such a way that the given control objective is achieved.
- **Household units** (smart meters) that are installed in each household with controlled EWH, which receive signals to turn the EWH on or off from the LV controller and also send load measurements and/or EWH state estimates to the LV controller (depending on the household unit capabilities).

The required capabilities of the LV controller and the household units may be summarized as:

- The **LV controller** is essentially a computer capable of performing the dispatch reference and the dispatch schedules optimization and optionally also measuring power balance of the LV (power flow through the MV/LV transformer).
- The requirements on the **household units** differ depending on available communication bandwidth between the household units and the LV controller, required precision of EWH state estimates and availability of measurement of the power balance of the area in the LV controller. The required and optional capabilities of the household units are as follows:
  - **Ability to switch the EWH on and off based on signals from the LV controller** (Required). This kind of functionality is typically available in most smart-meters.
  - **Capability to measure load at the household interconnection with the LV network** (Required). Household load measurements are essential in order to perform EWH state estimation.
  - **Capability to measure voltage at the household interconnection with the LV network** (Required only if power balance measurement is not available in the LV controller). This kind of functionality is needed in sufficient number of household units if a network state estimation functionality should be implemented in the LV controller. The network state estimation module may be used to estimate the power balance of the controlled area as well as other network characteristics.

- **Capability to estimate the current EWH state** (Required if household units to LV controller communication bandwidth is very limited or more precise EWH state estimates are required). If the EWH state estimation is done directly in the household unit, it may be based on much more frequent household load measurements or even on measurements provided by additional sensors installed in the EWHs. It reduces the requirements on communication since only the resulting state estimates need to be transferred to the LV controller with low frequency.

The actual configuration of the LV controller and household units will naturally depend on the baseline situation in the area where the system is to be installed - whether there are appropriate household units already in place or new ones are to be installed, what communications are they capable of and other factors. The influence of frequency and precision of household load measurements on EWH state estimation was one of the goals of the SIRES project and is briefly mentioned in Section 5.3.2.1.

Regarding the communication bandwidth requirements, the most demanding in this respect is communication between the LV controller and the household units. The bandwidth requirements of this communication depend on how the functions of the LV system are distributed between the household units and the LV controller as described above.

The author believes, that based on the above considerations, in real world, the proposed system should be applicable to a wide variety of hardware configurations of household units and LV controllers and communication links between them. One such combination that could be effective in terms of the system functions and cost-effective at the same time could be as follows:

- **Hardware**
  - **Household units** formed by smart meters only capable of measuring household load and switching the EWH on or off based on control signals from the LV controller.
  - **LV controller** in form of a programmable smart concentrator installed at the MV/LV substation capable of measuring power flows through the substation, computing EWH state estimates and dispatch schedules of the EWHs in the LV area. Depending on the computation capabilities of the smart concentrator, the dispatch schedules computation may be performed utilizing a MILP optimization as described in this thesis

or utilizing a more simple algorithm such as a form of a priority queue mentioned in Section 5.3.

- **MV controller** represented by a computer located either at the HV/MV substation or elsewhere, capable of measuring (or receiving measurements of) power flows through the HV/MV substation and performing the dispatch reference optimization.

- **Communication between the household units and the LV controller** should ideally be implemented by utilizing some form of broadband link in order to be able to send out the household measurements to the LV controller with sufficient frequency to perform reliable EWH state estimation and also to ensure reliable relay of control signals from the LV controller to the household units. This should be achievable using existing technologies for short range communications such as broadband power line communication (BPL) or other technologies that were presented for example in [56].

5.3.2 Implementation of individual functions of the system

This section describes the implementation of the key functions of the LV DSM system. The presented implementations were in most cases also tested in the pilot installation realized within the SIRES project and were also used in the simulations that formed the basis of the case study.

5.3.2.1 Electric water heater state estimation

The estimation of the EWHs state is essential for proper function of the DSM system since having an accurate EWH state estimate is required for the DSM system to ensure that at any instant the EWHs contain enough hot water to satisfy the households needs. The state of the EWH at any time instant as used throughout this thesis is defined by the following variables:

- **Stored energy** [kWh] - represents amount of energy stored in the EWH, which is directly proportional to the average temperature of the water stored in the EWH according to the following principle:

  - The amount of energy is zero, if the EWH is full of cold water, i. e. the average temperature equals to the temperature of the cold water that is used to refill the EWH.

  - A non-zero value of energy represents the energy that had to be delivered by the heater in order to heat the water from the temperature of the cold water to the current average temperature of water in the EWH.

- **Currently delivered power by the heating element** [kW] - i. e. the power at which the EWH is being 'charged'.
- **Currently drawn power by using the hot water** [kW] - i. e. it expresses a rate at which hot water is being drawn from the EWH. By using some of the hot water stored in the EWH and replacing it by cold water, the average temperature of water in the EWH decreases and so does the stored energy.
- **Energy losses** [kW] - a rate at which the stored energy in the EWH is being reduced as a result of energy losses through the EWH surface.

In principle, the (discrete) state equation could be written as:

$$\begin{aligned} \text{energy}\,(k+1) = \text{energy}\,(k) \\ + \left(\text{heating}\,(k) - \text{consumption}\,(k) - \text{losses}\,(k)\right) \cdot \Delta t. \end{aligned} \tag{5.28}$$

Note that the above equation only illustrates the principle of how energy stored in the EWH changes in time. A proper state equation used in optimization was given in the LV DSM system problem formulation in Section 5.2. The equation (5.28) indicates that in order to correctly estimate the EWH state, the following information is needed:

- determine the initial stored energy,
- identify periods when the EWH is heating water and what is the heating power,
- estimate hot water consumption and energy losses.

As will be shown later, knowing the initial state is not essential, since the correct state may be identified as soon as the EWH reaches its full capacity for the first time.

The other two factors are more important, but also more difficult to estimate. Regarding the identification of periods when the water in the EWH is being heated up, the second point, i. e. identification of the heating power, is simplified

by the fact that due to the construction of EWHs, they are always heating water at a constant power, which is a design parameter of the specific EWH. Even if the design heating power is not known, it can be derived with sufficient precision from observations of household load. The identification of heating periods is a more complicated task. Basically, it is performed by detection of household load step changes with magnitude of such change being equal to the design heating power of the EWH. The difficulties of the identification process result from

- possible confusion of EWH with another appliance,
- aggregation of the household load data (i. e. having measurements of overall household load only instead of a three-phase measurement or having only 15-minute averages of household load).

The above complicating factors were discussed and evaluated in thesis [57]. The thesis concluded, that these factors indeed influence precision of EWH state estimates, however, even with aggregated load measurements, the heating period detection can be performed with sufficient precision.

The hot water consumption estimation is the most challenging task. Without additional measurements, such as water flow meter at the EWH hot water extraction point, the estimate may only be based on typical hot water consumption patterns such as those presented in [58]. The typical hot water consumption patterns may be adjusted to better reflect hot water consumption of the given household by matching the total energy of water consumed over a selected time period and the electrical energy that was delivered to the EWH. It should be noted that such a modification only corrects magnitude of the water consumption estimate, not its shape. A method that also allows to determine shape of a hot water consumption curve was proposed in [57], however, its main deficiency lies in the fact, that the identification cannot be performed when the EWH is controlled by the DSM system and can therefore be used only for limited learning period. The energy losses of the EWH are typically negligible in comparison to the consumption of hot water by household users. In the models used in this thesis, they are incorporated into hot water consumption estimates by using a empirical value of 8 W per day per one litre of EWH volume which is the value generally quoted by EWH manufacturers.

In any case, the uncertainty in hot water consumption is the most important factor influencing the precision of the EWH state estimate. A comparison of a real energy stored in an EWH and its estimate based on the typical consumption pattern is shown in Fig. 5.5a. The figure displays a relative 'charge' where zero charge represents the state when the EWH contains only cold water and

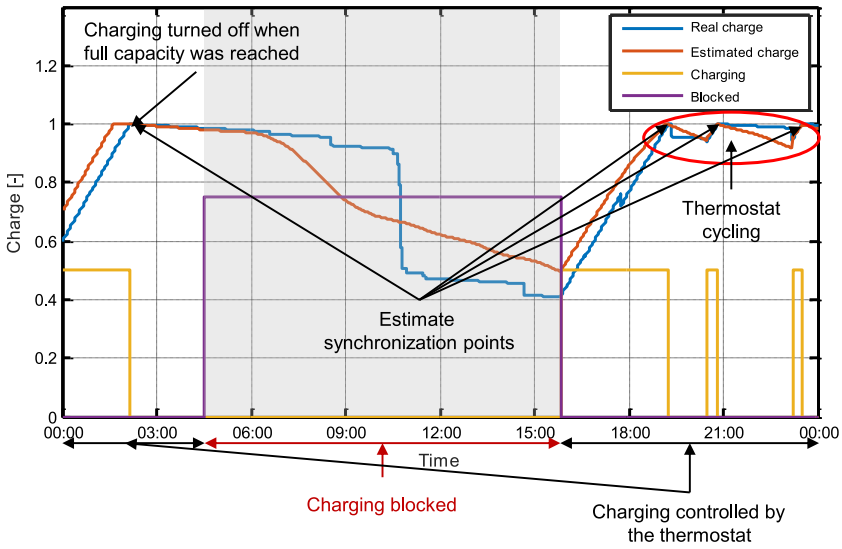

(a) : Comparison of stored energy in EWH and its estimate.

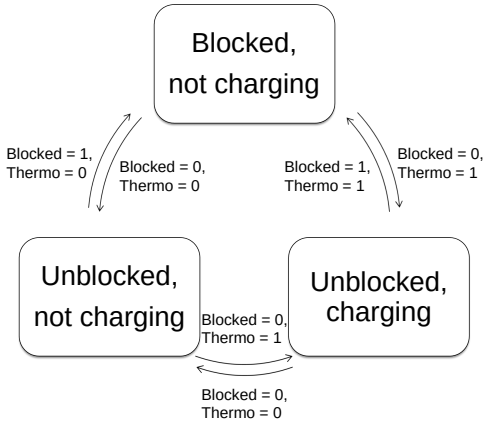

(b) : State diagram of EWH operation.

Figure 5.5: EWH state estimation.

charge equal to one represents the state when EWH is full of hot water. It is obvious, that the EWH state estimate becomes imprecise over the time due to the accumulation of differences between the real hot water consumption and the typical consumption diagram. However, by observing intervals when the water in the EWH is being heated, the EWH state estimate may be 'synchronized' with the actual state at certain time instants.

In order to better understand when such a synchronization event occurs, a state diagram describing the EWH operation is presented in Fig. 5.5b. There are two independent signals that decide whether the EWH is currently heating up the water (a term 'charging' as an analogy to energy storage devices is used to describe this state in further text):

- external control signal (from the DSM system, CRC or other system) denoted ***blocked*** in Fig. 5.5b that effectively 'blocks' or 'unblocks' charging by operating the circuit breaker of a circuit, where the EWH is connected,
- internal thermostat denoted ***thermo*** in Fig. 5.5b installed in the EWH which switches the EWH charging off when the water temperature reaches the desired value (set by the user) and resumes charging as soon as temperature drops below value specified by the thermostat hysteresis.

Naturally, the *blocked* signal has preference over the *thermo* signal, since the former physically disconnects the EWH from the power source. When the EWH is unblocked, the thermostat decides when the charging takes place. It is obvious, that whenever a transition from state *unblocked, charging* to state *unblocked, not charging* occurs, the EWH is fully charged, i. e. is at its maximal storage capacity. At these instants, which are also labelled in Fig. 5.5a it may be safely assumed that the charge is equal to one and the EWH state estimate may be corrected accordingly. The transitions from and to the *blocked* state do not carry any additional information on the actual EWH state, but the knowledge that the EWH is in the *blocked* state may be used to help with identification of heating periods since it prevents other household appliances to be confused with the EWH in periods when the EWH is *blocked*. Note that the aforementioned method of identifying the hot water consumption curve proposed in [57] is based on the principle described above - the *blocked* signal is always disabled, i. e. the EWH is always connected to the power source, hence the thermostat cycling (switching of *unblocked, charging* and *unblocked, not charging* states) occurs with high frequency (essentially after any larger hot water draw) which allows to estimate the hot water consumption with relatively high precision.

5.3.2.2 Power balance prediction

Precisely predicting the power balance of the area to be controlled by the DSM system is important in order to ensure that the dispatch reference and dispatch schedules are correctly computed so that the DSM system may appropriately distribute the EWH load to achieve the given objective (i. e. to minimize

exports of energy from and imports of energy to the controlled area). Note that the *uncontrolled* power balance prediction is of interest in this respect, i. e. a prediction of power balance that consists of household demand that cannot be controlled and production of RES which is also assumed not to be controllable.

The uncontrolled household load prediction used in the pilot installation and the simulations is based on the typical daily load profiles provided by the Czech electricity and gas market operator [59]. These profiles give normalized load predictions for certain types of residential and commercial consumers based on predominant characteristics of appliances installed in the households (i. e. different load profile would be used for a household that uses electrical space heating, heat pump, EWH or uses no such appliance). In order to obtain load prediction for a specific household, the following information is needed:

- *consumer type* to select the correct load profile (this can be usually inferred from the distribution tariff used by the consumer),
- *location* since some of the profiles [59] are geographically dependent,
- *yearly energy consumption of the household* which is used to obtain a correct magnitude of the load profile.

While the load profiles do not give precise uncontrolled load estimates for each individual household (such an estimate could possibly be obtained from observations of historical load of the specific household), they should be reasonably accurate for estimating the total load of large number of households and should therefore be accurate enough for the task of predicting the load of the whole LV area.

Since the PV sources are the only type of RES present in the SIRES pilot installation area, the prediction of RES generation only concerns this type of energy sources. Similarly to the household load predictions, the PV generation is based on typical generation profiles. These profiles were obtained from long-term observations of generation of rooftop PV array installed at the Czech Technical University and provide a mean power and a power variance for a given time instant and a cloud coverage at that time. The generation prediction for a specific PV source is therefore obtained based on:

- *typical PV power generation profiles*,
- *weather forecast* for the given location (forecasts from [60] were used in the simulations),

- *time interval for the prediction* which is needed to select the correct generation profile as the PV power generation depends on the yearly season,
- *installed capacity of the PV array* which is again used to obtain a correct magnitude of the load profile.

The resulting power balance prediction is computed as a sum of predictions of load of all households and generation of all power sources in the controlled area.

5.3.2.3 Dispatch reference and dispatch schedules optimization

For the purposes of rapid development and testing and also for simulations in the case study, the formulations of dispatch reference and dispatch schedules optimization problems were implemented in Matlab using Yalmip toolbox [61] and solved using the commercial solver Gurobi on a state-of-the-art computer capable of solving the optimization problems in a very short time. The dispatch reference was optimized on a 48-hour time horizon with 1-hour sampling period. It was executed 2 times per day at 6:00 and 18:00, i. e. at time when a new weather forecast is typically available. The dispatch schedules optimization was executed each 5 minutes on a 6-hour optimization horizon with the time samples lengths ranging from 5 minutes to 1 hour. Shorter time sample length at the beginning of the optimization horizon facilitates precise modelling of the EWH effects on power balance, while longer time samples towards its end reduce the number of variables thus making the problem easier to solve.

Since the hardware used for the simulations was significantly more capable than the hardware that is expected to be available in the real-world operation of the LV DSM system (as described in Section 5.3.1), a thesis [62], which was originated within the SIRES project, dealt with a problem how to compute the dispatch reference and dispatch schedules using a performance-limited hardware platform.

The basic tasks set out for the thesis [62] were:

- test whether it is possible to solve the optimization problems dealt with in the dispatch reference and dispatch schedules optimizations using an ARM based development board which should have similar capabilities to the typical smart-concentrators while using LP and MILP solvers that are open-source and available for commercial use,
- develop heuristic algorithms as a substitute for any task that is not possible to perform using optimization methods due to the performance limitations of the selected platform.

The thesis [62] concludes that the selected hardware platform is capable of solving the LP problem dealt with in the dispatch reference optimization, however, the MILP problem dealt with in the dispatch schedules optimization is beyond the capabilities of the platform. As a result, a heuristic priority-queue based algorithm for dispatching the EWHs was developed and tested. The thesis concluded, that the quality of the resulting EWH dispatch computed by the heuristic algorithm is comparable to the EWH dispatch obtained by solving the MILP optimization problem and that the heuristic algorithm is therefore a viable alternative that can be used on a performance-limited platform.

5.4 Pilot installation and the network used for low-voltage DSM system case study

As mentioned in Chapter 1, the presented DSM system has been designed to facilitate dealing with the issues introduced by the increased penetration of RES in distribution networks. As a part of the DSM system development within the SIRES project, a small-scale pilot installation of the proposed system was set up in a part of LV distribution network in the Czech Republic with very high penetration of PV sources.

The pilot installation network (Fig. 5.6) supplies approximately 100 households, is fed by a 250 kVA transformer, its peak load reaches 80 kW and the total installed peak PV capacity reaches 142 kW. In the area, around 40 EWHs with an aggregate power input reaching 80 kW are installed. The aggregate power input of EWHs in the households that participated in the pilot project is 20 kW, which is around 20 % of the highest measured export from the area. Its parameters are summarized in Tab. 5.1.

Nominal voltage	400 V
Number of buses	295
Number of lines	290
Number of households	104
Number of EWHs	43
Aggregate PV sources peak power	142 kW
Aggregate peak uncontrolled load	57 kW
Aggregate peak EWHs power input	85 kW

Table 5.1: Characteristics of the pilot LV network.

The main targets of the pilot installation were:

- to verify existence and extent of the issues associated with RES presented in Section 2,
- to find out how the existing load control - the centralised ripple control (CRC) - contributes to the above problems,
- to determine the required hardware configuration of the household units and the LV controller and test the key functional elements of the LV DSM system that were described in Section 5.3.2 in practice.

Since only 10 household units were deployed within the pilot installation network, the pilot installation could not be utilized to fully assess the benefits of the proposed DSM system. However, since the topology, line parameters, consumers'

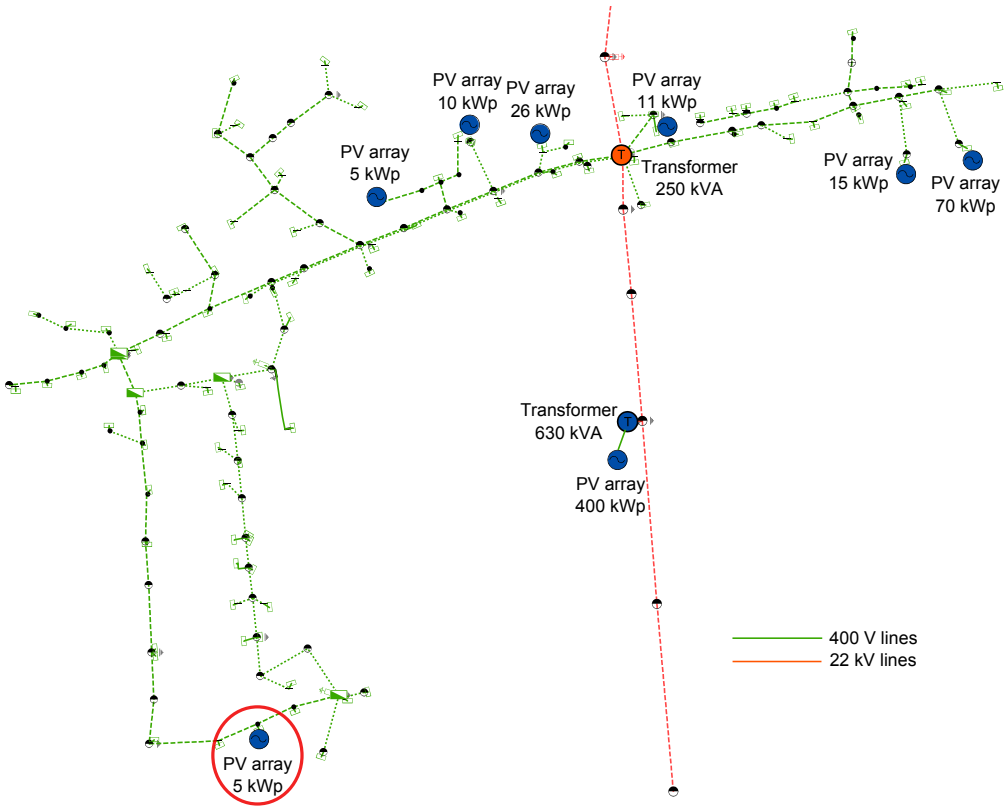

Figure 5.6: Topology of the pilot LV network.

structure and information on RES in the network were available, it allowed to use the aforementioned information to create a model of the network and use it to simulate the operation of the LV DSM system in a full-participation scenario. The results of such simulations are presented in a case study in Section 5.7.

5.4.1 Hardware setup used in pilot installation

As mentioned earlier, the main target of the pilot installation was to verify existence of negative phenomena associated with RES in the pilot network and to develop and test elementary functions of the proposed system. For this reason, the hardware used in the pilot installation was significantly more universal and capable of more precise measurements than it is needed for the system to function in the final configuration.

The household installation in the pilot network consisted of the following components:

- *Central unit* - a compact x86 compatible computer used to run local control algorithms or relay control signals from a LV controller (connected via internet) and to collect data and send control signals from/to measuring/load switching units.
- *Wireless gateway* - used to transmit signals from the central unit to measuring/load switching units using ZigBee protocol.
- *Measuring/load switching unit* - installed on the distribution board rack in order to measure the overall household voltage and power (three-phase) and to switch controlled appliances on or off based on signals from the central unit.

Using this setup facilitated testing of the following:

- Having a three-phase measuring unit allowed to test whether a three-phase measurement is actually needed in order to estimate the EWH state with sufficient precision.
- The central unit was capable of aggregating the household load measurements to simulate the data that are usually available from standard smart-meters, namely: Aggregating the three-phase measurement into a single value to obtain the overall household load and computing 15-minute averages of the household load.

- It allowed to verify impacts of the aforementioned aggregations on required communication bandwidth between the household units and the LV controller and on the quality of the EWH state estimation.
- The central unit was also capable of directly computing the EWH state estimates in order to test what benefits does it bring in terms of the DSM system performance and communication bandwidth requirements.
- The voltage measurements (along with the load measurements) allowed to test functionality of the network state estimation module which was based on [63].

The functions of the LV controller - dispatch reference optimization, dispatch schedules optimization, computation of load and generation predictions, estimation of EWH states (in scenarios when it was not done directly in household units), etc. - were carried out by a computation server located at the Czech Technical University. The required two-way communication was established using a secured channel over a standard internet connection available at the participating households.

5.4.2 Current situation in the pilot LV installation area and effects of the centralised ripple control

Due to the high installed capacity of PV sources, comparatively low load and the fact, that the peak production is achieved during the day while the consumption peaks at night, the power balance of the area is very uneven with distinct import and export peaks. The current situation is demonstrated in Fig. 5.7a which shows a 2-day power balance of the area measured at the feeding transformer and reveals, that the network exhibits peak power exports reaching 100 kW. Since the high power flows through the power lines in the area induce higher voltage drops or rises (depending on the power flow direction), the area also exhibits high voltage volatility as illustrated in Fig. 5.7b. As may be observed, the voltage exceeds the 10% tolerance allowed by the norm for approximately 4 hours a day, which should be avoided. The power balance and voltage measurements include the effects of the CRC-controlled EWHs, since the CRC is routinely used in the Czech distribution system.

As described in Section 3.3.2.2, the CRC system presents a form of DSM which is based on time-of-use tariffs supplemented with a remote control system, which physically disconnects controlled appliances from electricity in periods of high

tariff price. The CRC system is operated by DSOs and is set up to pursue two main objectives: levelling the distribution network load and shifting peaks of the overall transmission system load. The system works well for passive distribution networks (i. e. for networks without power sources) since consumption of such networks is well predictable. However, it may not be flexible enough to deal with the increasing diversity and uncertainty brought about by the increasing penetration of energy sources, especially RES in the distribution networks.

The drawbacks of CRC include:

- *CRC controls groups of appliances spread over a large area.* This prevents the DSO from being able to control load in specific part of the network.

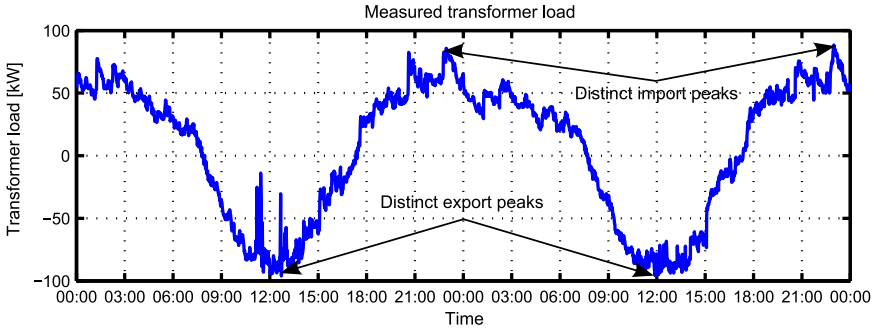

(a) : Measured power flow through the transformer feeding the low voltage network.

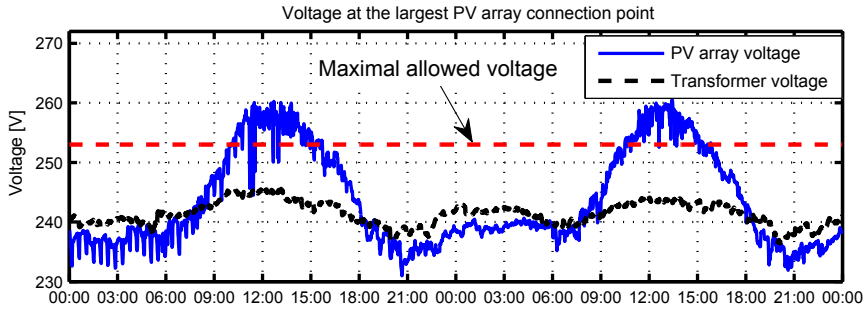

(b) : Voltage measured at the 70 kW PV array connection point.

Figure 5.7: Observed effects of RES in the pilot network.

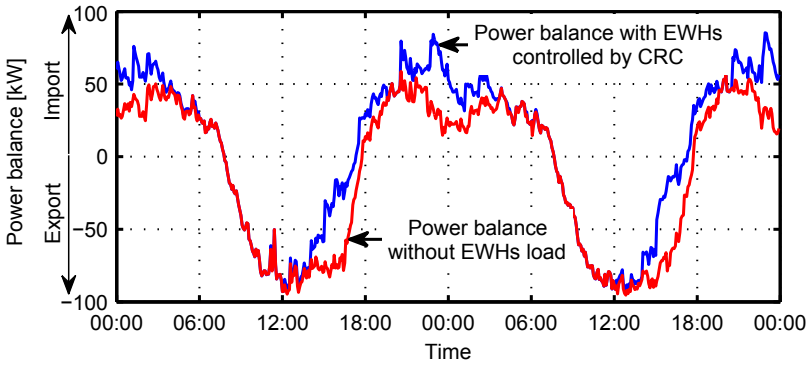

Figure 5.8: Comparison of power balance of the pilot area with EWHs controlled by CRC and estimated power balance without EWHs load.

- *CRC provides no feedback on its effects.* Therefore only overall effects of CRC control may be observed based on measurements available in distribution network.
- *CRC dispatch schedules cannot be changed in real time.* Due to the current legislation, the CRC schedules need to be published 7 days prior to any change.

The most important deficiency of the CRC is that the number of time-of-use tariffs settings is technically limited by the number of code combination that can be transmitted to the CRC receivers in households. As a result, the same time-of-use tariffs are valid for appliances spread over a large area. Therefore if the DSO wanted to modify the schedules so that the CRC improves operation of one part of the network, it may adversely affect other parts of the network.

The aforementioned deficiency is illustrated on example of the CRC contribution to the power balance in the pilot installation network shown in Fig. 5.8. The figure compares the measured power balance of the area and the estimated power balance without the EWHs load, which was computed based on known CRC schedules. The CRC schedules are set up to turn on most of the EWHs in the afternoon and overnight with an intention not to contribute to the typical morning load peak in the transmission system. However, in this particular part of the network, such a setting allows the export peak caused by PV production to fully develop over the day and also creates an import peak by turning on the EWHs overnight. It is also apparent that with a proper control, taking into account the specifics of the network, the EWHs load may be distributed in such

a way that the both peaks are reduced, which in turn reduces network losses on feeding lines and requires the DSO to reserve lower transmission capacity for feeding the network.

In all further comparisons, the CRC control will be considered a base case to which the performance of the proposed DSM system will be compared in order to answer the question how could the proposed DSM system improve the operation of the LV networks with high RES penetration compared to the current state.

5.5 Model of the low-voltage network used for simulations

As already stated, in order to verify the LV DSM system effectiveness in a full penetration scenario, the DSM system operation was simulated using a network model. It was therefore important model individual aspects of the studied network so that the model matches the real network as closely as possible. This involves modelling of the following aspects of the network:

- network topology,
- household electricity consumption,
- EWH energy consumption and household water consumption,
- production of PV sources.

The following sections describe how models of these aspects were set up in order to obtain the best possible match of the model and reality.

5.5.1 Network topology

The pilot installation network shown in Fig. 5.6 was modelled in order to assess what effects the LV DSM system has on power quality and other aspects of operation of a LV the distribution network. As mentioned in 5.4, all important parameters of the network, such as line parameters, locations and installed capacities of PV sources, number and types of households connected at each bus etc. were known.

5.5.2 Household electricity consumption

The real household consumption measurements obtained in the pilot installation network were the basis for the simulation of the uncontrolled load of households.

A distribution tariff and yearly consumption was known for each individual household. Since as pointed out in Section 5.3.2.2 the distribution tariff provides information on what appliances are used in the household, it allowed to select an appropriate measurement from a household with similar appliances composition. From this measurement a random working or non-working day data was used for simulating the load of the given household.

The magnitude of the resulting household load was adjusted such that it would match the known household yearly consumption. The yearly consumption of households equipped with a controlled EWH was lowered by the amount of energy that would be consumed by the EWH over a year to obtain the estimate of the uncontrolled load (i. e. a sum of the resulting uncontrolled load and simulated consumption of the EWH would yield the known yearly consumption of the household).

5.5.3 Electric water heater energy consumption and household water consumption

In order to simulate the electrical energy consumed by the EWH a model described in Section 5.3.2.1 was used with and important modification that instead of a typical hot water consumption profile, a random realization of household hot water consumption for an appropriate month based on study [58] was used.

Based on data from the pilot installation, the average hot water consumption was set to 80 % of the total EWH capacity while individual daily consumption of each EWH were set up in range from 40 % to 150 % of the EWH capacity.

The design parameters of EWHs (design power input and volume) and a CRC schedule used to control each EWH were known for each household with EWH.

5.5.4 Production of photovoltaic sources

The same power generation profiles that were described in Section 5.3.2.2 were used to simulate the real production of PV sources with the following alternations:

- As noted in Section 5.3.2.2, the power generation profiles provide mean and standard deviation of PV generation for the given cloud coverage. The prediction described in Section 5.3.2.2 only uses the mean value, whereas the simulation also uses the standard deviation to simulate the random component of the PV generation.
- Real cloud coverage observations collected from [64] were used instead of weather forecasts.

The installed capacities and locations of PV sources used in simulations of the LV network were as shown in Fig 5.6.

5.5.5 Model verification

To illustrate how the individual aspects of the LV area, which are important inputs to the LV controller, are simulated and predicted, Fig. 5.9 shows simulations and predictions of uncontrolled load (Fig. 5.9a), uncontrolled production (Fig. 5.9b), households water energy consumption (Fig. 5.9c) and the resulting uncontrolled power balance (Fig. 5.9d).

The simulations and predictions are based on models described in Sections 5.3.2 and 5.5 and are given for a two-day period with the first day being mostly cloudy, especially in the afternoon, while the second day was mostly sunny.

It may be observed that while the predictions naturally cannot predict short term variations of the given variable, the mean value is generally predicted with good accuracy, except for the PV generation on the cloudy first day, since fast changes in cloud coverage are difficult to predict and also induce substantial fluctuations of the PV sources production.

Moreover, an advantage of the fact that measurement of the power flow through the transformer feeding the pilot installation area was available for the simulated time interval was taken, allowing to compare the simulations against real data. The aforementioned comparison is presented in Fig. 5.10.

First, the Fig. 5.10a shows how the simulation of individual power balance elements, i. e. the uncontrolled power balance and the energy consumption of

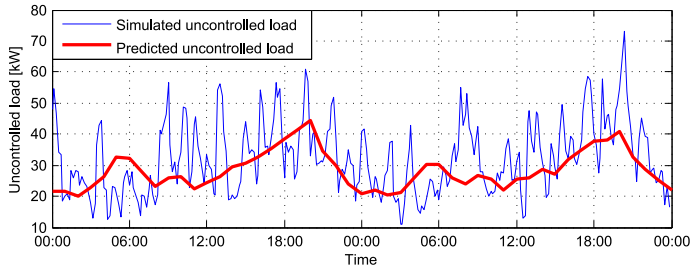

(a) : Uncontrolled load.

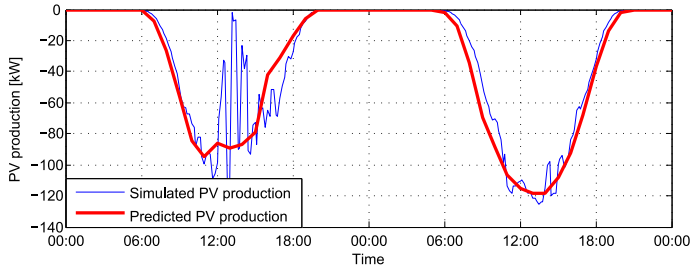

(b) : Uncontrolled generation.

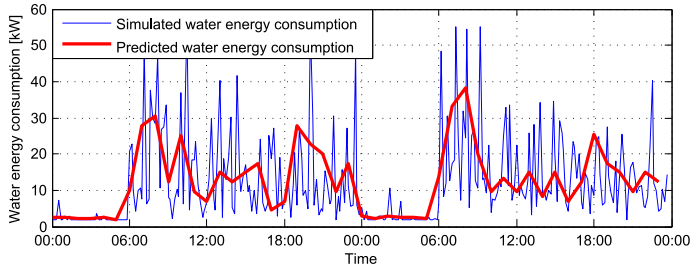

(c) : Household water energy consumption.

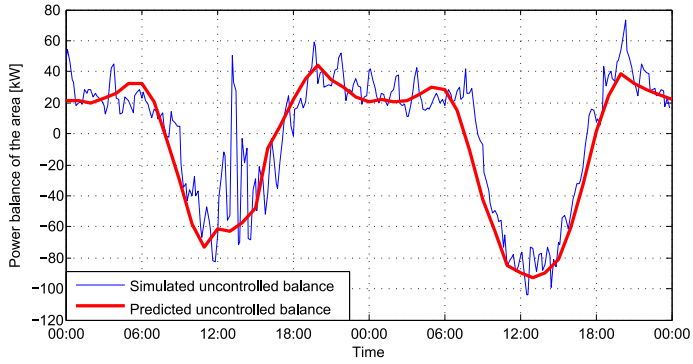

(d) : Uncontrolled power balance.

Figure 5.9: Illustration of simulation and prediction of individual aspects of the LV area.

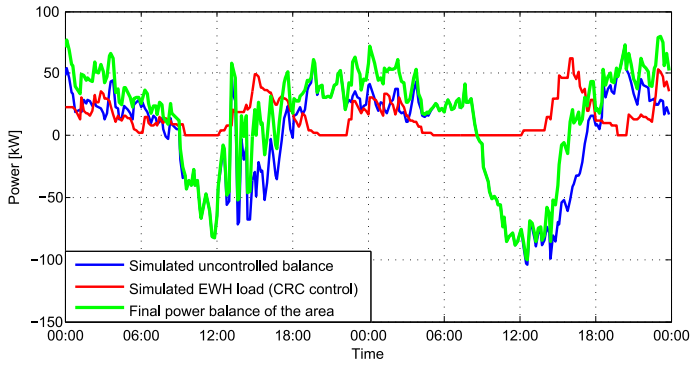

(a) : Illustration of composition of the simulated power balance of the LV area.

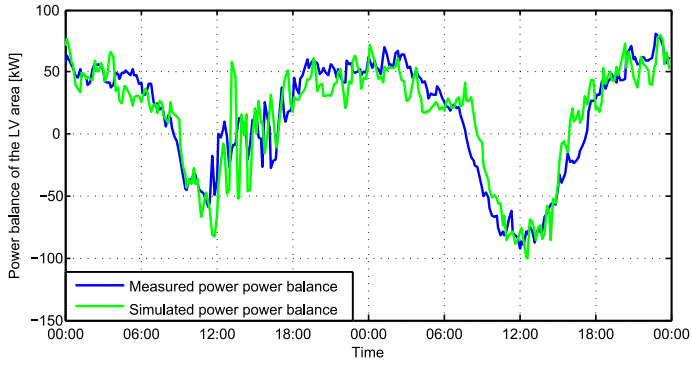

(b) : Comparison of measured and simulated balance of the LV area.

Figure 5.10: Comparison of simulation of power balance of the LV area and measured data.

the EWHs, contribute to the resulting power balance of the LV area. When simulating the EWH energy consumption, CRC schedules that were valid for the simulated time interval were used to control the EWHs.

The Fig. 5.10b then shows how the resulting simulated power balance compares to the real measurement. Although some differences between the measurement and simulation may be observed, the model fit is generally reasonable, considering the uncertainties present in each component forming the resulting simulated power balance of the LV area.

5.6 Simulation of low-voltage DSM system operation

The preceding sections described how individual functions of the LV DSM system were implemented (Section 5.3.2) and how the model of the network used for simulations of LV DSM system was created (Section 5.5). This section explains how the aforementioned elements are used to simulate the operation of the LV DSM system, i. e. how the process described in Section 5.1 is implemented in simulations used for the case study.

At the beginning, the following inputs are generated for the whole simulated time interval:

- uncontrolled load of each household,
- hot water consumption for each household with EWH,
- production of each PV source.

Moreover, at the beginning of simulation, the initial amount of hot water in each EWH is randomly set in range of 45 % to 90 % of its capacity. The estimate of the amount of hot water in the EWH is randomly set to value in range ±20 % around the simulated amount.

Then, the process of operation of the LV DSM system is simulated as follows:

- At the first time step and then when the simulation time equals the time when the dispatch reference should be computed, the dispatch reference optimization is performed. The inputs of dispatch reference optimization are:
  - estimated states of the EWHs in each household,
  - current power balance of the area,
  - predictions of uncontrolled load, uncontrolled generation and hot water consumption of EWHs generated for the time horizon of the dispatch reference optimization (e. g. 48 hours).
- With a time step with which the dispatch schedules optimization is performed (e. g. 5 minutes), the following operations are performed:
  1. Current uncontrolled load of each household is determined from the pre-generated data.

2. Current production of each PV source is determined from the pre-generated data.
3. The simulated state of EWH in each household is updated based on the simulated hot water consumption and based the fact whether the heating was turned on between the last step and the current.
4. The estimated state of the EWH is updated in the same way, but the hot water consumption estimate is used instead of the simulated hot water consumption. Whether the EWH was on or off between the last step and the current is determined based on observation of the given household load.
5. The network state is calculated using method [63] based on the current production of each PV source, uncontrolled load of each household and simulated power input of each EWH.
6. Dispatch schedules optimization is performed based on
   - the dispatch reference for the time horizon of the dispatch schedules optimization,
   - estimated states of the EWHs in each household,
   - current power balance of the area,
   - predictions of uncontrolled load, uncontrolled generation and hot water consumption of EWHs generated for the time horizon of the dispatch schedules optimization (e. g. 6 hours).
7. Based on the new dispatch schedules, the EWHs are turned on or off or left in the current state.
8. The simulation progresses to the next time step.

- If operation of the network with CRC is simulated, the above process simplifies to the following operations, which are performed with desired time granularity (e. g. 5 minutes):

1. Current uncontrolled load of each household is determined from the pre-generated data.
2. Current production of each PV source is determined from the pre-generated data.
3. The simulated state of EWH in each household is updated based on the simulated hot water consumption and based the fact whether the heating was turned on between the last step and the current.

4. The network state is calculated using method [63] based on the current production of each PV source, uncontrolled load of each household and simulated power input of each EWH.
5. Based on the CRC schedule that is valid for the given household, the EWHs are turned on or off or left in the current state.
6. The simulation progresses to the next time step.

5.7 Case study

In order to verify the performance of the LV DSM system in a full penetration scenario (i. e. in a scenario that assumes that all EWHs in the area can be controlled by the LV DSM system), its operation in the pilot installation network (Fig. 5.6) was simulated according to the process described in Section 5.6. Additionally, the simulations also attempted to answer a question what is the influence of having a more precise estimate of the EWH state. This was accomplished by simulating presence of sensors which would detect that there is a certain level of hot water in the EWH tank. Such sensors would provide additional events when the EWH state estimate could be synchronized with the real state as described in Section 5.3.2.1. Physically, such sensors could be implemented by installing temperature sensors at specified height of the EWH tank, which could be used to indicate that there is more than the specified level of hot water in the EWH tank.

As a result, the operation of the LV DSM system was simulated in the following three scenarios:

1. no sensors in EWHs, minimal relative energy[1] 45 %, maximal average relative energy 90 %, all EWHs were forced to turn on each day in period from 14:00 to 17:00 and remain on until reaching maximal capacity to ensure EWH energy estimates synchronization (only if the last synchronization event occurred more than 24 hours ago),
2. a sensor of 25 % of hot water in EWH, minimal relative energy 20 %, maximal average relative energy 90 %,
3. sensors indicating 25 % and 75 % of hot water in EWH, minimal relative energy 20 %, maximal average relative energy 95 %.

[1] The term minimal relative energy is equivalent to a ratio obtained by substituting $\hat{E}_i$ with the minimal energy $\hat{E}_{min,i}$ in the formula (5.12).

Scenario	1	2	3
Avg. power export peak reduction [%]	42.4	46.9	51.1
Avg. power import peak reduction [%]	26.5	25.3	24.9
Avg. peak to peak power reduction[a] [%]	34.7	36.4	38.0
Avg. energy transfer reduction[b] [%]	24.1	26.5	26.7
Abs. energy transfer reduction[c] [MWh]	1.13	1.25	1.26
Avg. min to max voltage reduction[d] [%]	28.6	26.1	27.5
Number of EWH depletion occurrences	4	2	2
Avg. depletion period length [min]	23	5	7.5

[a]Peak export to peak import reduction.
[b]Sum of avoided daily energy import and export.
[c]In the 4-day period shown in Fig. 5.11a.
[d]Measured in south-western part of the pilot installation area.

Table 5.2: Performance characteristics with the proposed DSM system in a LV network.

In all scenarios, the minimal on time was set to 30 minutes. The objective weights in both optimization stages were set in line with considerations presented in sections 5.2.1 and 5.2.2.

The Fig. 5.11a shows a comparison of the power balance with the current control of EWHs by CRC and simulations of the proposed DSM system in all aforementioned scenarios on a 4-day interval. The Fig. 5.11b compares voltage profiles at the node near the PV array in the south-western part of the pilot installation area marked by the red circle in Fig. 5.6. The Table 5.2 summarizes selected performance characteristics illustrating the DSM system effectiveness. All reductions are relative to the reference case with EWHs controlled by the CRC.

As may be observed, the proposed DSM system is capable of shifting the EWHs load such that a large portion of energy, that is exported in the reference case, is stored in EWHs. This results in considerable reductions in the peak power exports and imports, as well as reduction of energy transfers from and to the pilot installation area. As expected, most of the performance characteristics, especially the export peak reduction, improve with increasing quality of EWH state estimates. The peak import reductions are comparable in all scenarios since the EWHs are generally off during the night unless the energy estimate decreases under the minimal relative energy setting.

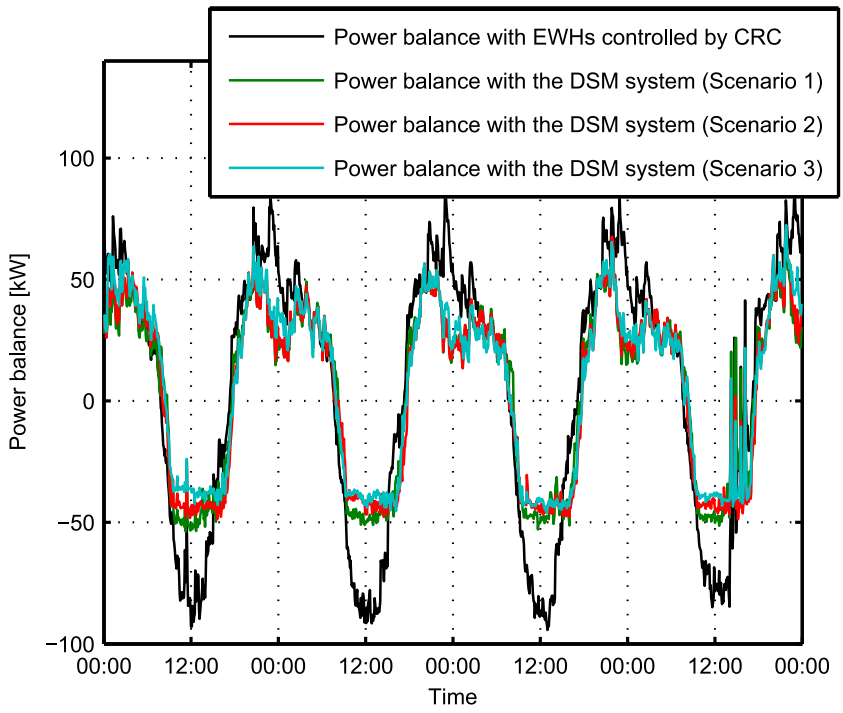

(a) : Power balance of the area.

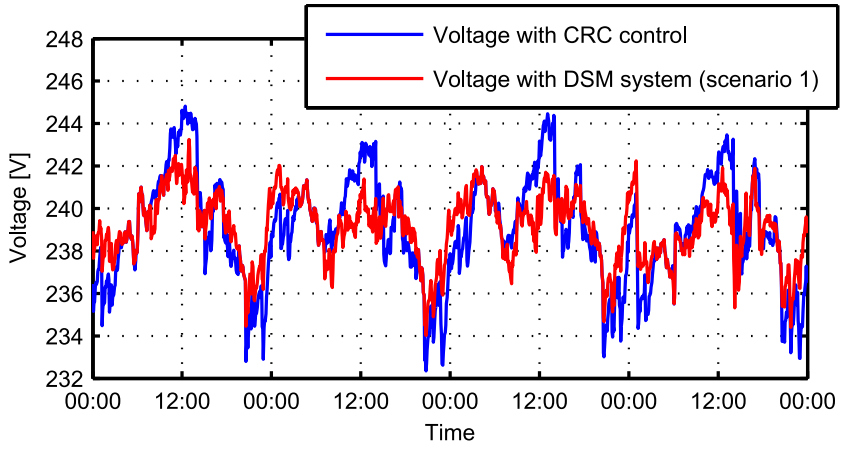

(b) : Voltage in south-western part of the area.

Figure 5.11: Performance of the proposed DSM system in a LV network.

The simulation results also indicate a considerable reduction in the voltage volatility, which may be attributed to the fact that in periods of high PV

production, a part of the produced energy is consumed near the PV sources. This lowers the loading of other lines through which the energy is exported in the reference case and reduces associated voltage rises. Analogously, during the night, the load of the area is reduced, which lowers the voltage drops associated with energy transfers to heat the EWHs in the reference case.

In the reference case, the EWH depletion occurred two times in the simulated period with an average depletion duration of 35 minutes. In scenario with no EWH sensors, the occurrence of depletions increased, however, the average depletion length was lower. In both scenarios with sensors in EWHs, the number of depletions did not increase and the duration of the depletions was reduced as a result of improved EWH state estimates.

Chapter 6

Medium-voltage demand side management system

This chapter presents the second level of the proposed control concept - the MV DSM system. The system coordinates operation of several LV DSM systems connected in the same MV network so that load control potential in all LV areas could be exploited. This concept was presented at the AUPEC 2014 Conference in Perth, Australia in the author's article [65]. The chapter is composed as follows: the basic principles of the MV DSM system are outlined in Section 6.1, the optimization problem solved by the MV controlled is given in Section 6.2, the Section 6.3 describes the network used in the MV DSM system case study and the case study itself is presented in Section 6.4.

6.1 Basic principles

As shown in Fig. 6.1, the MV DSM system expands the capabilities of the LV DSM system by introducing a MV controller which coordinates operation of multiple LV DSM systems connected in one MV network. The objective of the MV controller is to reduce energy imports and exports of the MV network as a whole by generating appropriate dispatch references for each LV DSM system. As will be further explained, this allows to effectively use all controllable loads even in LV areas with low penetration of RES, where the LV DSM systems in autonomous operation would be ineffective since with low penetration of RES or no RES in their LV area, the EWHs in the area would not be able to store any energy produced by RES and their objective would reduce to avoiding import peaks that may be caused by the EWHs themselves. Moreover, if the

network topology and parameters are known, the MV controller may also control the EWHs with respect to constraints imposed by the network or even make reduction of line loading a part of its objective.

The Fig. 6.2 explains the differences between the two operations modes, i. e. the mode when the LV DSM system operate autonomously (further denoted *autonomous mode*) and when their operation is coordinated by the MV controller (further denoted *hierarchical mode*). In the autonomous operation mode (Fig. 6.2a), the LV controller is installed only in areas that contain both - the controlled EWHs as well as substantial amount of RES. The LV controller predicts the RES generation, uncontrolled load (i. e. any load that cannot be controlled by the system) and available EWH capacity and attempts to shift the EWH consumption so that it matches the expected production of the RES in the LV area. It focuses on eliminating or reducing the RES production export and import peaks as well as reducing the amount of energy exported from and imported to the LV area. The reduction of energy export in turn reduces loading of the feeding lines in the MV area and the associated line losses. Moreover, it also reduces voltage fluctuations caused by the RES since some of the energy is consumed very close to the point of its production which reduces loading and associated voltage drops or increases on the upstream power lines.

In the hierarchical operation mode (Fig. 6.2b) the system includes the additional MV controller that takes over the role of predicting the RES generation and receives uncontrolled load and EWH capacity predictions from the LV controllers in the connected LV areas. It then combines this information and instructs the LV controllers how to control the EWHs in their LV area in order to achieve reduction of RES energy export of the whole controlled MV interconnection. The important difference from the autonomous operation mode is that with the

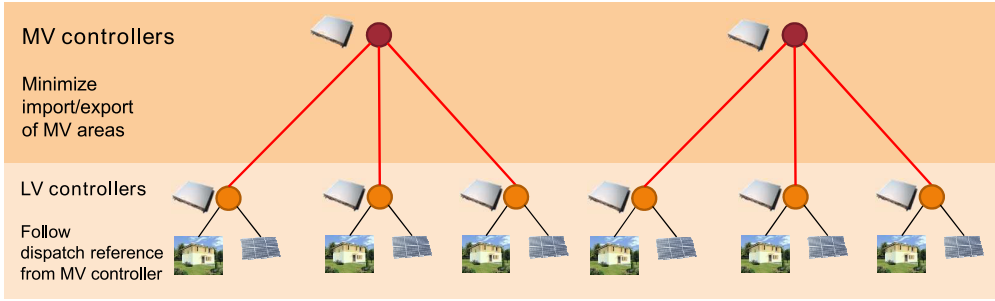

Figure 6.1: LV and MV levels of the proposed DSM concept.

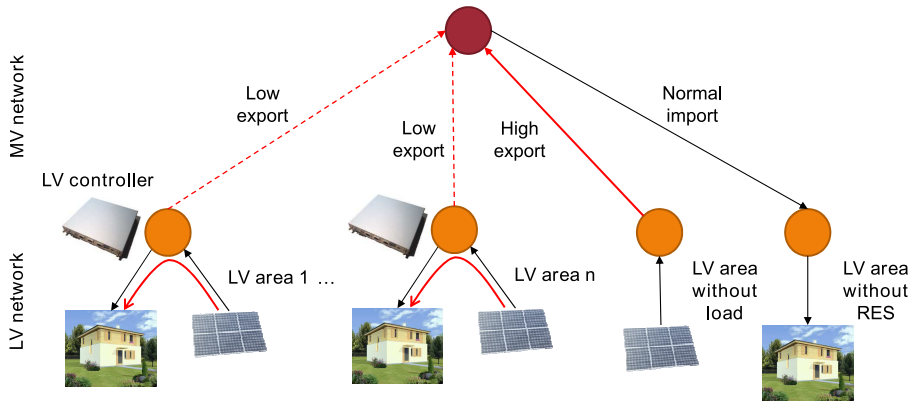

(a) : Autonomous operation.

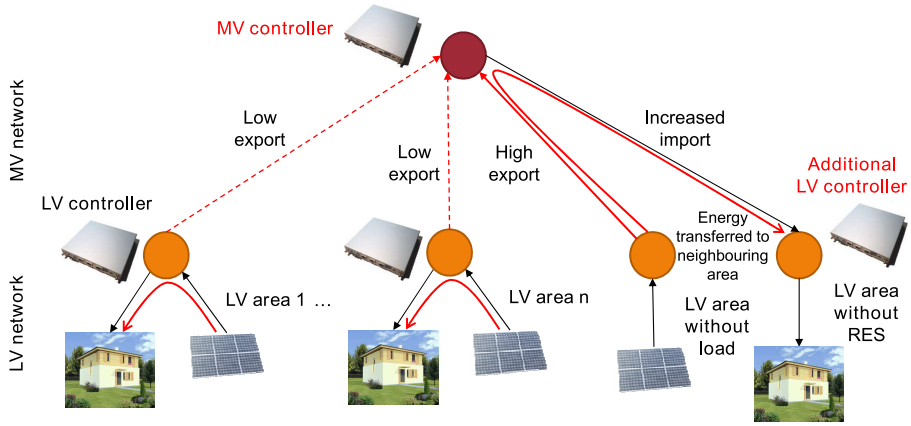

(b) : Hierarchical operation.

Figure 6.2: Operation of MV network with the proposed DSM system in autonomous and in hierarchical operation mode.

MV controller in place, it is beneficial to install the LV controller also in LV areas with no or low amount of RES sources. The MV controller may instruct such LV areas to decrease or increase their load based on RES production in the neighbouring areas, making them contribute to achieving the control target of the whole MV interconnection.

As explained above, the cooperation between the MV controller and the LV controllers is ensured in a way that the dispatch references are generated by the MV controller instead of the individual LV controllers. As such, it modifies the

sequence of the individual actions performed by the MV DSM system compared to that of the LV DSM system presented in Section 5.1 in the following way:

1. *Generation of power balance prediction:* Prediction of the power balance of the MV area (i. e. the difference between the predicted energy production and the predicted load in the area) for a selected horizon (e. g. 48 hours) is computed by the MV controller based on predictions received from each LV area.

2. *Dispatch reference optimization:* Based on the current EWHs state estimates received from the LV controllers and the aforementioned power balance prediction, the dispatch reference (i. e. the power balance of the MV area with optimal distribution of EWHs load in all LV areas according to the selected criterion) is computed and passed on to the appropriate LV controllers.

3. *Dispatch schedules optimization:* With a specified frequency (e. g. 5 minutes) the following steps are performed by the LV controllers, similarly to the receding horizon optimization principle, until new relevant information for the power balance prediction of the MV area are available:

   i) The power balance prediction of the LV area is updated with measured or estimated instantaneous power balance.

   ii) The optimal dispatch schedules of each EWH (i. e. switching schedules of the controlled EWHs, such that the difference from the dispatch reference is minimized) for a shorter time interval (e. g. 6 hours) are computed and sent to the household units.

   iii) First action in the EWH dispatch schedules is executed in each household unit. The rest of the dispatch schedule is kept in a household unit and used only in case of the failure of communication with the LV controller.

4. *Power balance prediction update:* If new information used for the power balance prediction of the MV area is available (e. g. a new weather forecast) the process is repeated from the step 1. Typically, this would happen several times a day.

The above process is illustrated in Fig. 6.3, in particular, it compares how the process changes when the DSM system operates in the autonomous mode (Fig. 6.3a) and in the hierarchical mode (Fig. 6.3b).

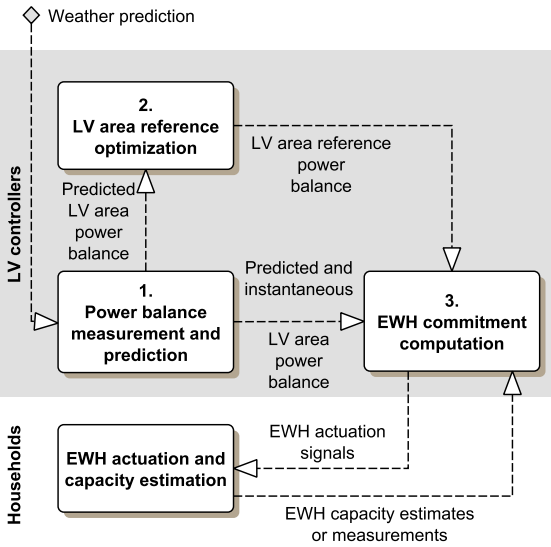

(a) : Autonomous operation mode.

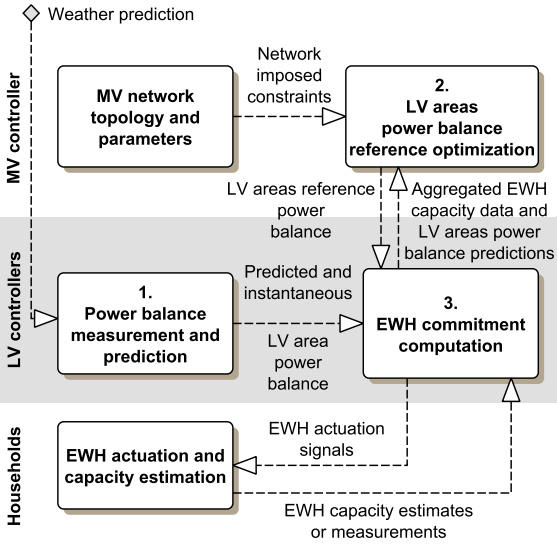

(b) : Hierarchical operation mode.

Figure 6.3: Detailed description of the DSM system operation in different operation modes.

As may be also seen in Fig. 6.3b, in the hierarchical operation mode, the system needs to perform additional communication in order to coordinate actions of the MV controller and the LV controllers. This communication involves sending aggregate power balance predictions, EWH state estimates and water consumption predictions from each LV controller to the MV controller and distribution of the dispatch references from the MV controller to the LV controllers. Although the amount of data that needs to be transmitted is higher compared to the autonomous operation mode, the overall communication requirements remains low since, as already mentioned, the dispatch reference optimization is only performed several times a day. Moreover, this communication is non-critical for the system operation because the LV controllers may still work with the previous dispatch reference in case the distribution of new dispatch references is delayed.

6.2 Optimization problem formulation

As noted in the previous section, the responsibility of the MV controller is to compute the dispatch references for the individual LV areas. This task was facilitated by integrating the DSM constraints into power system simulator [66]. The simulator provides means to perform the optimization of the MV network while respecting the transmission constraints by employing DC load flow modelling of the MV network. This section will therefore explicitly describe only required modifications and extensions of the simulator; the remaining constraints may be found in [66]. As mentioned above, the generation of dispatch schedules for individual EWHs remains a responsibility of the LV DSM systems even in the hierarchical mode and is therefore a solution of the optimization problem formulated in Section 5.2.2. For this reason, it will not be repeated in this section.

The hierarchical composition of the system also allow the MV controller to only optimize the MV level of the controlled part of the distribution network when computing the dispatch references. Control of the network elements at the LV level of the network is a responsibility of the corresponding LV controller. As a result, the LV areas were represented by aggregate values of uncontrolled load, PV sources generation and EWH characteristics (i. e. controllable part of the load). The network model used in computation of dispatch references by the MV controller therefore comprises:

- a *slack bus* modeling the point of interconnection of the MV network with the HV network,
- *MV transmission lines*,
- *other buses* representing interconnection of the MV network and LV networks (i. e. MV distribution substations where the LV controllers are located).

In order to use the simulator [66] for optimization of dispatch references of LV areas, the objective had to be modified to reflect the control target, i. e. to maximize local utilization of the energy produced by the PV sources in the whole MV area. To achieve this goal, a quadratic criterion penalizing energy flows through a slack node was chosen for the following reasons:

- As opposed to the linear criterion 5.2 used in the LV DSM system, the quadratic criterion not only penalizes import and export peaks but also amount of imported and exported energy. Basically, it ensures minimizing export and import of the area whenever possible, whereas the linear form of criterion 5.2 does not penalize imports and exports that are lower than the achievable import or export peak, but could have been avoided by proper distribution of the EWH load.
- The utilization of the quadratic criterion is made possible since it is reasonable to expect that the MV controllers will be formed by more computationally capable computers since their number is much lower than that of the LV controllers. As a result, this will not dramatically increase the system roll-out costs, but will allow to solve more complex optimization problems in the MV controller.

Moreover, additional element penalizing the loading of the lines in the MV area was added to the objective in order to further accentuate the requirement to consume the produced energy as close to the point of its production as possible so that the line loading and associated voltage fluctuations in the MV area are reduced. The resulting problem formulation may be summarized as follows:

minimize

$$\sum_{k}\left[c_{slack}\cdot P_{slack}^{2}\left(k\right)+c_{lines}\cdot\sum_{l}\left(\frac{P_{l}\left(k\right)}{P_{l,max}}\right)^{2}\right], \tag{6.1}$$
$$k=1\ldots N_{S},$$
$$l=1\ldots N_{L},$$

subject to

(DC load flow constraints [66])

(LV areas balance constraints)

$$\hat{B}_{A,j}\left(k\right)=\hat{D}_{A,j}\left(k\right)-\hat{G}_{A,j}\left(k\right)+P_{A,j}^{EWH}\left(k\right), \tag{6.2}$$
$$0\leq P_{A,j}^{EWH}\left(k\right)\leq P_{Atot,j}^{EWH}, \tag{6.3}$$
$$k=1\ldots N_{S}.$$

(LV areas EWH energy constraints)

$$\hat{E}_{A,j}^{EWH}\left(k+1\right)=\hat{E}_{A,j}^{EWH}\left(k\right)+P_{A,j}^{EWH}\left(k+1\right)\cdot T_{S}\left(k+1\right)-\hat{E}_{Aconsumed,j}^{EWH}\left(k+1\right), \tag{6.4}$$

$$\hat{E}_{Amin,j}^{EWH}\leq\hat{E}_{A,j}^{EWH}\left(k\right)\leq\hat{E}_{Amax,j}^{EWH} \tag{6.5}$$
$$0.9\cdot\hat{E}_{A,j}^{EWH}\left(0\right)\leq\hat{E}_{A,j}^{EWH}\left(N_{S}\right)\leq1.1\cdot\hat{E}_{A,j}^{EWH}\left(0\right) \tag{6.6}$$
$$k=0\ldots N_{S}-1,$$

where

$P_{slack}, P_{l}, \hat{B}_{A,j}, P_{A,j}^{EWH}, \hat{E}_{A,j}^{EWH}$ are continuous decision variable vectors,
$\hat{D}_{A,j}, \hat{G}_{A,j}, T_{S}, \hat{E}_{Aconsumed,j}^{EWH}$ are real number vectors,
$c_{slack}, c_{lines}, P_{l,max}, P_{Atot,j}^{EWH}, \hat{E}_{Amin,j}^{EWH}, \hat{E}_{Amax,j}^{EWH}$ are real number scalars,
j is LV area index, $j=1\ldots N_{A}$,
k is time index (bounds given in each constraint set),
N_{S} is number of samples in the optimization horizon,
N_{L} is number of lines in the MV area,
N_{A} is number of the controlled LV areas.

The term c_{slack} represents an objective weight of the energy flows P_{slack} [kW] between the MV and HV areas. The term c_{lines} is an objective weight of the line flows P_{l} relative to their maximal loading $P_{l,max}$. The equation (6.2) states that

the power balance of the LV area $\hat{B}_{A,j}$ [kW] is obtained by subtracting the predicted aggregate PV sources generation in the area $\hat{G}_{A,j}$ [kW] from the predicted aggregate uncontrolled demand of the area $\hat{D}_{A,j}$[kW] and adding aggregate instantaneous power of the controlled EWHs $P^{EWH}_{A,j}$ [kW]. The equation (6.3) complements the power balance equation by specifying bounds on the aggregate EWH power input, i. e. the power input has to be higher than zero (no EWHs are committed) and lower than $P^{EWH}_{Atot,j}$ [kW] which represents the total power input of all controlled EWHs in the area.

The estimated aggregate amount of energy stored in the EWHs in the LV area $\hat{E}^{EWH}_{A,j}$ [kWh] in each time sample is given by the constraint (6.4) where $T_S\,(k)$ [h] is the length of the time sample k and the term $\hat{E}^{EWH}_{Aconsumed,j}\,(k)$ [Wh] denotes the energy of water that is expected to be consumed in time k by all households with EWH in the LV area. The expected water energy consumption also includes estimated heat losses of EWHs. The term $\hat{E}^{EWH}_{A,j}\,(0)$ represents the estimated initial energy stored in the EWHs in the LV area at the beginning of the optimization horizon. The energy stored in the EWHs in the LV area is constrained according to equation (6.5). The maximal amount energy that the EWHs in the LV area are capable of storing is given by summing up the maximal capacities of the individual EWHs $\hat{E}_{max,i}$ [kWh] which are defined according to (5.10), i. e. they are equivalent to electrical energy consumed by the EWH to heat volume of water contained in the EWH V_i [l] from feed-in water temperature $t_{in,i}$ [°C] to the desired temperature given by the thermostat setting $t_{out,i}$ [°C]. While in practice, the minimal energy in the EWHs in the LV area $\hat{E}^{EWH}_{Amin,j}$ [kWh] should be equal to zero (which represents a state when temperature of water in all EWHs is equal to the feed-in water temperature $t_{in,i}$), depending on the EWH energy estimation quality, it might be necessary to set $\hat{E}^{EWH}_{Amin,j}$ to a non-zero positive value as a safety margin to avoid hot water depletion as explained in Section 5.2.1.

Finally, the constraint (6.6) ensures that the aggregate energy stored in the EWHs in the LV area at the end of the optimization horizon does not differ significantly from the value at the beginning of the optimization. This compensates for the lack of foresight that the optimizer has at the end of the optimization horizon and prevents it from letting the EWHs deplete in order to improve the objective value.

6.3 Network used for medium voltage demand side management system simulations

In order to test the MV DSM system performance, its operation was simulated on a part of an existing MV network in the Czech Republic. The topology of the selected network is shown in Fig. 6.4 and its main characteristics are given in Table 6.1. The topology of the network is simplified in a way that it only contains connections on a MV level. Each node in the network represents one LV area (one of which is the pilot installation network) and presence of the LV controller in each such LV area is assumed. As may be seen, the penetration of the PV sources in the network is high, with the peak PV power reaching 2 MW, which is twice the maximal observed uncontrolled load. The network is also appropriate for comparison of the autonomous and hierarchical operation mode of the DSM system since it contains LV areas with high amount of RES as well as areas where RES are almost non-existent.

Unlike for the LV network used for simulations of the LV DSM system, where information on distribution tariff, yearly consumption EWH parameters and CRC schedule was available for each household, for the MV network, more aggregated data consisting of number of households using a given distribution tariff, total yearly consumption of these households and total number of EWHs was available for each node (LV area). In order to estimate the yearly consumptions of individual households, a distribution function obtained from yearly consumptions of households with the given tariff from the pilot installation network was applied to the aggregated data under the assumption that distribution of households among the different tariffs will be roughly the same in all LV areas. Also, since only the number of EWHs was known for each LV area, the aforementioned principle was also applied in order to obtain power inputs, volumes and CRC

Nominal voltage	22 kV
Number of buses	66
Number of lines	65
Number of households	1720
Number of EWHs	805
Aggregate PV sources peak power	2107 kW
Aggregate peak uncontrolled load	1044 kW
Aggregate peak EWHs power input	1704 kW

Table 6.1: Characteristics of the MV network.

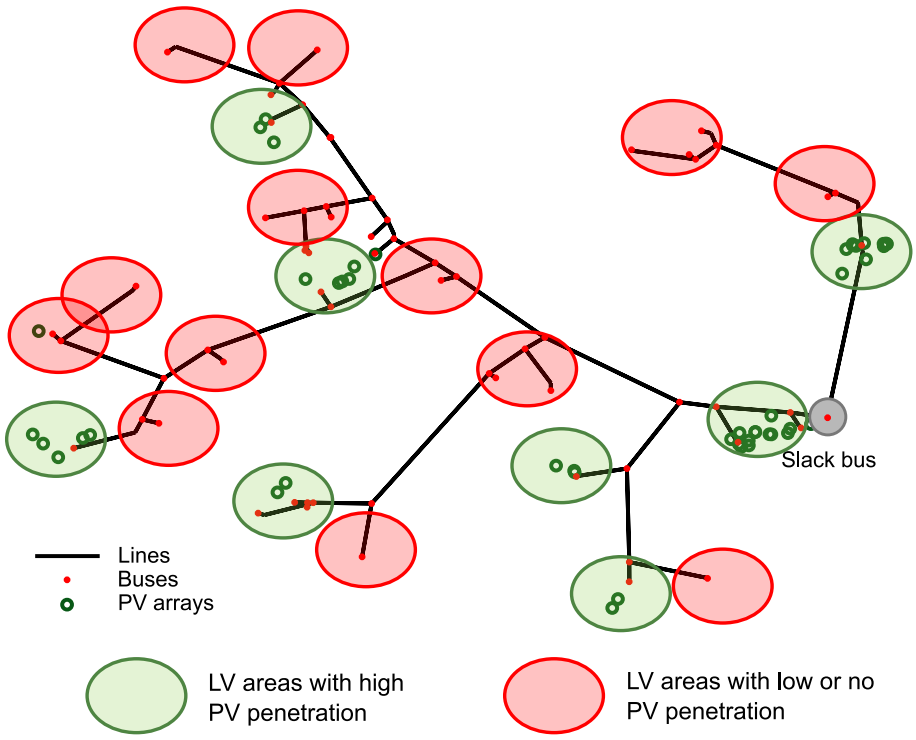

Figure 6.4: Topology of the MV network.

schedules of the EWHs in each LV area. The locations and peak power of the PV sources in the MV area were obtained from the energy production licenses available at [67].

6.4 Case study

The performance of the DSM system in the hierarchical operation mode was evaluated based on model of the network as shown in Fig. 6.4 using simulation process described in Section 5.6. Unlike in simulations of the autonomous operation of the DSM system in the LV network, no additional sensors in EWHs were considered in simulations; the EWH state estimation was performed based on principles described in Section 5.3.2.1 utilizing overall household consumption data with 1-minute resolution.

In order to show the advantages of the hierarchical operation mode of the DSM system compared to the autonomous operation and also to the current state of the controlled network, the following cases were simulated:

- **Case 1: Centralised ripple control.** This test case is the reference case representing the current situation in the selected MV area. The EWHs are controlled remotely according to their tariff by the centralised ripple control (CRC).
- **Case 2: Autonomous operation mode.** In this case, the EWHs are controlled by LV DSM systems. The LV DSM systems operate autonomously as described in Section 5.1.
- **Case 3: Hierarchical operation mode.** The operation of the LV DSM systems is coordinated by the MV controller.

The Fig. 6.5 compares the resulting MV area power balances, aggregate load of EWHs and aggregate energy stored in the EWHs in the test cases while the Table 6.2 gives overview of selected performance characteristics.

The first conclusion that may be drawn from the results is that both variants of DSM systems perform noticeably better than the CRC in terms of supporting local consumption of RES produced energy. Comparison of the case with CRC to the balance without EWHs in the Fig. 6.5a reveals that the CRC do not reduce exports from the area and even increase peak imports to the area. As described in Section 5.4.2, this originates from the fact that the CRC schedules cannot be flexibly set to make them more appropriate for areas with high RES penetration and as a result, the EWH heating periods do not coincide with periods of high RES production as may be observed in Fig. 6.5b and Fig. 6.5c.

Comparison of the autonomous and hierarchical variants of the DSM system confirms the assumption that the hierarchical DSM system allows to better exploit energy storage capabilities of all LV areas including areas with low RES penetration. By using areas with low RES penetration to store energy surplus from the areas with high RES penetration, the hierarchical DSM system was capable of almost eliminating the energy exports from the MV area. The peak export was reduced by 79% and exported energy was reduced by 92% compared to the case with CRC. The autonomous variant of the DSM system was less effective in this respect with peak export reduction of 45% and energy export reduction of 60%. These conclusions are also supported by Fig. 6.5d which shows that the hierarchical DSM system was able to exploit wider range of the EWH storage capacity compared to the autonomous system. The import

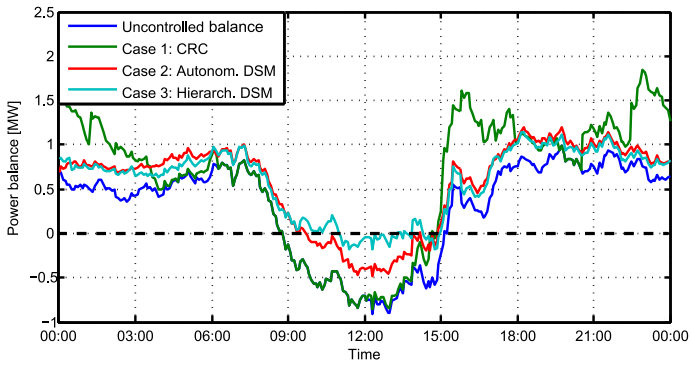

(a) : Power balance of the MV area.

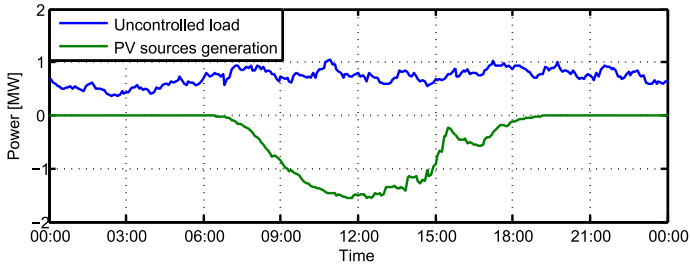

(b) : Details of uncontrolled load and PV sources generation.

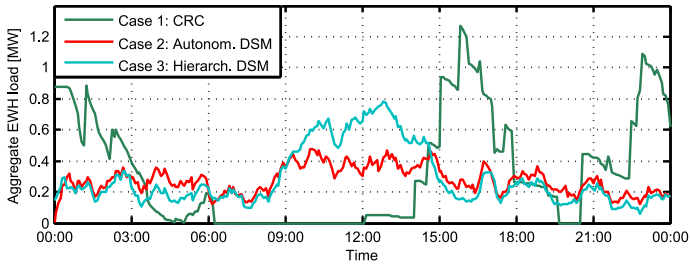

(c) : Aggregate EWHs load.

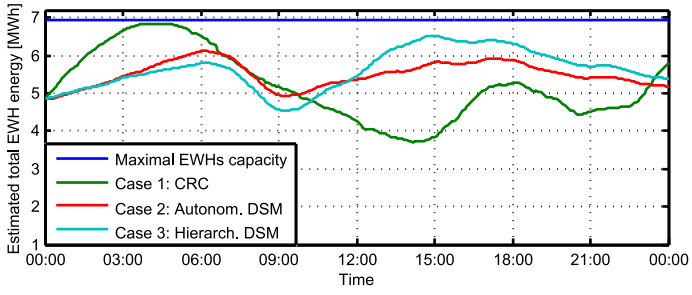

(d) : Energy stored in the EWHs.

Figure 6.5: Comparison of DSM systems performance in a MV network.

Case	1	2	3
Export peak [MW][a]	0.85	0.48	0.18
	100%	56.5%	21.2%
Import peak [MW]	1.84	1.19	1.14
	100%	64.7%	62.0%
Peak import to peak export [MW]	2.70	1.68	1.32
	100%	62.2%	42.9%
Exported energy [MWh]	3.10	1.23	0.26
	100%	39.7%	8.4%
Imported energy [MWh]	18.14	15.14	14.50
	100%	83.5%	79.9%

[a]The percent values represent relative value to the case with EWHs controlled by time-of-use tariffs.

Table 6.2: Comparison of performance characteristics of the DSM system in the MV network.

characteristics are comparable in both variants of the DSM system since they are mostly influenced by the uncontrolled load and both variants of the DSM system ensured levelled EWH load outside the RES production periods in order to not contribute to the import peaks.

In order to show how the MV DSM system influences power quality in the simulated MV network, an AC load flow analysis of the simulation network was performed. Selected load flow analysis results are summarized in Tab. 6.3. They indicate that the studied network is well dimensioned and even in the case when the EWHs are controlled by the CRC, the maximum loading of the distribution lines reaches only 24 % of the respective line capacity. Despite this fact, the benefits of the DSM system are clearly observable since it was capable of reducing the maximal line loading to around 16 % in case of the autonomous operation and to about 15 % in the hierarchical operation, i. e. the line loading was reduced by 33 % and 37 % respectively. The influence of the DSM system on line loading is also shown in Fig. 6.6, which compares line loading of the studied network at the time of peak PV production and at the time of maximal consumption in the three simulation scenarios. As expected, when the DSM system is in operation at the time of peak PV production, the loading of the lines within the MV network is increased since the energy from PV sources, which are mainly located near the HV/MV transformer (slack bus), needs to be

Case	1	2	3
Maximal line load [%][a]	23.9	15.8	15.1
Maximal voltage [V]	22 021	22 012	22 006
Minimal voltage [V]	21 823	21 884	21 898
Max-to-min voltage [V]	198	129	108

[a]The percent values represent relative value to the respective line capacity.

Table 6.3: Results of load flow analysis of the MV network with the DSM system.

transferred to the EWHs. Conversely, at the time of maximal consumption, the DSM system significantly reduces the the loading of the lines since the EWHs were already charged at the time of peak PV production. Overall, the DSM system ensures substantially more uniform loading of the distribution lines over the day.

The reduction of line loading also manifests itself in reduction of voltage volatility. While in the case of CRC control, the difference between the maximal and minimal observed voltage in the network reached 198 V, it was reduced to 129 V in case of the DSM system in autonomous mode and to 108 V in case of the hierarchical operation mode. Again, the observed voltage variations are relatively small, being under 1 % of the nominal voltage (22000 V).

It should be noted, that the benefits of the DSM system were not as pronounced in case of the MV network under study since it is very compact (the whole area fed by the network is around 40 square kilometres), the lines are well dimensioned and the penetration of RES sources is such that the network parameters are within permissible limits even without the DSM system. To test how effective the MV DSM system would be in case of networks with worse dimensioning or in networks where more RES sources are installed, two additional scenarios resulting from modifications of the MV network explained in Fig. 6.7 were also simulated:

1. *Dimensioning scenario*, where the line connecting the larger part of the network to the HV/MV transformer was supposed to be 5 times longer, i. e. its length was increased from 360 m to 1800 m and its parameters were modified accordingly. Moreover, it was assumed that all the lines have 50% higher resistance and reactance.

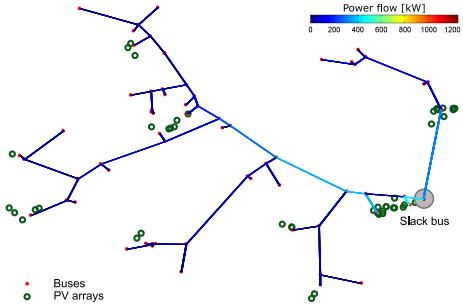

(a) : CRC control (maximal production).

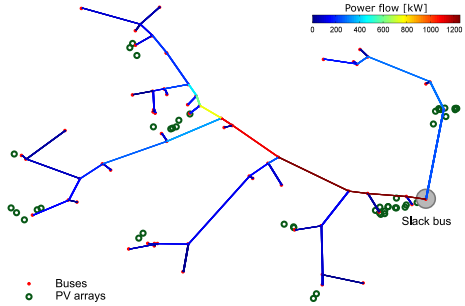

(b) : CRC control (maximal load).

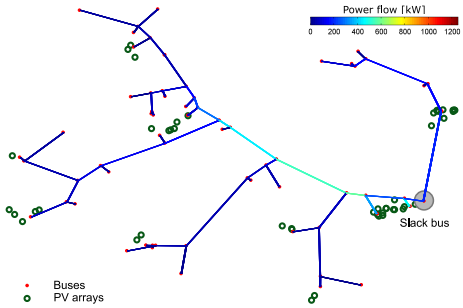

(c) : Autonomous mode (maximal production).

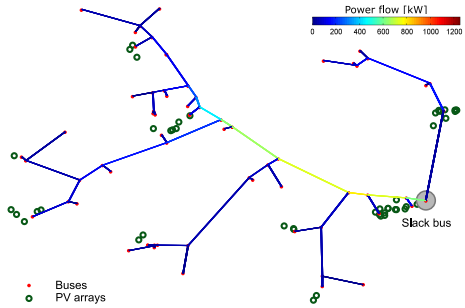

(d) : Autonomous mode (maximal load).

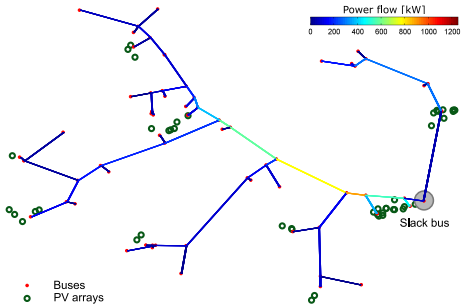

(e) : Hierarchical mode (maximal production).

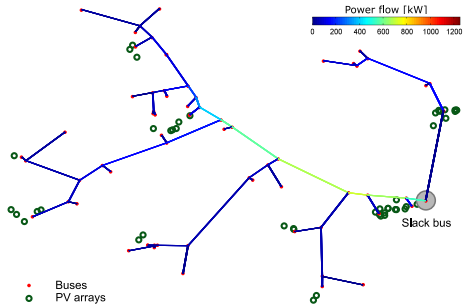

(f) : Hierarchical mode (maximal load).

Figure 6.6: Comparison of line loading in different operation modes at time of maximal production and maximal load.

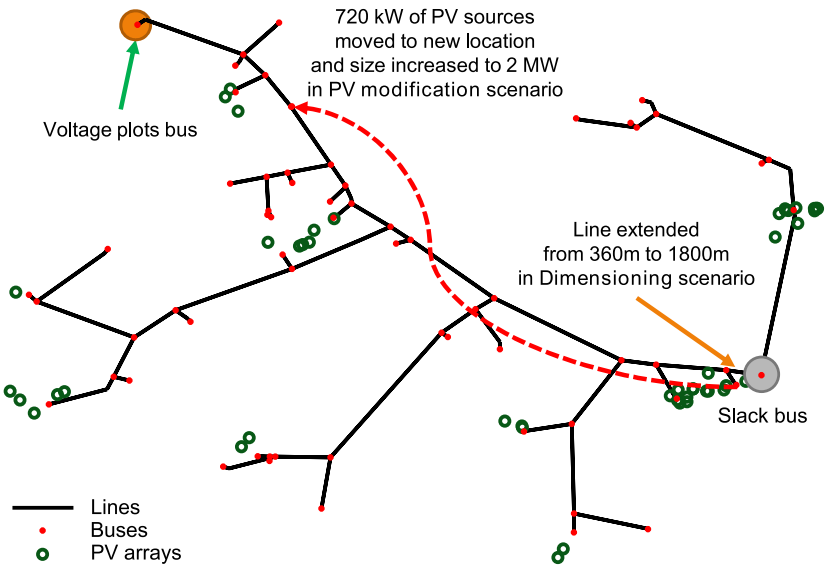

Figure 6.7: Modifications of MV network carried out in the alternative power flow analysis scenarios.

2. *PV modification scenario* in which the line parameters were not altered, but the largest PV array located near the HV/MV transformer was moved further downstream the network and its size was increased from 720 kW to 2 MW.

Load flow analysis of these scenarios is compared to the results of the original load flow analysis (as shown in Tab. 6.3), which is always denoted *nominal* in all comparisons. In the comparison tables, the term *Scenario* denotes the power flow analysis scenario (*Nominal, Dimensioning* or *PV modification*) while the term *Case* denotes the MV DSM operation mode (*Case 1: CRC, Case 2: Autonomous operation mode, Case 3: Hierarchical operation mode*).

Naturally, in the *Dimensioning* scenario the modified line parameters do not influence how the DSM system distributes the EWH load, since the uncontrolled load and PV sources generation remain the same. For the *PV modification* scenario, new simulations of the DSM system needed to be performed in order to determine, how the change in location and size of the PV sources would affect the way the DSM system optimizes the EWH operation. The resulting power balance of the MV area in this scenario is presented in Fig. 6.8 and the relevant performance characteristics are shown in Tab. 6.4. The results indicate that

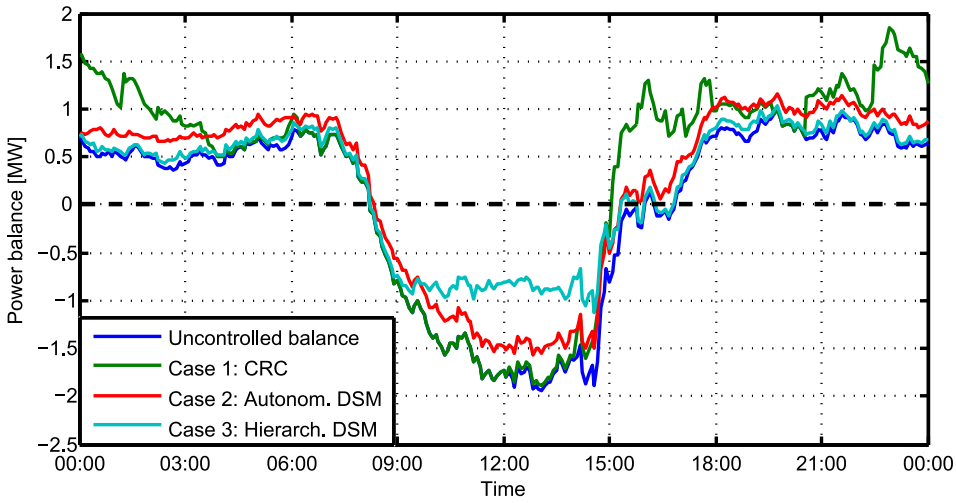

Figure 6.8: Power balance of the MV area in scenario with PV sources modification.

Case	1	2	3
Export peak [MW][a]	1.89	1.58	1.13
	100%	83.6%	59.8%
Import peak [MW]	1.84	1.16	1.03
	100%	63.0%	56.0%
Peak import to peak export [MW]	3.75	2.74	2.16
	100%	73.1%	57.6%
Exported energy [MWh]	9.16	7.70	5.49
	100%	84.1%	59.9%
Imported energy [MWh]	16.73	13.35	10.63
	100%	79.8%	63.5%

[a]The percent values represent relative value to the case with EWHs controlled by time-of-use tariffs.

Table 6.4: Comparison of performance characteristics of the MV DSM network in scenario with PV sources modification.

in this scenario, the EWHs cannot store all the energy produced in the area, however, the resulting energy imports and exports of the controlled MV area are

Scenario	Nominal			Dimensioning			PV modification		
Case	**1**	**2**	**3**	**1**	**2**	**3**	**1**	**2**	**3**
Maximal voltage [V]	22 021	22 012	22 006	22 032	22 019	22 009	22 179	22 158	22 125
Minimal voltage [V]	21 823	21 884	21 898	21 661	21 778	21 811	21 840	21 891	21 909
Max-to-min voltage [V]	198	129	108	371	241	198	339	267	216

Table 6.5: Results of load flow analysis of the modified MV DSM scenarios.

still considerably reduced in comparison to the CRC control. More specifically, the import and export peaks are reduced by more than 40 % in case of the hierarchical operation mode and by 37 % and 16 % respectively in case of the autonomous operation mode. The amount of imported and exported energy was again reduced by approximately 40 % by the DSM system in hierarchical operation mode and by 20 % and 16 % respectively in case of the autonomous operation mode.

The Tab. 6.5 presents selected results of the load flow analysis of all the scenarios. Namely, it shows the maximal and minimal voltages that were experienced in the MV network at any time and place. Also the difference of these values is presented, expressing the total voltage range in which the whole MV network operates. As expected, the Tab. 6.5 indicates, that this voltage range is significantly increased in both alternative scenarios compared to the nominal one. The effects of the DSM system in the different scenarios on voltage are also illustrated in Fig. 6.9 which shows simulated voltage at a terminal node denoted *voltage plots bus* in Fig. 6.7. Being a terminal node this node is one of the most susceptible to voltage fluctuations brought about by changes of feeding lines loading.

In the *dimensioning* scenario, the observed minimal voltage drops as with longer and less conductive lines, higher voltage drops are experienced, especially at the time of peak load. Compared to the nominal scenario, the difference between the maximal and minimal voltage increases by 173 V in case of CRC control, by 112 V in case of autonomous operation mode of the DSM system and by 90 V in case of the hierarchical operation mode. Hence, the benefit of the DSM system clearly becomes evident. The operation parameters in terms of voltage are approximately the same in case of hierarchical operation of the MV DSM system in the worse dimensioned network as they are with the CRC in the original well-dimensioned network. The increased voltage fluctuations are also illustrated in Fig. 6.9b. Since as already mentioned, in this scenario, the load and injections at each node are the same as in the nominal scenario, the

shape of the voltage curve remains the same, however range in which the voltage fluctuates is increased.

In the *PV modification scenario* it is the maximal observed voltage in the MV network which is increased compared to the nominal scenario as a result of substantial reversed flows from the PV sources to the HV/MV transformer since all the produced energy could not be consumed locally. Similarly to the previous scenario, the most noticeable increase of maximal to minimal voltage range is experienced in case of the CRC with the increase being 141 V. In case of DSM system in the autonomous operation mode, the increase over the nominal scenario is 138 V and finally in the hierarchical operation mode, the increase reduces to 108 V. The Fig. 6.9c presents how the voltage volatility increases at the terminal node under study in the PV modification scenario. It may be observed that the voltage at this node increases markedly over the nominal voltage as a result of the aforementioned reversed flows. Again the voltage volatility in case of the scenario with increased amount of PV sources and EWHs controlled by the MV DSM system in the hierarchical operation mode is roughly equivalent to the CRC control in nominal scenario. The result indicates, that the DSM system could allow to install more RES into the network without the need to increase the dimensioning of the distribution lines.

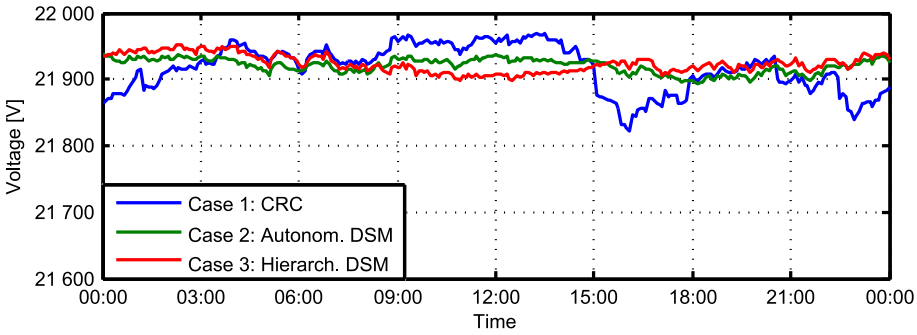

(a) : Nominal scenario.

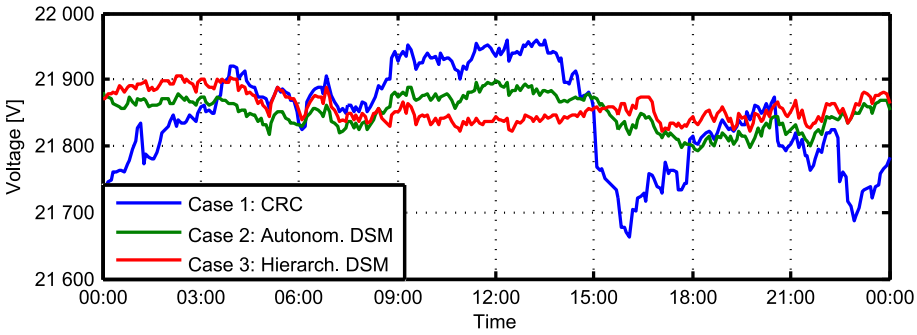

(b) : Dimensioning modification.

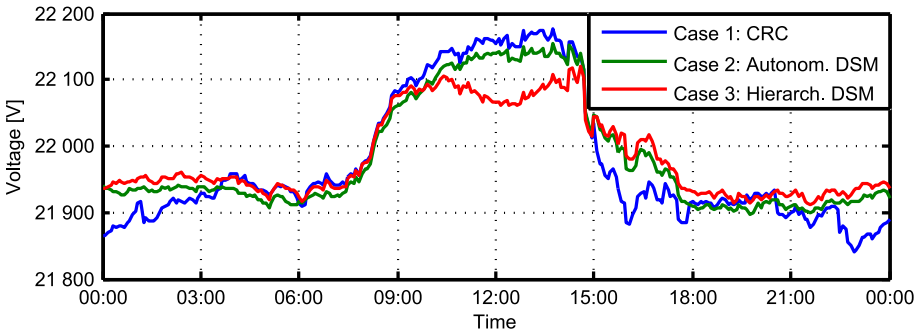

(c) : PV sources modification.

Figure 6.9: Illustration of voltage volatility reduction in the MV network.

Chapter 7

Provision of the DSM capabilities to the transmission system operator

In the previous text it was mentioned that the design of the proposed DSM system is flexible enough to be able to perform wide range of tasks, including provision of ancillary services to the TSO. By aggregating sufficient number of areas where the DSM system is installed, a significant volume of load increase potential can be offered to the TSO as concluded in the DSM potential analysis shown in Section 3.3.2.1. It should be also noted, that the load increase (or generation decrease) service is recently much more frequently utilized than it was in history as a direct result of increasing penetration of renewable energy sources, which under certain conditions may bring about situations when the generation exceeds load.

However, unlike typical ancillary services which are in most cases provided in form of reserving of part of the generator capacity to be used by the TSO, utilizing DSM resources for ancillary services has an important restriction that the controlled appliances primary purpose is not to be a service for the TSO but rather satisfy the needs of their users. As a result, in order for the DSM to be used to provide ancillary services while respecting the constraints imposed by the utilization patterns of the controlled appliances, these constraints need to be reflected in a way how the DSM resources are used by the TSO.

Since it may be inconvenient or even impossible for the human TSO operators to incorporate these constraints into the way they decide when to activate ancillary services, which services to activate and for how long (especially in case that a large number of DSM aggregators offered their services to the TSO), a use of an automated control system or advisory system is envisaged. This links the proposed DSM system with an earlier work that dealt with designing a

decision support system that was intended to help TSO dispatcher to reduce costs of ancillary services activation by computing cost-optimal ancillary services activation schedules. With a small modification, the system may be used to recommend when to activate the DSM-based ancillary services while respecting the aforementioned constraints that they may have.

The original decision support system along with a case study that showed how such a system influences costs for ancillary services activation was presented in the author's article [68] that was published in International Journal of Electrical Power & Energy Systems.

This chapter is divided into the following sections: First, the basic principles of cooperation of all three levels of the proposed DSM system in order to be able to provide ancillary services to the TSO are briefly outlined in Section 7.1. Then, to provide insight into how the decision support tool functions and also to allow to better understand how it may be integrated with the DSM system, the basic principles of the decision support tool itself and its optimization problem formulation are described in Section 7.2. Finally, the Section 7.3 describes the modifications of the decision support tool and the MV and LV levels of the DSM system required to integrate the systems and a brief case study presenting an example of such integration is presented in Section 7.4.

7.1 Basic principles

As noted earlier, this section deals with a problem how the DSM capabilities could be offered to and also efficiently used by the TSO. The proposed integration concept is depicted in Fig. 7.1. As will be explained in more detail in Section 7.2.1, one of the tasks performed by the TSO is a load-frequency control, objective of which is to maintain an area control error (ACE) of its control area as close to zero as possible. This, explained in a simplified way, equals to keeping the exchange of energy with neighbouring control areas at a scheduled value or at zero if no exchange is scheduled. As a result, the task is very similar to a task dealt with in the LV and MV DSM systems.

In order to achieve this objective, the TSO uses control reserves in a form of ancillary services to compensate for unexpected changes of generation or load in its control area. The ancillary services are control reserves that allow to increase or decrease generation or increase or decrease load either automatically or at the command of the TSO dispatcher. The DSM fits in this scheme in a way that it can be offered to the TSO as load-increase ancillary service. Since the TSO

typically operates with much larger magnitudes of power than it was dealt with in the LV DSM and MV DSM systems (hundreds of megawatts or more instead of hundreds of kilowatts or several megawatts dealt with in the proposed LV DSM or MV DSM systems) an additional entity, a DSM capacity aggregator, is envisaged to provide a link between multiple MV DSM systems and the TSO so that the aggregate offered DSM capacity becomes interesting for the TSO.

The basic concept of integration of DSM into the load-frequency control is therefore as follows: The DSM capacity aggregator aggregates DSM capacity available in multiple areas equipped with the MV DSM system and offers the aggregated capacity to the TSO as an ancillary service. If the TSO decides to activate the ancillary service (for example with help of the presented decision support tool), it sends the activation request to the capacity aggregator, which further distributes the request among the MV areas in the aggregation. The MV controllers then compute dispatch references for the individual LV areas and the LV controllers then compute dispatch schedules for individual EWHs in a way similar to the concept presented in the preceding sections. The Fig. 7.2 illustrates the differences between operation of the MV DSM system with the original objective to minimize import/exports of the MV area and when it is

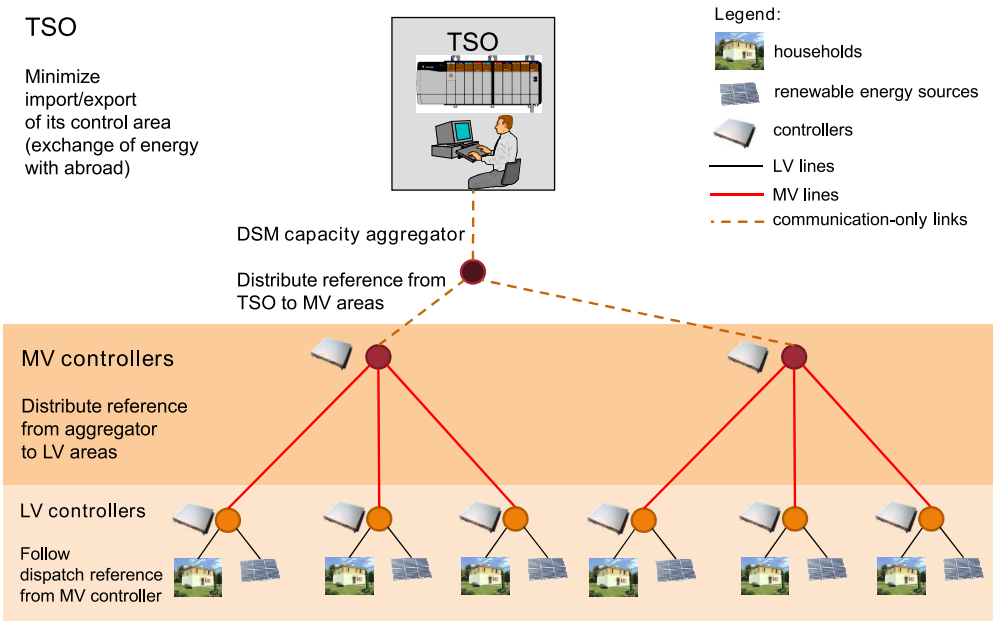

Figure 7.1: Cooperation of all levels of the proposed DSM concept.

used to provide the DSM-based ancillary service. The main differences between the two operation modes may be summarized as follows:

- Additional TSO control level is added. This control level generates requests to activate the DSM-based ancillary service.
- Since the TSO/DSM capacity aggregator requests to activate a specified aggregate EWH power, the MV controller computes references for aggregate EWH power of the LV areas instead of references for power balance of the LV areas that were generated by the MV controller with the original objective.
- The LV controllers do not use power balance predictions to compute dispatch of individual EWHs. The objective of the dispatch schedules optimization changes to achieving such aggregate power of EWHs in the LV area so that the EWH power reference of the given LV area is achieved.
- However, the LV controllers still compute power balance predictions of their LV area and send them to the MV controller, which uses them to compute the EWH power references for the LV areas with respect to the MV network transmission constraints and to minimize the MV lines loading.

As a result, the sequence of control actions of the DSM system is modified compared to the sequence used in the MV DSM system with the original objective presented in Section 6.1 to allow the cooperation of all the control levels. The modified control actions sequence is as follows:

1. *Update of current EWH states and EWH energy utilization predictions of the DSM-based ancillary services:* The DSM capacity aggregators send the current estimated aggregated EWH state estimates to the TSO along with EWH energy utilization predictions (i. e. the expected aggregated consumption of hot water).
2. *Ancillary services activation optimization:* The decision support tool takes information from the step 1 as one of its inputs and computes optimal activation of ancillary services that minimizes costs for reserve energy for a selected horizon (e. g. 6 hours).
3. *Distribution of aggregate EWH power references to the MV areas:* The DSM aggregator receives the required activation of the DSM-based ancillary service for the next period (e. g. 6 hours). If it is different from the existing reference, the aggregator distributes appropriate EWH power references to the MV areas that form the aggregation.

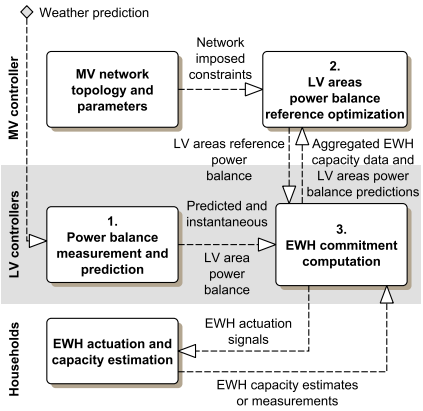

(a) : Minimization of import/exports of the MV area.

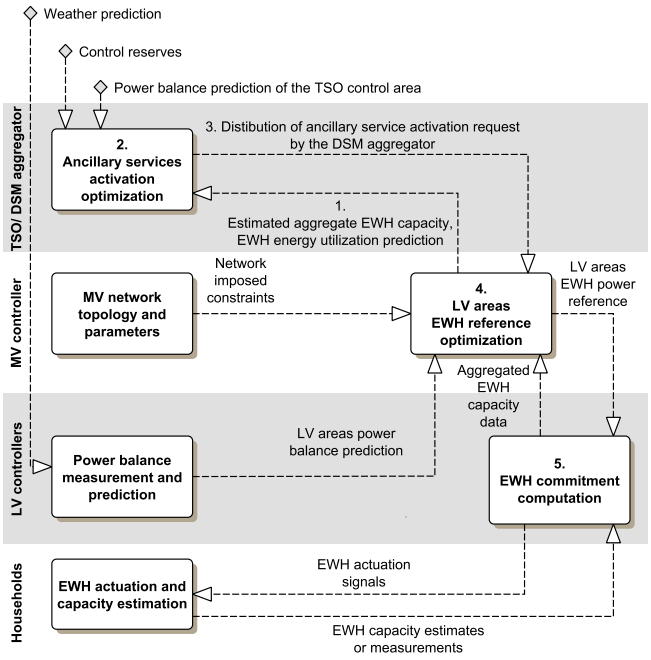

(b) : Provision of ancillary service.

Figure 7.2: Comparison of the DSM system operation MV DSM system with the original objective and when used to provide DSM-based ancillary service.

4. *EWH dispatch references optimization:* The MV controller computes EWH dispatch references for the individual LV areas so that the reference received from the DSM aggregator is achieved.

5. *Dispatch schedules optimization:* With a specified frequency (e. g. 5 minutes) the following steps are performed by the LV controllers until new reference from the MV controller is received:

   i) The EWH state estimates are updated based on the most recent information.

   ii) The optimal dispatch schedules of each EWH (i. e. switching schedules of the controlled EWHs, such that the difference from the EWH dispatch reference is minimized) are computed and sent to the household units.

   iii) First action in the EWH dispatch schedules is executed in each household unit. The rest of the dispatch schedule is kept in a household unit and used only in case of the failure of communication with the LV controller.

6. *Activation request update:* If the TSO needs to modify the required activation of the DSM-based ancillary service, the whole process is repeated from step 1.

It should be noted that detailed discussion of a role of the DSM capacity aggregator is out of scope of this thesis. For the purposes of this thesis, it is assumed, that the DSM capacity aggregator simply aggregates the DSM capacity of MV areas and then distributes the activation requests proportionally to the capacity offered by the given MV area.

7.2 Decision support tool and its optimization problem formulation

This section presents a more detailed description of load-frequency control performed by the TSO and how the decision support tool helps the TSO dispatchers to efficiently perform the given task. The principles of the decision support tool are explained in Section 7.2.1 and formulation of the optimization problem dealt with in the decision support tool is presented in Section 7.2.2. The presented information should help to better understand how the extension

of the decision support tool described later in this chapter, which allows the TSO to use the DSM-based control reserves, fits into the concept of the decision support tool. Additional information including how the decision support tool concept relates to other concepts presented in literature may be found in [68].

7.2.1 Principles of the decision support tool

Load-frequency control is an important control task, which maintains generation-demand balance in a transmission system and thus prevents large network frequency excursions and associated phenomena like load tripping or even black-outs. In large interconnected areas, such as the networks integrated in the European Network of Transmission System Operators for Electricity (ENTSO-E), the load-frequency control is a responsibility of the TSO in each control area. Fig. 7.3a shows a typical setting of a load-frequency control system for a single control area which complies with the policies in the Operation Handbook [69]. The load-frequency control is organised in three levels with different deployment times and a way the reserves are activated:

- **Primary control** is a distributed automatic control - the primary controller is located at each generation unit providing primary control reserve. Its action is proportional to a frequency deviation from a nominal frequency and the reserve must be fully deployed within 30 seconds of the incident which caused the frequency excursion.
- **Secondary control** is activated automatically by a central proportional-integral (PI) controller in each control area. The controller attempts to maintain the Area Control Error (ACE) at zero value, i. e. to balance the generation with load and scheduled export in the control area (Fig. 7.3a). The deployment of the reserve starts within seconds of an incident in the control area and the reserve must be fully deployed in no more than 15 minutes after the incident.
- **Tertiary control** encompasses all other control reserves different from primary and secondary control. Tertiary control reserves are usually under manual control of TSO's dispatchers and they are activated in order to free up the secondary control reserves.

The tertiary control reserves may be further divided into two categories according to a way they are activated:

- directly activated control reserves which may be activated at any time instant,

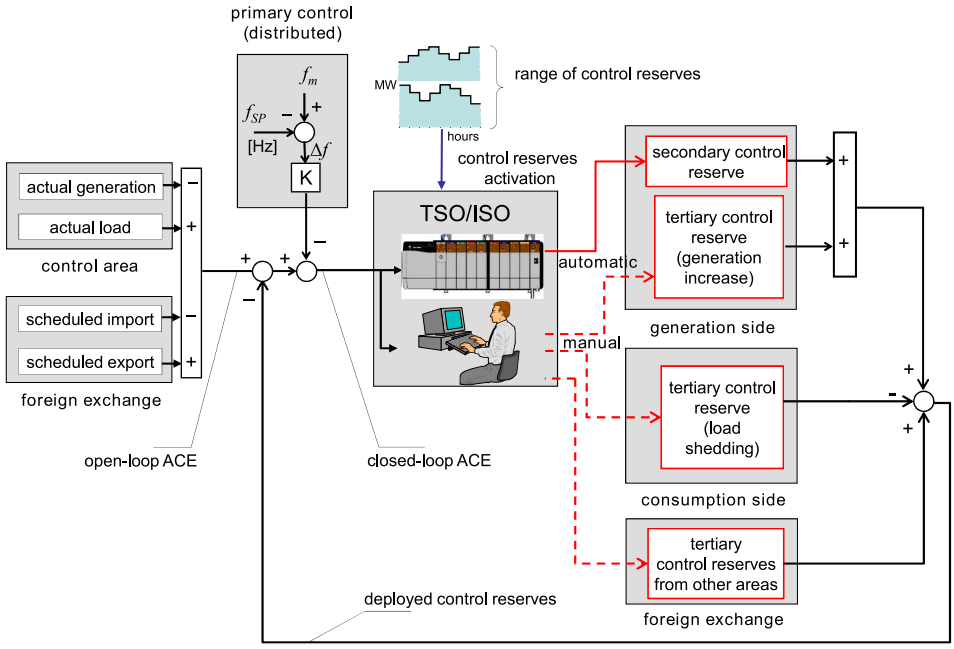

(a) : Typical load–frequency control system for a single control area in the ENTSO-E.

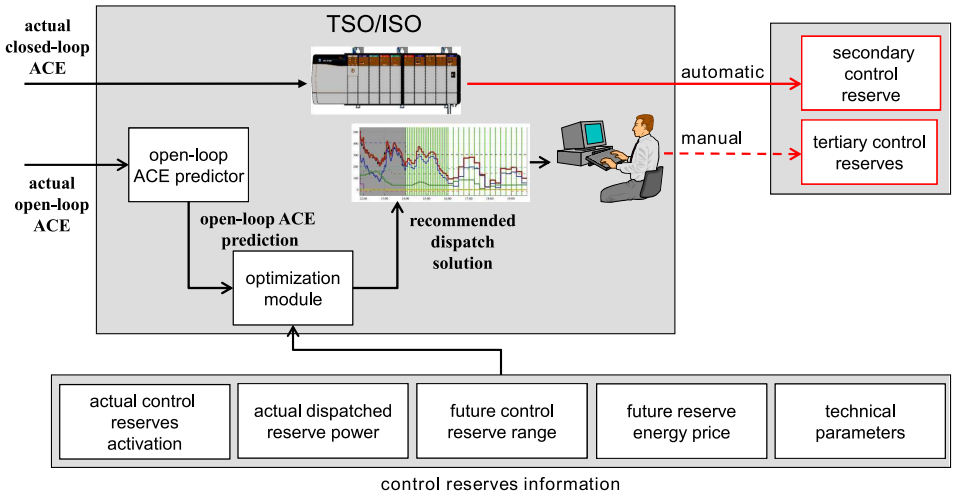

(b) : Proposed modification of tertiary control reserves dispatch procedure.

Figure 7.3: Load-frequency control principles and the proposed modification of tertiary control reserves dispatch.

- schedule activated control reserves which may be activated only in specific time instants (e.g. each hour), related for example to foreign exchange schedules etc.

Furthermore, the tertiary control reserves may be categorized according to their availability:

- spinning control reserves which are provided at generation units synchronized with the grid,
- non-spinning control reserves which are provided at generation units not synchronized with the grid, but are standing-by to be synchronized and deliver required power at the dispatcher's request.

Since pattern of utilization of the automatic primary and secondary control in the ENTSO-E is prescribed in the Operation Handbook [69], the presented decision support tool mainly deals with dispatch of tertiary control reserves. Dispatch of tertiary control reserves is done primarily with an aim to ensure secure operation of the transmission system, while the costs associated with utilization of the control reserves are traditionally of less importance. When making the decision which reserves to activate, several factors need to be simultaneously considered to perform the task in an economic manner, such as

- expected open-loop ACE (i. e. the ACE if no load-frequency control is performed as shown in Fig. 7.3a) in future minutes or hours,
- different prices of reserve energy from individual ancillary services providers versus their different time responses,
- limited energy capacity,
- other dynamic characteristics (activation delays, minimum up- and down-times, generation constraints etc.).

Making a decision which reserves to dispatch considering all the aforementioned factors is a difficult task for a human operator, especially because such a decision has to be made in very short time. The presented tool optimizes the dispatch of control reserves, so that the recommended control actions minimize the costs for the control reserves utilization and ensure secure operation of the transmission system at the same time.

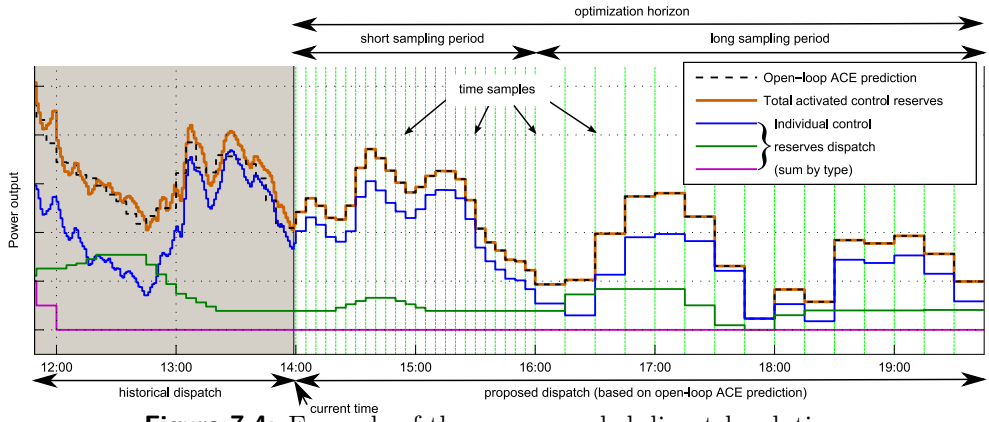

Figure 7.4: Example of the recommended dispatch solution.

The principles of the decision support tool are depicted in Fig. 7.3b, which illustrates the proposed modification of the TSO/ISO block in Fig. 7.3a. First, based on the actual open-loop ACE, the prediction of the open-loop ACE for the whole optimization horizon is generated. Then, the optimization module uses the prediction and information about control reserves to compute a cost-optimal dispatch of the tertiary control reserves which compensates the predicted open-loop ACE. The typical utilization pattern of the decision support tool would go as follows:

1. Based on the current state of the transmission system, a prediction of the open-loop ACE for the following 6 hours is generated.

2. The current state of the control reserves and their parameters are loaded into the optimization module.

3. The optimization is executed and the cost-optimal dispatch of the tertiary control reserves which compensates the predicted open-loop ACE is found.

4. The dispatch solution is visualised to the dispatcher (Fig. 7.4).

5. Actions from the first time-sample (i. e. the changes in the dispatch of the control reserves recommended for the following 5 minutes from the current time as shown in Fig. 7.4) are recommended to the dispatcher. The dispatcher then accepts the recommended actions or modifies them based on his evaluation of the current situation in the control area.

6. The whole process is repeated from step 1 in selected time intervals (e.g. 5 minutes) or at the dispatcher's command.

7.2.2 Decision support tool optimization problem formulation

The fundamental part of the decision support tool is the mixed-integer linear programming (MILP) based optimization module. MILP was selected for the problem formulation since using binary variables, it is possible to model nonlinearities dealt with in the problem. The optimization module incorporates models of tertiary control reserves and also model of secondary control, which is necessary to assess its influence on the load-frequency control in the control area (i. e. to determine when it is beneficial to dispatch tertiary control reserves to reduce load-frequency control costs or to determine when the secondary control reserve range is insufficient to compensate the predicted open-loop ACE). The primary control is not included in the optimization, since it is not used to compensate the ACE in the control area and is not operated by the TSO dispatch centre (Fig. 7.3a).

The arrangement of the optimization horizon used in the optimization of tertiary control reserves dispatch is shown in Fig. 7.4. The length of the optimization horizon is 6 hours, for which the open-loop ACE prediction may be obtained with reasonable accuracy and which allows optimization of control reserves with long deployment times or long minimal up and down times. The sampling of the optimization horizon is non-uniform with 5-minute sampling period for the first 2 hours and 15 minutes for the rest. Such a non-uniform sampling reduces problem complexity and computation time, while it does not seriously affect solution quality since actions towards the end of the optimization horizon have little influence on the actions taken at its beginning (i. e. on the actions suggested the dispatchers).

The problem of the cost-optimal dispatch of the tertiary control reserves may be generally formulated as follows:

Minimize utilization costs
Subject to

- load – generation balance (zero closed-loop ACE)
- dynamics and limits of control reserves
- dispatch constraints and rules

The utilization costs typically consist of energy costs and start-up costs associated with start-up of non-spinning control reserves. In the real world, the fluctuations of ACE are often very fast, hence in order to achieve zero closed-loop ACE,

large quantities of fast control reserves would be needed. Since procuring such quantities of fast control reserves would excessively increase the procurement costs, certain non-zero closed-loop ACE is permitted as defined by the control performance standards [70, 71], which lowers the amount of required fast control reserves. Also, in some cases, the open-loop ACE may be so high, that the total range of control reserves is insufficient to compensate it, which would make the problem infeasible. Hence, in the proposed concept, the load-generation balance constraint is relaxed and the following problem is solved:

Minimize utilization costs + $C_{ACE} \cdot |ACE_o$ prediction – dispatched control reserves|
Subject to

- dynamics and limits of control reserves
- dispatch constraints and rules

The term inside the absolute value is the uncompensated open-loop ACE (ACEo) prediction. The coefficient C_{ACE} sets a penalization for each MWh the uncompensated open-loop ACE prediction - if it set higher than reserve energy price of any unit, it ensures, that all available control reserves will be dispatched if necessary. If the control reserves are insufficient to compensate the predicted open-loop ACE, the penalization will be non-zero, which may serve the dispatchers as an indication that additional emergency control reserves need to be called up.

7.2.2.1 Used terms

The term *unit* denotes an entity (usually a generation unit) providing control reserve that can be activated by the TSO's dispatcher. Each such a unit labelled with an index i has its control reserve range $< P_i^{min}, P_i^{max} >$ [MW] provided to the TSO together with a given price C_i per MWh of supplied reserve energy and other technical parameters. The optimization is performed over a fixed 6-hour horizon with non-uniform sampling, consisting of N_S samples, each time-sample k having length $T_S\,(k)$ [min]. The total number of participating units will be denoted N_U.

The terms used to describe the behaviour of the control reserves in this paper are shown in Fig. 7.5. The terms *activation* and *deactivation* of the control reserve denote the time instants when the unit was instructed to deploy its

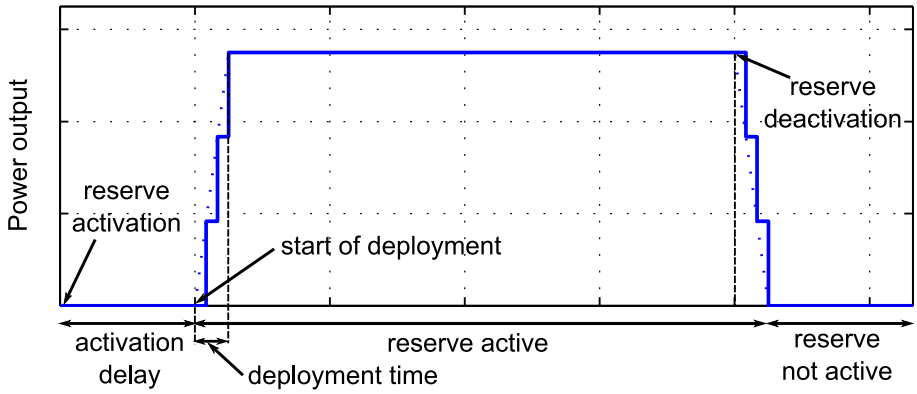

Figure 7.5: Terms used for the description of the control reserves behaviour.

control reserve or stop the reserve delivery, respectively. The term *activation delay* denotes the time between the unit activation and actual start of its control reserve deployment. The *deployment time* denotes the time required to fully deploy the control reserve at the unit from the start of its deployment.

7.2.2.2 Decision variables

The base set of decision variables vector for each unit i is a vector of binary variables u_i with length N_S. If $u_i\,(k)$ is 1, the control reserve at the unit is active at time k, otherwise, the control reserve is not active. To completely describe the state of the control reserve at the unit, the vector u_i is supplemented by the vector of continuous decision variables P_i of length N_S, where $P_i\,(k)$ denotes the reserve power supplied by the unit i in time k. In some models, the vector u_i is substituted by two binary vectors Δu_i^{ON} and Δu_i^{OFF}, each of length N_S. Such a substitution doubles the number of the required binary variables but allows modelling of units whose control reserve range may change during the optimization horizon. The value of the variables Δu_i^{ON} and Δu_i^{OFF} is 1 if the reserve at the unit was activated or deactivated at time k. If needed, the vector u_i may be reconstructed from Δu_i^{ON} and Δu_i^{OFF} using the following equality constraint:

$$\begin{aligned} u_i\,(k+1) =& u_i\,(k) + \Delta u_i^{ON}\,(k+1) - \Delta u_i^{OFF}\,(k+1)\,, \\ & k \in 0, \ldots, N_S - 1, \end{aligned} \tag{7.1}$$

where $u_i\,(0)$ indicates, whether the reserve at the unit was active at the beginning of the optimization horizon.

7.2.2.3 Objective function

With the decision variables defined above, the objective presented in Section 7.2.2 may be rewritten as:

$$J = \sum_{i=1}^{N_U} \sum_{k=1}^{N_S} \left[C_i\left(k\right) P_i\left(k\right) T_S\left(k\right) \right] + \tag{7.2}$$

$$+ \sum_{i=1}^{N_U} \sum_{k=1}^{N_S} \left[C_i^{SU}\left(k\right) \Delta u_i^{ON}\left(k\right) \right] + \tag{7.3}$$

$$+ \sum_{k=1}^{N_S} \left[C_{ACE}\left(k\right) \cdot \sum_{i=1}^{N_U} \left| P_i\left(k\right) - ACE_o\left(k\right) \right| \cdot T_S(k) \right], \tag{7.4}$$

where $C_i^{SU}\left(k\right)$ denotes start-up costs of the unit being activated. The part of the objective (7.2) represents energy costs, the part (7.3) represents the unit start-up costs and the part (7.4) represents the penalization for uncompensated open-loop ACE prediction. To preserve the linearity of the objective, the nonlinear absolute value operator in (7.4) needs to be reformulated to a linear form, e. g. using the conversion presented in [72].

7.2.2.4 Problem constraints

The problem constraints may be divided into two groups – models of control reserves, which model the dynamics of the control reserves, and dispatch constraints, which may be imposed on units so that their activation conforms to standard usage patterns (e. g. minimal up and down times, activation frequency limits etc.).

Models of control reserves. In this section, the models of control reserves will be presented. Each model will be supplemented with a figure describing the typical activation of the modelled reserve and illustrating reserve dynamics, properties and parameters.

Model 1: Control reserves with ability to continuously change delivered power. The model is designed for the control reserves which, when active, may continuously change the delivered power in a given range $< P_i^{min}, P_i^{max} >$, while respecting their ramping limits and minimal and maximal power output. The typical activation of the control reserve with this model is shown in Fig. 7.6.

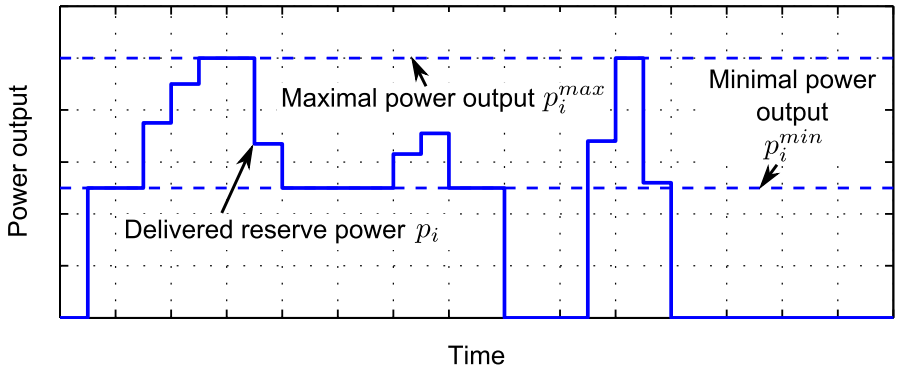

Figure 7.6: Typical activation of control reserve with dynamics described by model 1.

When the control reserve at the unit is active, the reserve power must remain within the control reserve range as expressed by the following constraint:

$$P_i^{min}(k) \cdot u_i(k) \leq P_i(k) \leq P_i^{max}(k) \cdot u_i(k), \quad k \in 1, \ldots, N_S. \tag{7.5}$$

The ramping limits are modelled by constraints

$$\begin{aligned} P_i(k+1) - P_i(k) &\leq \Delta P_i^{max}(k), \\ -[P_i(k+1) - P_i(k)] &\leq \Delta P_i^{max}(k), \\ k &\in 0, \ldots, N_S - 1, \end{aligned} \tag{7.6}$$

where $\Delta P_i^{max}(k)$ is the maximal ramping rate which respects the current sampling period:

$$\Delta P_i^{max}(k) = T_S(k) \cdot \frac{P_i^{max}(k)}{T_i^{SU}}, \quad k \in 0, \ldots, N_S - 1, \tag{7.7}$$

where T_i^{SU} is the deployment time. The first constraint in (7.6) limits the ramp-up rate, the second limits the ramp-down rate. This model is suitable for example for control reserves provided on pumped-storage power plants. The dispatch constraints limiting the frequency of control reserve activations or power output changes may be used with this model, as will be further shown in the dispatch constraints section.

Special case 1a: Constantly active control reserves. Certain control reserves are constantly active, hence the states when the reserve is active and not active do not need to be distinguished. This allows simplifying the constraint (7.5) by removing the term u_i or constraining it to 1 for all time-samples. Such a modification removes one set of binary variables and makes the problem less computationally intensive. This modification may be used for example for a simple continuous secondary control model with reserve range symmetric around zero.

Special case 1b: Schedule activated control reserves. The dynamics of schedule activated control reserves may be described by model 1 without ramping constraints, however, such control reserves are special in a way that the changes in dispatched reserve power may occur only in specific time instants (e.g. each hour). For such instants, the constraint (7.5) may be applied, for other time-samples, the following constraints are used to guarantee constant power output:

$$\begin{aligned} P_i(k) =& P_i(k-1), \\ u_i(k) =& u_i(k-1), \\ & k \notin DP, \end{aligned} \tag{7.8}$$

where DP is a set of decision points, i. e. the time-samples when the dispatched reserve power may change. This variant of model 1 is suitable for example for modelling of exchange schedules of reserve energy obtained from abroad.

Model 2: Control reserves with constant power delivery. This model is designed for the reserves which, if activated, have to be dispatched at their maximal power output and their deployment time is longer than sampling period of the optimization horizon, hence their deployment process needs to be modelled (Fig. 7.7).

It is assumed, that the reserve power increase and decrease is done at constant ramping rate. If the reserve range of the unit changes during the activation of the control reserve, the delivered reserve power has to change accordingly.

The dynamics described above may be modelled by the following constraint:

$$\begin{aligned} P_i(j+1) =& P_i(j) + \Delta P_i^{UP}(j)\,\Delta u_i^{ON}(k) - \Delta P_i^{DOWN}(j)\,\Delta u_i^{OFF}(k) + \\ & + \Delta P_i^{max}(j)\,\Delta u_i^{trans}(j), \\ j \in & k, \ldots, k + N_i^{SU}(k), \\ k \in & 1, \ldots, N_S - N_i^{SU}(N), \end{aligned} \tag{7.9}$$

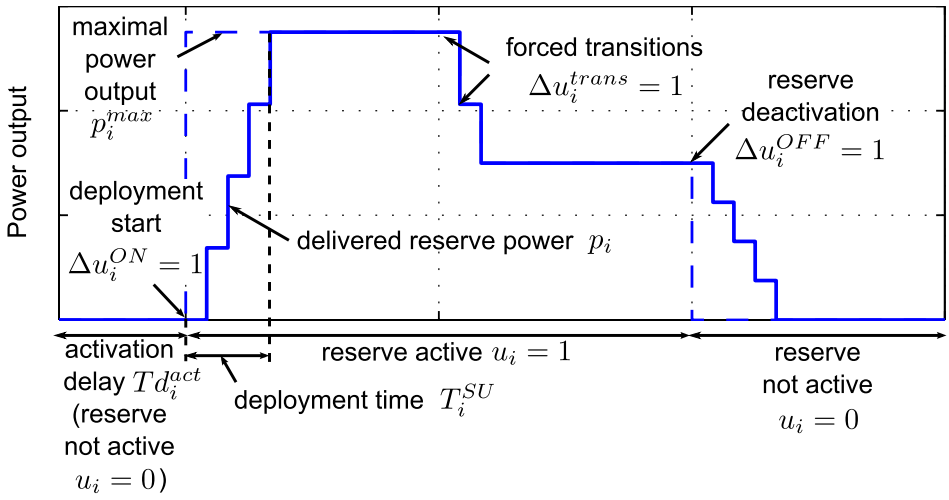

Figure 7.7: Typical activation of control reserve with dynamics described by model 2.

where $N_i^{SU}(k)$ is the number of time-samples which are required for the control reserve at the unit i to be fully deployed at a given sample of the optimization horizon k. The variables Δu_i^{ON} and Δu_i^{OFF} are used instead of u_i so that the activation and deactivation of the control reserve may be modelled separately, each having its own ramping rate ΔP_i^{UP} and ΔP_i^{DOWN} respectively. The ramping rate during the activation of the control reserve ΔP_i^{UP} is a parameter defined by the maximal power output at the end of the activation (i. e. by $P_i^{max}\left(k + N_i^{SU}(k)\right)$):

$$\begin{aligned} \Delta P_i^{UP}(j) =& T_S(j) \cdot \frac{P_i^{max}\left(k + N_i^{SU}(k)\right)}{T_i^{SU}}, \\ & j \in k, \ldots, k + N_i^{SU}(k), \\ & k \in 1, \ldots, N_S - N_i^{SU}(N_S), \end{aligned} \tag{7.10}$$

The rate used during deactivation of the control reserve ΔP_i^{DOWN} is based on the maximal power output at the beginning of deactivation (i. e. based on

$P_i^{max}(k)$)

$$\begin{aligned}\Delta P_i^{DOWN}(j) =& T_S(j) \cdot \frac{P_i^{max}(k)}{T_i^{SU}}, \\ & j \in k, \ldots, k + N_i^{SU}(k), \\ & k \in 1, \ldots, N - N_i^{SU}(N_S).\end{aligned} \tag{7.11}$$

The transitions forced by the change of control reserve range at the unit are modelled by the last term in 7.9. The parameter $\Delta P_i^{max}(j)$ corresponds to the reserve range change at time j and the binary variable Δu_i^{trans} indicates, whether the transition occurs or not. Since the transition cannot happen when the control reserve is not fully deployed, it is constrained as follows:

$$\begin{aligned}\Delta u_i^{trans}(k) \leq \frac{P_i(k)}{P_i^{max}(k)}, \\ k \in 1, \ldots, N_S.\end{aligned} \tag{7.12}$$

Moreover, the following constraint ensures that if the reserve is fully deployed at the time of the change of reserve range, either the transition occurs or the delivery of the control reserve is stopped:

$$\begin{aligned}\frac{P_i(k) - P_i^{\max}(k) + \varepsilon}{P_i^{max}(k)} \leq \Delta u_i^{trans}(k) + \Delta u_i^{OFF}(k) \leq 1, \\ k \in 1, \ldots, N_S.\end{aligned} \tag{7.13}$$

where ε is a small positive constant. To model activation delay at the beginning of the optimization horizon, the following constraint may be used

$$\begin{aligned}\Delta u_i^{ON}(k) = 0, \\ k \in 1, \ldots, Nd_i^{act},\end{aligned} \tag{7.14}$$

where Nd_i^{act} is the number of time-samples corresponding to the activation delay. After the first activation, the activation delay is modelled by using minimal down time dispatch constraint described in the dispatch constraints section and by modifying the minimal down time $T_i^{\min OFF}$ as follows:

$$T_i^{\min OFF} = \max\left(T_i^{\min OFF}, Td_i^{act}\right). \tag{7.15}$$

Any of the dispatch constraints described in the dispatch constraints section may be used with this model. The model 2 with activation delay may be used for example for non-spinning control reserves provided at cold start coal-fired power plants.

Special case 2a: Control reserves with constant reserve range. If the range of the control reserve with dynamics similar to model 2 is constant, a simplified variation of the model 2 may be used. Since the reserve range is constant, the ramping rates during activation and deactivation are identical, which allows simplifying (7.9) to

$$\begin{aligned} P_i(j+1) = P_i(j) + \Delta P_i(j)\left[u_i(k+1) - u_i(k)\right], \\ j \in & k, \ldots, k + N_i^{SU}(k), \\ k \in & 1, \ldots, N_S - N_i^{SU}(N_S), \end{aligned} \tag{7.16}$$

where $\Delta P_i(j)$ is the ramping rate of activation or deactivation of the control reserve defined as follows:

$$\begin{aligned} \Delta P_i(j) = T_S(j) \cdot \frac{P_i^{\max}}{T_i^{SU}}, \\ j \in & k, \ldots, k + N_i^{SU}(k), \\ k \in & 1, \ldots, N_S - N_i^{SU}(N_S). \end{aligned} \tag{7.17}$$

It is beneficial to use this modification for any reserve with dynamics similar to model 2 and constant reserve range, since it lowers the number of used binary variables. The modification cannot be used for the control reserves with activation delay, since the implementation of activation delay presented in model 2 is based on the minimal down-time dispatch constraint, which requires variables Δu_i^{ON} and Δu_i^{OFF}.

Dispatch constraints. The dispatch constraints allow the dispatcher to influence the way the optimization module utilizes the control reserves. The main purpose of using the dispatch constraints is to reduce wear of the units providing the control reserves.

Dispatch constraint 1: Dispatch changes frequency limit. Two types of changes in the control reserves dispatch are considered in this paper – changes in control reserves activation and changes in dispatched power. A constraint expressing for example a requirement 'limit the number of dispatch changes to N_{ch} per hour' may be formulated as follows:

$$\begin{aligned} \sum_{j=k}^{k+N^{int}} \Delta v^{ind}(j) \leq N_{ch}, \\ k \in 0, \ldots, N_S - N^{int}, \end{aligned} \tag{7.18}$$

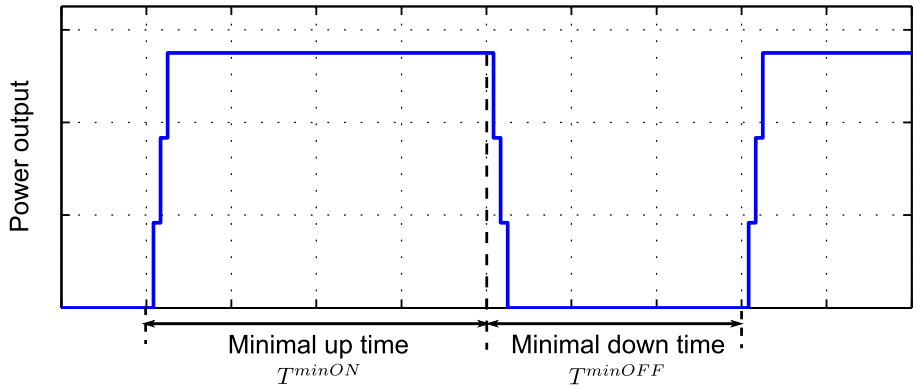

Figure 7.8: Illustration of the minimal up and minimal down time constraints.

where Δv^{ind} is a binary variable indicating the changes that should be limited and N^{int} is the number of time-samples corresponding to the length of an interval, over which the number of changes should be limited. The constraint (7.18) may be directly applied to variables Δu_i^{ON} and Δu_i^{OFF}, e. g. by substituting the Δv^{ind} with Δu_i^{ON} to limit frequency of activations. For other variables, such as u_i or p_i, the change indicating variables may be derived in the following way:

$$\begin{aligned} \Delta v^{ind}(k) &\geq \frac{v(k) - v(k-1)}{V^{max}}, \\ \Delta v^{ind}(k) &\geq -\frac{v(k) - v(k-1)}{V^{max}}, \\ k &\in 1, \ldots, N_S, \end{aligned} \tag{7.19}$$

where v is the variable for which the change indicator is being derived and V^{max} is its maximal value. The variable v may be either continuous or binary, hence (7.19) may be used for deriving changes in activation as well as for deriving changes in dispatched power.

Dispatch constraint 2: Minimal up and down times. For non-spinning reserves, the providers often set minimal up time $T_i^{\min ON}$ and minimal down time $T_i^{\min OFF}$ requirement as illustrated in Fig. 7.8. As $T_i^{\min ON}$ and $T_i^{\min OFF}$ may be different, the dispatch change frequency limit cannot be used. In the proposed formulation, the minimal up and down times may only be used with models

based on variables Δu_i^{ON} and Δu_i^{OFF} and are modelled as follows:

$$\sum_{j=k}^{k+N^{\min ON}} \Delta u_i^{OFF}(j) \leq \left[1 - \Delta u_i^{ON}(j)\right], \quad k \in 0, \ldots, N_S - N^{\min ON}, \tag{7.20}$$

$$\sum_{j=k}^{k+N^{\min OFF}} \Delta u_i^{ON}(j) \leq \left[1 - \Delta u_i^{OFF}(j)\right], \quad k \in 0, \ldots, N_S - N^{\min OFF}, \tag{7.21}$$

where $N^{\min ON}$ and $N^{\min OFF}$ are number of samples corresponding to minimal up and down times.

Dispatch constraint 3: Capacity constraint. The energy that certain types of control reserves are able to deliver is limited. This is particularly true for the control reserves provided at pumped-storage power plants, which may deliver the reserve energy only as long as their water reservoir is not depleted. As a result, the following constraint may be used to reflect such limitation:

$$\sum_{k=1}^{N_S} P_i(k) \cdot T_s(k) \leq cap_i, \tag{7.22}$$

where cap_i [MWh] is the available reserve energy at the beginning of the optimization horizon.

7.3 Integration of the decision support tool with DSM-based ancillary services providers

This section will describe the required modifications of the optimization problems dealt with in the MV and LV DSM systems in order to allow seamless interoperation of all the control levels to be able to provide ancillary services to the TSO.

7.3.1 Extension of the decision support tool

In order to determine what changes need to be done in the decision support tool so that it could be used to optimize dispatch of the DSM-based ancillary services, the following list reviews what constraints are associated with using the DSM potential offered to the TSO by the DSM capacity aggregator:

- *Maximal power* is limited by the aggregated power input of all EWHs in aggregation,
- *Energy storage capacity* is limited by the total energy storage capacity of the EWHs in aggregation,
- *Use of hot water* influences the available energy storage capacity,
- *Ramping limits are almost non-existent* since EWHs may be turned on instantaneously.

Based on the above, it can be concluded, that a combination of model and dispatch constraints typically used for ancillary services provided by pumped-storage power plants may be used for incorporation of the DSM-based ancillary services into the optimization problem solved by the decision support tool, i. e. the combination would be as follow:

- Model 1 as described in Section 7.2.2.4,
- Dispatch constraint 1 to limit number of power changes requests since each such request involves computing new references for the MV and LV DSM systems, which also increases communication requirements.
- Dispatch constraint 3 to take the EWH storage capacity limits into account.

However, the capacity constraint has to be modified in order to incorporate the expected consumption of hot water by the EWHs. This constraint may be formulated equivalently to the form used in the LV and MV DSM systems formulation:

$$\hat{E}_i\left(k+1\right) = \hat{E}_i\left(k\right) - P_i\left(k+1\right) \cdot T_S\left(k+1\right) - \hat{E}_{consumed,i}\left(k+1\right), \tag{7.23}$$

$$\hat{E}_{min,i} \leq \hat{E}_i\left(k\right) \leq \hat{E}_{max,i} \tag{7.24}$$

$$k = 0 \ldots N_S - 1,$$

where

$E_i(k)$ is the aggregated amount of energy stored in all EWHs provided by the aggregator at time k,

$E_i(0)$ is the energy stored in EWHs at the beginning of the optimization (i. e. the current estimate obtained from the aggregator),

$P_i(k)$ is the total power drawn by all EWHs provided by the aggregator at time k,

$\hat{E}_{consumed,i}(k)$ is the predicted hot water energy consumption of all EWHs provided by the aggregator at time k,

$\hat{E}_{max,i}$ is the maximal energy that all EWHs provided by the aggregator may store,

$\hat{E}_{max,i}$ is the required minimal energy that may be used as a safeguard against hot water depletion.

It should be also noted that in comparison to the equivalent used in LV DSM problem formulation given in Section 5.2.1 the sign convention used here is modified. From the TSO point of view, the DSM supplies negative power (i. e. it compensates for surplus of energy in the control area, which is traditionally associated with negative sign). As a result, the power of EWHs is included with negative sign in equation (7.23).

7.3.2 Modification of medium-voltage DSM and low-voltage DSM problem formulations

As explained in Section 7.1 the main modification proposed in connection with provision of DSM potential to the TSO concerning the operation of MV DSM and LV DSM system lies in the fact that instead using objective to achieve certain power balance of the MV or LV area, an objective to achieve certain power input of EWHs in the LV or MV area is used. This allows the MV DSM and LV DSM to be used to directly control the power of EWHs irrespective of what is the uncontrolled load and generation of the area. As will be further seen, this modification actually only involves changing objective functions of the dispatch reference optimization (which in this case is always performed by the MV controller; in the autonomous operation mode of LV DSM system, the reference cannot be set from an external entity such as the TSO) and the dispatch schedules optimization and also dropping of constraints that modelled the power balance of the MV or LV area in case of original formulations.

The dispatch reference optimization problem solved by the MV controller therefore reduces to:

minimize

$$\sum_k \left[c_{ref} \cdot \left(\sum_j \left(P_{A,j}^{EWH}(k) \right) - P_{ref}^{EWH}(k) \right)^2 + c_{lines} \cdot \sum_l \left(\frac{P_l(k)}{P_{l,max}} \right)^2 \right], \quad (7.25)$$

$$k = 1 \dots N_S,$$
$$l = 1 \dots N_L,$$
$$j = 1 \dots N_A,$$

subject to

(DC load flow constraints [66])
(LV areas EWH power input constraint (6.3))
(LV areas EWH energy constraints (6.4)-(6.6))

where

c_{ref} is objective weight of deviation from the EWH power reference P_{ref}^{EWH},
$P_{A,j}^{EWH}(k)$ is aggregate power of EWHs in area j at time k,
$P_{ref}^{EWH}(k)$ is the required power of all EWHs in the MV area at time k,
c_{lines} is objective weight of line capacity utilization,
$P_l(k)$ is power flow through line l at time k,
$P_{l,max}$ is capacity of line l,
k is time index,
j is LV area index,
l is line index,
N_S is number of samples in the optimization horizon,
N_L is number of lines in the MV area,
N_A is number of the controlled LV areas.

The first part of the objective (7.25) is a penalization for deviating from the EWH power reference P_{ref}^{EWH} received from the aggregator, while the second part is, similarly to the original MV DSM problem formulation, penalization of line loading. From the second term and also from inclusion of load flow constraints, it is immediately obvious that despite directly controlling the EWH power instead of power balance of the area, the transmission constraints may still be taken into account so that the required power of EWHs in individual LV areas $P_{A,j}^{EWH}$ may be optimized in a way, that line loading is minimized which should ensure that adverse effects of the EWH control on power quality in the

MV area are minimized. Note that in order to optimize the line loading, the MV controller still needs predictions of the uncontrolled load, generation and naturally also of the EWH hot water consumption.

The resulting EWH power requirements $P_{A,j}^{EWH}$ are then passed on to the appropriate LV controller which then optimizes performs the dispatch schedules optimization modified to the following form:

minimize

$$c_{ref} \cdot \sum_{k} \left(\sum_{i} \left(P_i \left(k \right) \right) - P_{A,j}^{EWH} \left(k \right) \right), \tag{7.26}$$

$$k = 1 \ldots N_S, \tag{7.27}$$
$$i = 1 \ldots N_{EWH},$$

subject to

(deviation from the dispatch reference constraints (5.13-5.15))
(EWH power input constraints (5.22))
(EWH energy constraints (5.8-5.10))
(minimum on time constraints (5.23-5.27))

where

c_{ref} is objective weight of deviation from the EWH power reference of the given area $P_{A,j}^{EWH}$,
$P_i \left(k \right)$ is power of EWH i at time k,
$P_{A,j}^{EWH} \left(k \right)$ is the required power of all EWHs in the LV area at time k,
k is time index,
i is EWH index,
j is LV area index,
N_S is number of samples in the optimization horizon,
N_{EWH} is number of the controlled EWHs.

The objective 7.26 simply states that difference of the total power input of all controlled EWHs from the reference received from the MV controller $P_{A,j}^{EWH}$ should be minimized at any time. The constraints are used in exactly the same form as formulated in Section 5.2.2, only constraints related to the power balance of the LV area are not used.

Finally, it should be noted that the above presented modifications of MV DSM and LV DSM systems optimization problems formulations should rather be perceived as extensions to the original systems rather than modifications as they

actually may be combined with the original objective in case that only a part of the total number of EWHs in each area was dedicated for use as an ancillary service. The aforementioned combination of objectives is also facilitated by the fact, that the forms of the objectives are kept the same as in the original formulations, i. e. a quadratic objective is used in the MV DSM problem formulation and linear objective in the LV DSM problem formulation.

7.4 Case study

In order to verify functionality of the concept presented in this chapter, a brief case study was performed using the following setup:

- One day of load-frequency control of the control area with dimensioning similar to the Czech Republic utilizing the TSO dispatcher decision support tool was simulated. The inputs were as follows:
  - The control reserves used by the Czech TSO as defined in [21] and shown in Tab. 7.1 were included in the optimization. The Tab. 7.1 also shows models and dispatch constraints used for each such control reserve.
  - The control ranges and regulation energy prices were set-up according to typical values for the Czech Republic.
  - The open-loop ACE prediction were used as described in [68].
  - It was assumed that after every optimization step, the actions from the first time-sample of the tertiary reserves dispatch recommended by the decision support tool were accepted and realised by the dispatchers.
- The DSM-based ancillary services were included in the following way:
  - It was assumed that the DSM capacity aggregator offers aggregation of EWHs with the following overall parameters:
    - Maximal power input: 10 MW (the aggregation contained EWHs with total power input of 20 MW but only 10 MW of the total range was allowed to be used at any time instant to avoid too large increases of energy imports into the MV areas),
    - Energy storage capacity: 82 MWh (the total capacity is equal to the total capacity of the whole 20 MW aggregation, i. e. capacity of all EWHs may be used by the TSO, but not all EWHs at the same time)

        - Regulation energy prices were set-up in a way that assumes that the energy produced by the PV sources in the area is also available to the DSM capacity aggregator at low price, therefore the regulation energy price is higher at times of no or little production and low at time of high PV production as illustrated in Fig. 7.9.
        - The estimated hot water consumption predictions provided to the TSO were computed as described in Section 5.3.2.2.
    - The model used for the DSM-based ancillary service was as described in Section 7.3.2. The power changes frequency constraint was set-up to allow 1 change of required power in 30 minutes to avoid excessive transmission of reference change requirements between the individual parts of the DSM system.
    - It was assumed that the DSM capacity aggregator distributes the DSM-based ancillary service activation request among the MV areas proportionally to the total power inputs of the EWHs in the area.

- The resulting required activation of the DSM-based ancillary service was passed on to the MV controller of the MV area which was used for simulations in the MV DSM system case study and is described in Section 6.3. The operation of the MV network with the given EWH power reference was then simulated with the following assumptions:

    - The objectives of the EWH dispatch reference optimization in the MV area and dispatch schedule optimizations in individual LV areas were set up according to the description presented in Section 7.3.2.
    - Since the aggregate power of the EWHs in the simulated MV area is 1.7 MW, it forms approximately 1/12th of the total aggregation size (20 MW) which translates into:
        - The maximal power input of 10 MW is equivalent to 850 kW in the simulated MV area.
        - The maximal storage capacity of 82 MWh is equivalent to approximately 7 MWh in the simulated MV area.

It should be noted that this case study does not aim to present whether the inclusion of DSM-based ancillary services would impact the costs for ancillary services activation. Such a case study would require in-depth analysis of the economics of the DSM system which is not in scope of this thesis. Rather, it aims to show that with the presented modification of the decision support tool, it may be used to recommend such a dispatch of DSM-based ancillary services,

Deployment time	Control reserve			Model	Dispatch constraints
	Positive/negative	Spinning/non-spinning	Reserve type		
~ 30 sec.	Positive and negative	Spinning	**Primary reserve**	Not included	
Max. 5 min.	Positive	Non-spinning	**MZ$_5$** minute reserve (5 min)	1	1 (Power changes), 3
Max. 10 min.	Positive	Spinning	**SR+** secondary reserve (positive)	1a	None
	Negative	Spinning	**SR-** secondary reserve (negative)	1a	None
Max. 15 min.	Positive	Spinning	**MZ$_{15}$+** minute reserve (15 min) (positive)	2 or 2a	1 (Activation frequency)
	Negative	Spinning	**MZ$_{15}$-** minute reserve (15 min) (negative)	2 or 2a	1 (Activation frequency)
Max. 30 min.	Negative	Non-spinning	**Generation shedding**	Not included	
	Positive	Purchase of energy	**EmA+** emergency assistance from abroad (positive)	1b	1 (Power changes)
	Negative	Purchase of energy	**EmA-** emergency assistance from abroad (negative)	1b	1 (Power changes)

Table 7.1: Control reserves used by the Czech TSO.

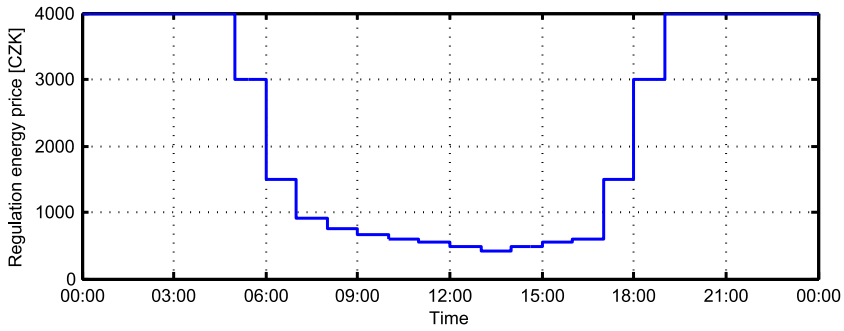

Figure 7.9: Regulation energy prices used for the DSM-based ancillary service.

that would positively contribute to the load-frequency control performed by the TSO and at the same time, that the DSM system would be capable to deliver the regulation energy as per the requirement of the TSO.

The resulting dispatch of the control reserves is shown in Fig. 7.10. Since as was already mentioned, the model used in the decision support tool is in many ways similar to the model used for pumped-storage power plants, the activation of the DSM-based ancillary service activation is shown as activation of negative part of the MZ$_5$ control reserve in Fig. 7.10. As expected, most of activations of this

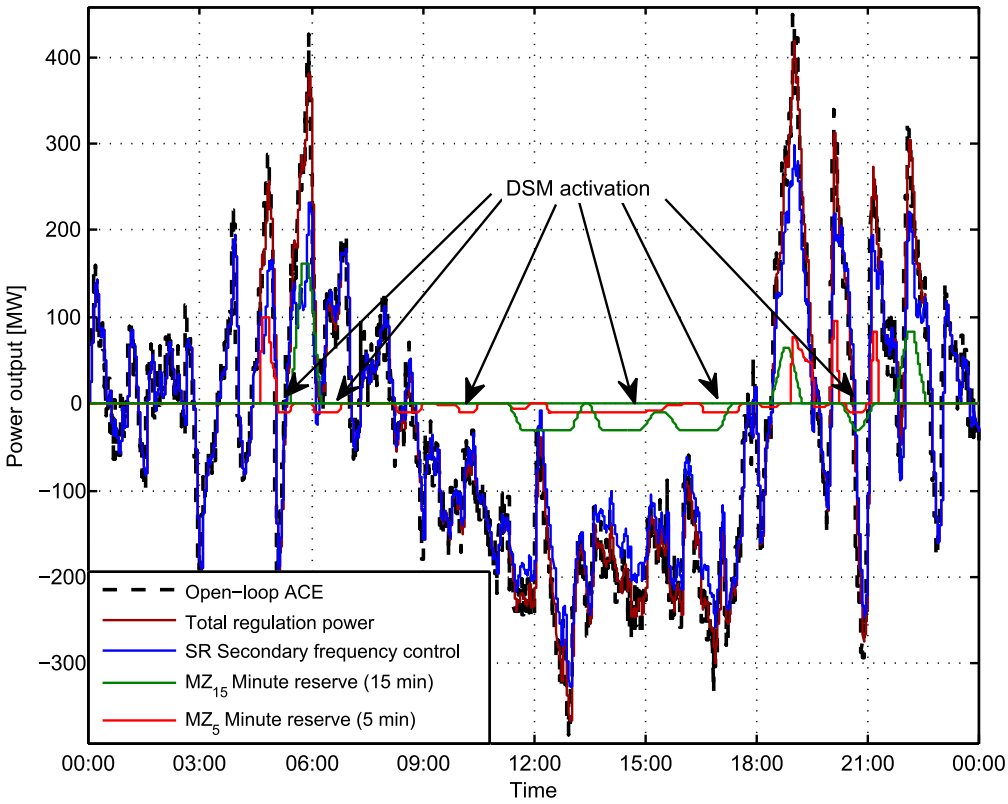

(a) : Activation of all control reserves.

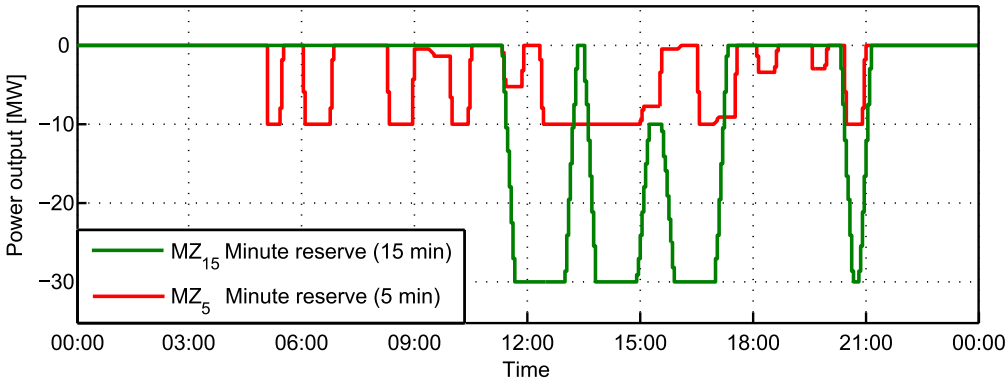

(b) : Detail of negative tertiary control reserves activation.

Figure 7.10: Activations of control reserves recommended by the decision support tool, including activation of the DSM.

ancillary service happens during the day, when the regulation energy price is the lowest. The activations that happen at night are caused by the requirement to ensure enough hot water in the EWHs since the minimal energy constraint of EWHs was set to 50 % of the EWH volume to avoid hot water depletion even in case of large errors in EWH state estimation.

How the required activation of the DSM-based ancillary service influences operation of the simulated MV area is presented in Fig. 7.11. First, the Fig. 7.11a shows the EWH power reference received from the DSM capacity aggregator and the resulting dispatch of EWHs in the area. As already mentioned, the reference from aggregator shown in Fig. 7.11a is approximately 1/12th of the total power that was requested to be delivered by the DSM-based ancillary service (i. e. 1/12th of the the activated negative part of the MZ_5 control reserve shown in Fig. 7.10b).

It may be observed that the total power input of EWHs in the area follows the given reference in most cases with good accuracy with the exception of a long activation that happens between 12:00 and 15:00 of the simulated day, which is caused by the fact that large number of EWHs were already fully charged but their state estimate incorrectly reported that there is still some of their capacity available. The estimation of the energy stored in the EWHs is shown in Fig. 7.11b and compared to the case when the EWHs are controlled by the CRC. Finally, the Fig. 7.11c compares the power balance of the MV area when controlled by DSM the system providing the ancillary service to the case of control by CRC. The power balance exhibits distinctive fluctuations caused by activation of the ancillary service in case of DSM system control, however the resulting import and export peaks do not exceed the peaks observed in case of CRC control.

Further, to verify impacts of the ancillary service activation on power quality in the simulated MV network, a load flow analysis was also performed. The Fig. 7.12 illustrates voltage fluctuations at the same node as was presented in the MV DSM system case study and is marked in Fig. 6.7. The Tab. 7.2 then presents selected results of the load flow analysis. Although it may be clearly observed that activation of the ancillary service causes notable fluctuations of the voltage at the terminal node, the range in which the voltage fluctuates is actually narrower than in case of CRC control. This is also confirmed by the maximal to minimal voltage range observed in the whole MV network which is 157 V in case of control by the DSM system and 198 V in case when the EWHs are controlled by the CRC. The maximal line loading observed in the MV network is also lower in case of the control by the DSM system which achieved

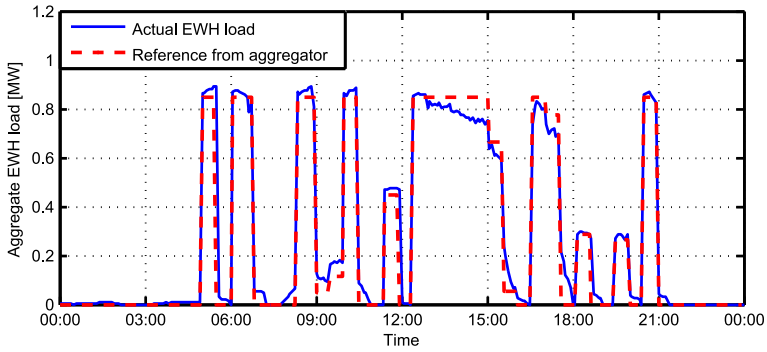

(a) : Reference sent to the MV network by the DSM aggregator and the resulting EWH dispatch.

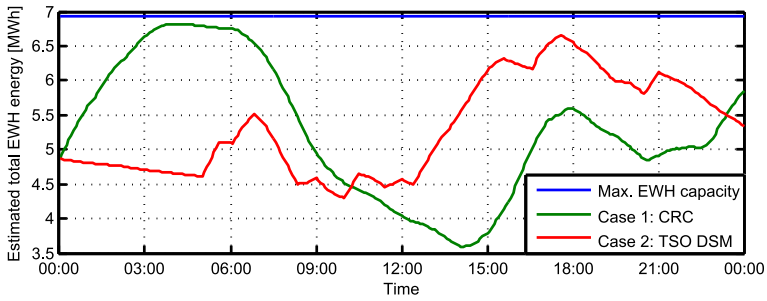

(b) : Estimated EWH energy.

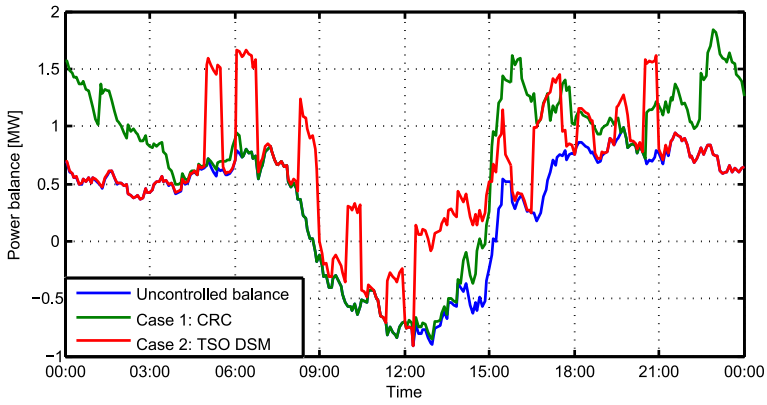

(c) : Resulting power balance of the MV area.

Figure 7.11: Operation of MV network with the EWH reference from the DSM aggregator.

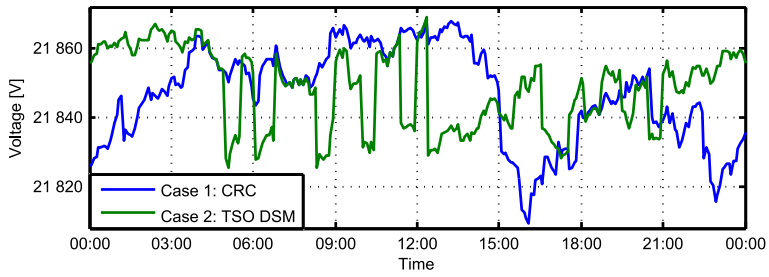

Figure 7.12: Voltage profile at the terminal node with MV network controlled based on reference from the DSM aggregator.

Control type	CRC	DSM system
Maximal line load [%][a]	23.9	20.3
Maximal voltage [V]	22 021	22 021
Minimal voltage [V]	21 823	21 864
Max-to-min voltage [V]	198	157

[a]The percent values represent relative value to the respective line capacity.

Table 7.2: Results of load flow analysis of the MV network controlled based on reference from the DSM aggregator.

maximal line loading of 20.3 % of the respective line capacity, whereas in case the CRC, the maximal line load reached 23.9 %.

Note, that achieving the relatively good results of power quality in the simulated network were partially achieved by the deliberate choice to provide only 50 % of the total power input of the EWHs area (but the whole energy storage capacity) to the TSO. This also suggests that there are methods that may be used to limit impacts of using the DSM to provide ancillary services on power quality of the controlled network which include:

- *Limit the maximal power offered to the TSO*, which reduces the power flow fluctuations resulting from the ancillary service and in turn reduce the voltage fluctuations in the network. This method was used in the presented case study. While this modification limits the control range of the offered control reserve, it allows to use the ancillary service for longer time periods, since the storage capacity of the EWHs is not altered.

- *Use ramping limits with the DSM-based ancillary service*, which would ensure that the requested activation of the ancillary service is applied gradually, resulting in less steep changes in power balance and voltage in the network.

Finally, it may be concluded that although the power quality in the simulated MV network was reduced compared to the original objective of minimizing exports and imports of the controlled area, it was shown that the proposed DSM system is flexible enough to also serve other purposes than improving power quality if such a purpose is more desirable for example for economic reasons. It was also shown that when the DSM system is used for such other purposes, the power quality may still be influenced by proper dimensioning of the amount of the service provided by the EWHs. Moreover such a dimensioning may be set individually for different areas based on parameters of the given network such as line capacities, RES penetration etc.

To generalize the above consideration, in practice, whenever the DSM potential is not used directly by the DSO to improve power quality of its network, but rather by an independent third party, a trade-off between the needs of the DSO and the needs of the third party operating the system must always be found. Aside from the technical perspective (i. e. ensuring acceptable power quality in the network), the economic balance also needs to be found to ensure return of investments of the third party into the control system roll-out, cover running costs of the system and assure a reasonable profit.

Chapter 8

Conclusions

This thesis dealt with a problem of integrating renewable energy sources into the electrical distribution networks. It proposed a three-level demand-side management system which directly controls electric water heaters in households. The proposed concept covers all important technical aspects that are needed to implement the system:

- principles of operation of each control level and interoperation of individual control levels,
- formulation of optimization problems dealt with at each control level,
- implementation of functions critical for the system operation such as power balance predictions, electric water heater state estimation etc.,
- discussion of hardware configuration of the system, distribution of individual functions of the system among different components in the system and communication between the individual parts of the system.

Implementations of most of the aforementioned functions critical for the proposed system operation were also tested in real-world small-scale pilot installation that was realized as a part of the Safe Integration of Renewable Energy Sources (SIRES) project.

The low-voltage and medium-voltage levels of the proposed demand side management system were primarily designed to counteract the issues experienced when a large amount of renewable energy sources, particularly photovoltaic sources, is installed into the distribution networks.

In order to show benefits of the demand side management system, a simulation framework allowing to simulate real-time operation of the proposed demand side management system was developed. Real data from existing low-voltage and medium-voltage networks in Czech Republic which suffer from the aforementioned problems were used to simulate operation of the low-voltage and medium-voltage demand side management systems. The simulations have shown that the demand side management system is capable of effectively reducing the adverse effects associated with renewable energy sources.

The third control level expands the possible use-cases of the proposed system. It presents a framework that allows to aggregate demand side management potential of several medium-voltage networks where the medium-voltage and low-voltage demand side management systems are installed in order to provide ancillary services to the transmission system operator. Moreover, it was shown that by integration of the proposed demand side management system with a decision support system proposed by the author in an earlier work, the ancillary services provided by the demand side management system can be effectively used by the transmission system operator for load-frequency control of its control area.

The key deliverables and results may be summarized as follows:

- A demand side management system for controlling electric water heaters in low-voltage distribution networks with an objective to match the local consumption with local renewable energy sources production was proposed, which, compared to the existing similar concepts, has the following qualities:
  - It is based on the direct load control to ensure predictable response [46] similarly to concepts [47, 48, 49, 50].
  - Compared to the real-time prices based systems [38, 39, 40], it allows for simpler and less expensive household units and requires minimum user interaction. It is designed to be operated with only standard smart-meters installed in households, no additional hardware is required for a basic functionality of the system.
  - Especially in the Czech Republic, the system could be seamlessly rolled-out as an upgrade of the existing centralised ripple control, bringing immediate benefits without requiring any additional interaction from the household users compared to the current state.
  - The proposed system is more autonomous than the presented real-time prices based systems and direct load control systems, since all inputs

are generated locally in the controlled low-voltage distribution network, no information from utility is required.

- By employing optimization techniques to compute optimal dispatch reference and by an appropriate dispatch of each individual controlled electric water heater, the system allows to optimally distribute the electric water heaters load over a longer time horizon, thus avoiding synchronization of controlled load experienced in real-time prices based systems as described in [41].

- The simulations of the low-voltage demand side management system in the SIRES project pilot area have shown that the system is capable of reducing energy export peak of the controlled area by up to 50%, while reducing energy transfer between the low-voltage and medium voltage networks by around 25% thus reducing energy losses associated with energy transmission as well as reducing requirements on feeding lines capacity. Moreover, it has been demonstrated, that the system improves the voltage quality in the controlled area by being capable of reducing the minimal to maximal voltage range in the most critical part of the controlled area by more than 25%.

- An extension of the demand side management system that allows to coordinate operation of multiple low-voltage demand side management systems interconnected within a medium-voltage network was proposed.

  - Unlike other existing concepts [52, 53, 54], which either assume presence of advanced in house energy management system required to support the demand side management system operation or assume presence of high-bandwidth communication links required to spread out control signals at various levels of the distribution networks, the proposed medium-voltage extension increases the required hardware and communications infrastructure compared to the autonomous operation of the low-voltage demand side management systems only marginally, since the communication bandwidth requirements are low thanks to the low frequency of communication between the medium-voltage and low-voltage controllers.
  - The simulations of the medium-voltage demand side management system have shown, that compared to the current state, it is able to reduce photovoltaic sources energy export by more than 90% and reduce the export power peak by almost 80% which is a notable improvement over operating the low-voltage demand side management

systems autonomously, which yielded reduction of energy export of 60% and peak export reduction of 45%.

- The AC load flow analysis of the medium-voltage network revealed that the demand side management system is capable of improving power quality in the network by reducing the peak line loading by 33% and voltage variations by 40%. Since the power quality in the studied medium-voltage network was within reasonable limits even with electric water heaters controlled by the centralised ripple control system due to the dimensioning of the network, additional analyses of operation of the demand side management system in the medium-voltage network with modified dimensioning of the network and also with increased capacity of photovoltaic sources in the area were performed. The results of these analyses indicated that in networks with worse dimensioning, the benefits of the demand side management system could be more substantial, allowing the medium-voltage network to operate with similar power quality to the quality that was achieved by the centralised ripple control system in the network with original dimensioning.

- Finally, it was shown that by aggregating demand side management potential of multiple medium-voltage areas and integrating the demand side management system with a decision support tool [68], the demand side management potential of households may be offered to the transmission system operator in form of ancillary service. While the decision support system helps the transmission system operator's dispatchers to generate such a dispatch of ancillary services that minimizes costs for ancillary services and respects the demand side management specific constraints at the same time, the demand side management system ensures that requirements to activate such an ancillary service are fulfilled in the medium-voltage and low-voltage parts of the network and the regulation energy is delivered to the transmission system operator as required. Furthermore, it was shown that although using the demand side management potential for ancillary services provision does impact power quality in the networks that provide the demand side management potential, the resulting power quality in the distribution networks actually improves compared to the current state, when the electric water heaters are controlled by the centralised ripple control system.

Although the thesis presented a detailed analysis of technical aspects of the proposed demand side management system, two important directions on which

a further development of the system could focus may be pinpointed. The first such direction is to perform a larger-scale pilot installation of the demand side management system than was realized within the SIRES project in order to verify the system performance in real-life scenario. The other important direction is to obtain a better insight into economics of the system and also into the legislative issues associated with operating such a system. Such an analysis would allow to show the potential economic benefits to the respective stakeholders and possibly also facilitate putting the system into routine practice in the future.

The main results presented in this thesis were published in selected scientific journals and international conferences: The initial demand side management potential analysis for the Czech Republic was presented at EEEIC 2011 Conference in Rome, Italy [73], the low-voltage demand side management system was published in IEEE Transactions on Sustainable Energy [55], the medium-voltage hierarchical extension was presented at the AUPEC 2014 Conference in Perth, Australia [65], a summary of the SIRES project was presented in [74] and finally the TSO dispatcher support tool was first presented at ICCA 2009 Conference in Christchurch, New Zealand in paper [75] and then the extended version was published in International Journal of Electrical Power & Energy Systems [68].

Appendix A

Bibliography

[1] K. F. Katiraei and J. R. Aguero, "Solar PV integration challenges," *IEEE Power and Energy Magazine*, vol. 9, no. 3, pp. 62–71, Jun. 2011.

[2] Y. Liu, J. Bebic, B. Kroposki, J. de Bedout, and W. Ren, "Distribution system voltage performance analysis for High-Penetration PV," in *Energy 2030 Conference, 2008. ENERGY 2008. IEEE*, 2008, pp. 1–8.

[3] T. Senjyu, Y. Miyazato, A. Yona, N. Urasaki, and T. Funabashi, "Optimal Distribution Voltage Control and Coordination With Distributed Generation," *Power Delivery, IEEE Transactions on*, vol. 23, no. 2, pp. 1236–1242, 2008.

[4] M. Thomson and D. Infield, "Impact of widespread photovoltaics generation on distribution systems," *Renewable Power Generation, IET*, vol. 1, no. 1, pp. 33–40, 2007.

[5] P. McNutt, J. Hambrick, and M. Keesee, "Effects of photovoltaics on distribution system voltage regulation," in *Photovoltaic Specialists Conference (PVSC), 2009 34th IEEE*, 2009, pp. 001 914–001 917.

[6] R. Tonkoski, L. A. C. Lopes, and T. H. M. El-Fouly, "Coordinated active power curtailment of grid connected PV inverters for overvoltage prevention," *Sustainable Energy, IEEE Transactions on*, vol. 2, no. 2, pp. 139–147, 2011.

[7] D. W. Paulus and D. W. Borggrefe, "Economic potential of demand side management in an industrialized country - the case of Germany," in *10th IAEE European conference, Vienna Austria*, 2009.

[8] (2009) A National Assessment of Demand Response Potential. Federal Energy Regulatory Commission (FERC). [Online]. Available: http://www.ferc.gov/legal/staff-reports/06-09-demand-response.pdf [Accessed: 2016-08-23]

[9] T. G. Hesser. (2010) The Future of Demand Response: Connecting the Dots between Smart Grid and Large Scale Wind Integration. [Online]. Available: http://www.maproyalty.com/downloads/the-future-of-demand-response.pdf [Accessed: 2016-08-23]

[10] (2009) Assessment of Achievable Potential from Energy Efficiency and Demand Response Programs in the U.S. Electric Power Research Institute (EPRI). [Online]. Available: http://www.edisonfoundation.net/iei/Documents/EPRI_AssessmentAchievableEEPotential0109.pdf [Accessed: 2016-08-23]

[11] (2010) AmerenUE Demand Side Management (DSM) Market Potential Study Volume 1: Executive Summary. Global Energy Partners, LLC. Walnut Creek, CA. 2010. 1287-1. [Online]. Available: https://www.ameren.com/-/media/missouri-site/Files/Environment/Renewables/AmerenUEVolume1ExecutiveSummary.pdf [Accessed: 2016-08-23]

[12] (2010) AmerenUE DSM Market Research Report: Volume 2: Market Research, Results from the Saturation, Program Interest and Trade Ally Research. Global Energy Partners, LLC. Walnut Creek, CA. 2010. 1287-1. [Online]. Available: https://www.ameren.com/-/media/missouri-site/Files/Environment/Renewables/AmerenUEVolume2MarketResearchReport2.pdf [Accessed: 2016-08-23]

[13] (2010) AmerenUE Demand Side Management (DSM) Market Potential Study Volume 3: Analysis of Energy-Efficiency Potential. Global Energy Partners, LLC. Walnut Creek, CA. 2010. 1287-3. [Online]. Available: https://www.ameren.com/-/media/missouri-site/Files/Environment/Renewables/AmerenUEVolume3PotentialReport.pdf [Accessed: 2016-08-23]

[14] (2010) AmerenUE Demand Side Management (DSM) Market Potential Study Volume 4: Program Analysis. Global Energy Partners, LLC. Walnut Creek, CA. 2010. 1287-4. [Online]. Available: https://www.ameren.com/-/media/missouri-site/Files/Environment/Renewables/AmerenUEVolume4ProgramReport.pdf [Accessed: 2016-08-23]

[15] (2011) Missouri Statewide DSM Market Potential Study. Kema, Inc. [Online]. Available: https://energy.mo.gov/energy/docs/Finalreport_041411.pdf [Accessed: 2016-08-23]

[16] (2010) Assessment of Demand Response and Energy Efficiency Potential for Midwest ISO. Global Energy Partners, LLC. Walnut Creek, CA 2010. Report Number 1314. [Online]. Available: http://pserc.wisc.edu/documents/publications/special_interest_publications/miso/Midwest-ISO_DR_and_EE_Potential_Assessment_Volume_1.pdf [Accessed: 2016-08-23]

[17] (2010) Assessment of Demand Response and Energy Efficiency Potential Volume 2: Eastern Interconnection Analysis. Global Energy Partners, LLC. Walnut Creek, CA 2010. Report Number 1314-2. [Online]. Available: http://pserc.wisc.edu/documents/publications/special_interest_publications/miso/Midwest-ISO_DR_and_EE_Potential_Assessment_Final_Volume%202.pdf [Accessed: 2016-08-23]

[18] A. Chardon, O. Almen, P. E. Lewis, J. Stromback, and B. Chateau, "Demand Response: A decisive breakthrough for Europe," 2008. [Online]. Available: http://sedc-coalition.eu/wp-content/uploads/2011/05/Capgemini-09-05-01-Demand-Response-Potential-in-Europe.pdf [Accessed: 2016-08-23]

[19] G. Strbac, "Demand side management: Benefits and challenges," *Energy Policy*, vol. 36, no. 12, pp. 4419–4426, Dec. 2008. [Online]. Available: http://www.sciencedirect.com/science/article/B6V2W-4TW0SWR-7/2/ff67656ebacc17b8322ff6e774643e0d [Accessed: 2016-08-23]

[20] N. Voropai, D. Efimov, and V. Khanaev, "Demand side management and load control in Russia: Experience and perspective view for the next two decades," in *2010 IEEE Power and Energy Society General Meeting*, 2010, pp. 1 –7.

[21] ČEPS, a.s., "Grid code, English extract," revision 15, May 2015. [Online]. Available: https://www.ceps.cz/CZE/Media/Tiskove-zpravy/Documents/en14_15_rev_part_I_II_III_fin.pdf [Accessed: 2016-08-23]

[22] ČEPS, a.s., "Web pages." [Online]. Available: http://www.ceps.cz/ [Accessed: 2016-08-23]

[23] Z. Brettschneider, "Potential to provide the Load Change ancillary service in the Czech Republic," ORGREZ, a.s., in Czech. [Online]. Available: http://svse.aem.cz/sd051103/orgrez_brettschneider.ppt [Accessed: 2016-08-23]

[24] Czech Statistical Office. Census 2001: Household technical equipment. In Czech. [Online]. Available: https://www.czso.cz/documents/10180/20536688/41320556.pdf/d8f5e481-8649-45ba-8253-146e95229660?version=1.0 [Accessed: 2016-08-23]

[25] "Residential monitoring to decrease energy use and carbon emissions in Europe (REMODECE) deliverable D9: Report with the results of the surveys based on questionnaires for all countries," 2008. [Online]. Available: http://remodece.isr.uc.pt/downloads/REMODECE_D9_Nov2008_Final.pdf [Accessed: 2016-08-23]

[26] P. Bertoldi and B. Atanasiu, "Electricity Consumption and Efficiency Trends in the Enlarged European Union," 2006. [Online]. Available: http://qualenergia.it/UserFiles/Files/Electricity%20Consumption%20in%20UE.pdf [Accessed: 2016-08-23]

[27] (2010) Energy Regulatory Office of the Czech Republic: Annual Data Summary of Electric Power System of the Czech Republic 2010. In Czech. [Online]. Available: https://www.eru.cz/documents/10540/462820/Rocni_zprava_provoz_ES_2010.pdf/e33fe1d5-b15c-4a0e-bcc8-08cfaf3252ae [Accessed: 2016-08-23]

[28] Heating costs 2011: How much do we pay for heat? In Czech. [Online]. Available: http://www.cenyenergie.cz/nejnovejsi-clanky/ceny-vytapeni-2011-kolik-za-co-zaplatime.aspx [Accessed: 2016-08-23]

[29] EIA Information System. In Czech. [Online]. Available: http://www.cenia.cz/EIA [Accessed: 2016-08-23]

[30] (2007) Federation of the Food and Drink Industries of the Czech Republic: The number of large grocery stores in the Czech Republic has risen to 215. In Czech. [Online]. Available: http://www.foodnet.cz/polozka/?jmeno=Pr%C5%AFzkum%3A+Po%C4%8Det+hypermarket%C5%AF+v+%C4%8Cesku+vzrostl+na+215&id=12383 [Accessed: 2016-08-23]

[31] (2006) First grocery store was opened 15 years ago. In Czech. [Online]. Available: http://ekonomika.idnes.cz/

pred-15-lety-otevrel-prvni-cesky-supermarket-fmj-/ekonomika.aspx?c=A060801_114604_ekonomika_plz [Accessed: 2016-08-23]

[32] P. Havel, P. Horacek, V. Cerny, and J. Fantik, "Optimal Planning of Ancillary Services for Reliable Power Balance Control," *Power Systems, IEEE Transactions on*, vol. 23, no. 3, pp. 1375 –1382, aug. 2008.

[33] ČEZ: Project FUTUREMOTION. [Online]. Available: https://www.cez.cz/edee/content/micrositesutf/odpovednost2011/en/environment/iniciativa-future-motion.html [Accessed: 2016-08-23]

[34] A. Neuberg, "Ripple control in the Czech Republic and Demand Side Management," in *Electricity Distribution - Part 1, 2009. CIRED 2009. 20th International Conference and Exhibition on*, 2009, pp. 1–5.

[35] P. Jiříček, "Numerical methods for evaluating power of CRC groups," CYGNI, spol. s r.o., in Czech.

[36] D. Raisz and A. Dan, "Ripple Control as a possible tool for daily load balancing in an open electricity market environment," in *2005 IEEE Power Tech, Russia*, 2005, pp. 1–6.

[37] J. Shen, C. Jiang, and B. Li, "Controllable Load Management Approaches in Smart Grids," *Energies*, vol. 8, no. 10, pp. 11 187–11 202, Oct. 2015.

[38] A. Conejo, J. Morales, and L. Baringo, "Real-Time demand response model," *IEEE Trans. Smart Grid*, vol. 1, no. 3, pp. 236 –242, Dec. 2010.

[39] H. Saele and O. Grande, "Demand Response From Household Customers: Experiences From a Pilot Study in Norway," *IEEE Trans. Smart Grid*, vol. 2, no. 1, pp. 102 –109, Mar. 2011.

[40] Y. Guo, M. Pan, and Y. Fang, "Optimal Power Management of Residential Customers in the Smart Grid," *IEEE Trans. Parallel Distrib. Syst.*, 2012.

[41] A. Mohsenian-Rad, V. Wong, J. Jatskevich, R. Schober, and A. Leon-Garcia, "Autonomous Demand-Side management based on Game-Theoretic energy consumption scheduling for the future smart grid," *IEEE Trans. Smart Grid*, vol. 1, no. 3, pp. 320 –331, Dec. 2010.

[42] J. A. Short, D. G. Infield, and L. L. Freris, "Stabilization of Grid Frequency Through Dynamic Demand Control," *IEEE Trans. Power Syst.*, vol. 22, no. 3, pp. 1284–1293, Aug. 2007.

[43] A. Molina-Garcia, F. Bouffard, and D. S. Kirschen, "Decentralized Demand-Side Contribution to Primary Frequency Control," *IEEE Transactions on Power Systems*, vol. 26, no. 1, pp. 411–419, Feb. 2011.

[44] J. Villena, A. Vigueras-Rodriguez, E. Gomez-Lazaro, J. Alvaro Fuentes-Moreno, I. Munoz-Benavente, and A. Molina-Garcia, "An Analysis of Decentralized Demand Response as Frequency Control Support under Critical Wind Power Oscillations," *Energies*, vol. 8, no. 11, pp. 12 881–12 897, Nov. 2015.

[45] R. Garcia-Valle, L. C. da Silva, Z. Xu, and J. Ostergaard, "Smart demand for improving short-term voltage control on distribution networks," *IET Generation, Transmission & Distribution*, vol. 3, no. 8, pp. 724–732, Aug. 2009.

[46] S. Lu, N. Samaan, R. Diao, M. Elizondo, C. Jin, E. Mayhorn, Y. Zhang, and H. Kirkham, "Centralized and decentralized control for demand response," in *Innovative Smart Grid Technologies (ISGT), 2011 IEEE PES*. IEEE, Jan. 2011, pp. 1–8.

[47] N. Lu and D. Chassin, "A state-queueing model of thermostatically controlled appliances," *IEEE Trans. Power Syst.*, vol. 19, no. 3, pp. 1666 – 1673, Aug. 2004.

[48] N. Lu, D. Chassin, and S. Widergren, "Modeling uncertainties in aggregated thermostatically controlled loads using a State queueing model," *IEEE Trans. Power Syst.*, vol. 20, no. 2, pp. 725 – 733, May 2005.

[49] J. Kondoh, N. Lu, and D. Hammerstrom, "An Evaluation of the Water Heater Load Potential for Providing Regulation Service," *IEEE Trans. Power Syst.*, vol. 26, no. 3, pp. 1309 –1316, Aug. 2011.

[50] N. Lu, "An evaluation of the HVAC load potential for providing load balancing service," *IEEE Trans. Smart Grid*, pp. 1 –8, 2012.

[51] (2016) NERC Operating manual. North American Electric Reliability Corporation. [Online]. Available: http://www.nerc.com/comm/OC/Operating%20Manual%20DL/Operating_Manual_20160809.pdf [Accessed: 2016-08-23]

[52] E. Vrettos and G. Andersson, "Combined Load Frequency Control and active distribution network management with Thermostatically Controlled

Loads," in *2013 IEEE Int. Conf. on Smart Grid Commun. (SmartGridComm)*, Oct 2013, pp. 247–252.

[53] C. Vivekananthan, Y. Mishra, G. Ledwich, and F. Li, "Demand Response for Residential Appliances via Customer Reward Scheme," *IEEE Trans. Smart Grid*, vol. 5, no. 2, pp. 809–820, March 2014.

[54] D. Wang, S. Parkinson, W. Miao, H. Jia, C. Crawford, and N. Djilali, "Hierarchical market integration of responsive loads as spinning reserve," *Appl. Energy*, vol. 104, no. 0, pp. 229 – 238, 2013. [Online]. Available: http://www.sciencedirect.com/science/article/pii/S0306261912007738 [Accessed: 2016-08-23]

[55] O. Malik and P. Havel, "Active Demand-Side Management System to Facilitate Integration of RES in Low-Voltage Distribution Networks," *IEEE Trans. Sustain. Energy*, vol. 5, no. 2, pp. 673–681, April 2014.

[56] D. D. Giustina and S. Rinaldi, "Hybrid Communication Network for the Smart Grid: Validation of a Field Test Experience," *IEEE Transactions on Power Delivery*, vol. 30, no. 6, pp. 2492–2500, Dec 2015.

[57] M. Hubík. (2013) Design of Algorithms for Electric Water Heater State Estimation. Bachelor thesis. [Online]. Available: https://cyber.felk.cvut.cz/theses/papers/373.pdf [Accessed: 2016-08-23]

[58] I. Knight, N. Kreutzer, M. Manning, M. Swinton, and H. Ribberink, "Residential cogeneration systems: European and Canadian residential non-HVAC electric and DHW load profiles for use in simulating the performance of residential cogeneration systems," Annex 42 report, IEA ECBCS, Tech. Rep., 2007. [Online]. Available: http://www.ecbcs.org/docs/Annex_42_Domestic_Energy_Profiles.pdf [Accessed: 2016-08-23]

[59] Normalized load profiles. OTE, a. s. [Online]. Available: http://www.ote-cr.cz/statistics/load-profiles-electricity/normalized-lp [Accessed: 2016-08-23]

[60] Yr.no - weather forecasts. [Online]. Available: http://www.yr.no [Accessed: 2016-08-23]

[61] J. Lofberg, "YALMIP : a toolbox for modeling and optimization in MATLAB," in *Computer Aided Control Systems Design, 2004 IEEE International Symposium on*, sept. 2004, pp. 284 –289.

[62] J. Müller. (2013) Development of algorithms for demand-side management in smart-grids. Diploma thesis. In Czech. [Online]. Available: https://support.dce.felk.cvut.cz/mediawiki/images/1/1c/Dp_2013_mueller_josef.pdf [Accessed: 2016-08-23]

[63] E. Janecek and D. Georgiev, "Probabilistic Extension of the Backward/Forward Load Flow Analysis Method," *IEEE Transactions on Power Systems*, vol. 27, no. 2, pp. 695–704, May 2012.

[64] Weather information from meteorological stations. Czech Hydrometeorological Institute. In Czech. [Online]. Available: http://pr-asv.chmi.cz/synopy-tab/ [Accessed: 2016-08-23]

[65] O. Malík, J. Zábojník, and O. Zlevor, "A hierarchical demand-side management system for MV networks with high RES penetration," in *Power Engineering Conference (AUPEC), 2014 Australasian Universities*, 2014, pp. 1–6.

[66] J. Zabojník and M. Dvořák, "Power grid simulation model for long term operation planning," *Applied Thermal Engineering*, vol. 70, no. 2, pp. 1294 – 1305, 2014. [Online]. Available: http://www.sciencedirect.com/science/article/pii/S1359431114004402 [Accessed: 2016-08-23]

[67] Licenses locator. Energy Regulatory Office of the Czech Republic. [Online]. Available: http://licence.eru.cz/ [Accessed: 2016-08-23]

[68] O. Malík and P. Havel, "Decision support tool for optimal dispatch of tertiary control reserves," *International Journal of Electrical Power & Energy Systems*, vol. 42, no. 1, pp. 341 – 349, 2012. [Online]. Available: http://www.sciencedirect.com/science/article/pii/S0142061512001299 [Accessed: 2016-08-23]

[69] Continental Europe Operation Handbook. European Network of Transmission System Operators for Electricity (ENTSO-E). [Online]. Available: https://www.entsoe.eu/publications/system-operations-reports/operation-handbook/Pages/default.aspx [Accessed: 2016-08-23]

[70] N. Maruejouls, T. Margotin, M. Trotignon, P. L. Dupuis, and J. M. Tesseron, "Measurement of the load frequency control system service: comparison between American and European indicators," *IEEE Transactions on Power Systems*, vol. 15, no. 4, pp. 1382–1387, Nov 2000.

[71] N. Jaleeli and L. S. VanSlyck, "NERC's new control performance standards," *IEEE Transactions on Power Systems*, vol. 14, no. 3, pp. 1092–1099, Aug 1999.

[72] D. Bertsekas and J. Tsitsiklis, *Introduction to Linear Optimization*, ser. Athena Scientific series in optimization and neural computation. Athena Scientific, 1997.

[73] O. Malík and P. Havel, "Analysing demand-side management potential: Situation in Europe and the Czech Republic," in *Environment and Electrical Engineering (EEEIC), 2011 10th International Conference on*, May 2011, pp. 1–4.

[74] O. Malík, O. Novák, and J. Zábojník, "Power management for the safe integration of renewable energy sources," *All for Power*, vol. 5, pp. 74 – 76, 2015, in Czech.

[75] P. Havel and O. Malík, "Optimal Dispatch of Regulation Reserves for Power Balance Control in Transmission System," in *2009 IEEE International Conference on Control and Automation, vols 1-3*. IEEE, 2009, pp. 807–812.

Appendix B

List of author's publications

Publications in journals indexed in Web of Science with impact factor in Journal Citation Reports

1. O. Malík and P. Havel, "Decision support tool for optimal dispatch of tertiary control reserves," International Journal of Electrical Power & Energy Systems, vol. 42, no. 1, pp. 341 – 349, 2012. Co-authorship: 80% - 20%. Citing articles from Web of Science: [Citations1, Citations2, Citations3, Citations4]

2. O. Malík and P. Havel, "Active demand-side management system to facilitate integration of RES in low-voltage distribution networks," IEEE Trans. Sustain. Energy, vol. 5, no. 2, pp. 673–681, April 2014. Co-authorship: 90% - 10%. Citing articles from Web of Science: [Citations5, Citations6, Citations7, Citations8, Citations9]

Publications in other peer-reviewed journals

1. O. Malík, O. Novák, and J. Zábojník, "Power management for the safe integration of renewable energy sources," All for Power, vol. 5, pp. 74–76, 2015, in Czech. Co-authorship: 80% - 15% - 5%

Conference publications indexed in Web of Science

1. P. Havel and O. Malík, "Optimal Dispatch of Regulation Reserves for Power Balance Control in Transmission System," in 2009 IEEE International Conference on Control and Automation, vols 1-3. IEEE, 2009, pp. 807–812. Co-authorship: 50% - 50%. Citing articles from Web of Science: [Citations10, Citations11]

Other conference publications

1. O. Malík and P. Havel, "Analysing demand-side management potential: Situation in Europe and the Czech republic," in 10th International Conference on Environment and Electrical Engineering (EEEIC), May 2011, pp. 1–4. Co-authorship: 90% - 10%.

2. O. Malík, J. Zábojník, and O. Zlevor, "A hierarchical demand-side management system for MV networks with high RES penetration," in 2014 Australasian Universities Power Engineering Conference (AUPEC), 2014, pp. 1–6. Co-authorship: 50% - 25% - 25%.

Appendix C

Citing articles from Web of Science

[Citations1] Z. Zhang, S. Zhang, S. Geng, Y. Jiang, H. Li, and D. Zhang, "Application of decision trees to the determination of the year-end level of a carryover storage reservoir based on the iterative dichotomizer 3," *INTERNATIONAL JOURNAL OF ELECTRICAL POWER & ENERGY SYSTEMS*, vol. 64, pp. 375–383, JAN 2015.

[Citations2] N. Rezaei and M. Kalantar, "Economic-environmental hierarchical frequency management of a droop-controlled islanded microgrid," *ENERGY CONVERSION AND MANAGEMENT*, vol. 88, pp. 498–515, DEC 2014.

[Citations3] P. Rabbanifar and S. Jadid, "Stochastic multi-objective security-constrained market-clearing considering static frequency of power system," *INTERNATIONAL JOURNAL OF ELECTRICAL POWER & ENERGY SYSTEMS*, vol. 54, pp. 465–480, JAN 2014.

[Citations4] G. Diaz, "Optimal primary reserve in DFIGs for frequency support," *INTERNATIONAL JOURNAL OF ELECTRICAL POWER & ENERGY SYSTEMS*, vol. 43, no. 1, pp. 1193–1195, DEC 2012.

[Citations5] J. Villena, A. Vigueras-Rodriguez, E. Gomez-Lazaro, J. Alvaro Fuentes-Moreno, I. Munoz-Benavente, and A. Molina-Garcia, "An Analysis of Decentralized Demand Response as Frequency Control Support under Critical Wind Power Oscillations," *ENERGIES*, vol. 8, no. 11, pp. 12 881–12 897, NOV 2015.

[Citations6] J. Shen, C. Jiang, and B. Li, "Controllable Load Management Approaches in Smart Grids," *Energies*, vol. 8, no. 10, pp. 11 187–11 202, OCT 2015.

[Citations7] L. Zhi-Xian, L. Xiao-Shu, and H. Guo-Xian, "Numerical modeling and research on nonlinear dynamic behaviors of two-stage photovoltaic grid-connected inverter," *ACTA PHYSICA SINICA*, vol. 64, no. 13, JUL 5 2015.

[Citations8] A. Kleidaras and A. Kiprakis, "A Roadmap for Domestic Load Modelling for Large-Scale Demand Management within Smart Grids," vol. 154, pp. 33–47, 7th International Conference on Wireless and Satellite Systems (WiSATS), Univ Bradford, Norcroft Ctr, Bradford, ENGLAND, JUL 06-07, 2015.

[Citations9] T. Niknam, B. Bagheri, M. M. Bonehkhater, and B. B. Firouzi, "A new teaching-learning-based optimization algorithm for distribution system state estimation," *JOURNAL OF INTELLIGENT & FUZZY SYSTEMS*, vol. 29, no. 2, pp. 791–801, 2015.

[Citations10] I. Saboya Bautista, I. Egido, and E. Lobato Miguelez, "Performance Evaluation of Start-Up Decisions of Rapid-Start Units for AGC," *IEEE TRANSACTIONS ON POWER SYSTEMS*, vol. 30, no. 6, pp. 3130–3138, NOV 2015.

[Citations11] I. Saboya, I. Egido, and L. Rouco, "Start-Up Decision of a Rapid-Start Unit for AGC Based on Machine Learning," *IEEE TRANSACTIONS ON POWER SYSTEMS*, vol. 28, no. 4, pp. 3834–3841, NOV 2013.